PRECISION OPTICAL INTERFEROMETRY IN SPACE

Grant NAGW-1647

Semiannual Status Report No's 1,2,3,4,5,6 and 7

For the period 6 February 1989 through 31 January 1993

Final Report

For the period 6 February 1989 through 31 January 1993

Principal Investigator
Robert D. Reasenberg

July 1993

Prepared for
National Aeronautics and Space Administration
Washington, DC 20546

Smithsonian Institution
Astrophysical Observatory
Cambridge, MA 02138

The Smithsonian Astrophysical Observatory
is a member of the
Harvard-Smithsonian Center for Astrophysics

The NASA Technical Officer for this grant is Ms. Dolores Holland, Code E, NASA Headquarters, Washington, DC 20546.

Final Report to Innovative Research Program
Precision Optical INTerferometry in Space (POINTS)

This is the final report, and incorporates the several semiannual reports listed on the cover, of the work done under NASA Innovative Research Program Grant NAGW-1647 for Precision Optical INTerferometry in Space (POINTS). During the tenure of the grant, the POINTS concept was developed and supporting technologies were investigated. One technology of particular importance to POINTS is laser gauging. Under the grant, we developed a new class of precision laser gauges. In our laboratory, we demonstrated a laser gauge at the picometer level (10^{-12} meter) required for the POINTS spaceborne instrument. This is a three order advance over the best commercial gauges available. A patent is pending, and industrial applications are being sought.

Appended are two recent invited papers on POINTS. The paper to appear in the special issue of Remote Sensing Reviews provides some historical perspective on the POINTS project, underscores the innovations, and indicates the work by students on the project. The paper for the SPIE Conference 1947, Spaceborne Interferometry, contains the most up-to-date description of the instrument. Between them, these papers summarize the status of the development at the end of the subject grant. (The SPIE Conference included five other papers on POINTS as indicated in the copy of the Conference agenda and the POINTS bibliography that follow. Copies of the papers in the bibliography are available on request.)

POINTS is now a collaborative effort between SAO and JPL. The development of POINTS at SAO is now supported by the PIDDP program of Code SL and by the Smithsonian Institution. We plan to propose to further develop POINTS in response to the NRA that is expected to be issued this summer for the TOPS-1 mission of Code SL. According to the agreed division of labor, JPL will buy or build the spacecraft and do the instrument-spacecraft integration; SAO will develop the instrument with the help of industry. After an evaluation of potential partners, we have selected Itek of Lexington, Mass. as our industrial partner for the instrument.

Also appended is a recent paper on a small astrometric interferometer named for Simon Newcomb. This is a spinoff of the POINTS work and is now the subject of a collaboration between SAO and the Naval Research Laboratory. "Newcomb" is intended for the Navy's Space Test Program, which is a fast-track low-cost program for technology development and evaluation. Under the established division of labor, SAO will be responsible for the instrument. Itek is designated as our industrial partner for the Newcomb instrument. NRL will build (or possibly buy) the spacecraft and do the integration. The Space Test Program will provide the launch.

POINTS: the first small step

R.D. Reasenberg, R.W. Babcock, M.C. Noecker, and J.D. Phillips

Smithsonian Astrophysical Observatory
Harvard-Smithsonian Center for Astrophysics

ABSTRACT

POINTS, an astrometric optical interferometer with a nominal measurement accuracy of 5 microarcseconds for the angle between a pair of stars separated by about 90 deg, is presently under consideration by two divisions of NASA-OSSA. It will be a powerful new multi-disciplinary tool for astronomical research. If chosen as the TOPS-1 (Toward Other Planetary Systems) instrument by the Solar-System Exploration Division, it will perform a definitive search for extra-solar planetary systems, either finding and characterizing a large number of them or showing that they are far less numerous than now believed. If chosen as the AIM (Astrometric Interferometry Mission) by the Astrophysics Division, POINTS will open new areas of astrophysical research and change the nature of the questions being asked in some old areas. In either case, it will be the first of a new class of powerful instruments in space and will prove the technology for the larger members of that class to follow. Based on a preliminary indication of the observational needs of the two missions, we find that a single POINTS mission will meet the science objectives of both TOPS-1 and AIM.

The instrument detects a dispersed fringe (channelled spectrum) and therefore can tolerate large pointing errors. In operation, the difficult problem of measuring the angular separation of widely spaced star pairs is reduced to two less difficult problems: that of measuring the angle between the two interferometers and that of measuring interferometrically the small offset of each star from the corresponding interferometer axis. The question of systematic error is the central theme of the instrument architecture and the data-analysis methods. Stable materials, precise thermal control, and continuous precise metrology are fundamental to the design of the instrument. A preliminary version of the required picometer laser metrology has been demonstrated in the laboratory. Post-measurement detection and correction of time-dependent bias are the essential elements in data analysis. In that post-measurement analysis, individual star-pair separations are combined to determine both the relative positions of all observed stars and several instrument parameters including overall time-dependent measurement bias. The resulting stellar separation estimates are both global and bias-free at the level of the uncertainty in the reduced (*i.e.*, combined and analyzed) measurements.

1. INTRODUCTION

New technologies have made possible construction of ground-based and space-based optical interferometers that could make routine observations of high scientific value. Early versions of the ground-based instruments are now working or near completion. However, ground-based interferometers and telescopes jointly suffer two classes of restrictions: (1) Observations are made through a turbulent atmosphere with limited windows of visibility; and (2) The platform (Earth) rotates slowly, necessitating compensatory pointing, restricting the portion of the sky that can be observed at one time, and setting the time between observations of points well separated on the sky. These restrictions are removed when the observations are made from space, where several optical interferometers can be expected during the 21st century. We expect that most of the starlight interferometers in space will be imaging devices on a grand scale, with corresponding price tags. Because they represent a new and complex technology, these "greater observatory" class instruments are not likely to be flown without the benefit of a smaller, less expensive precursor instrument such as POINTS.

POINTS, a space-based astrometric optical interferometer with a nominal measurement accuracy of 5 microarcseconds (μas), will be a powerful new multi-disciplinary tool for astronomical research.[1,2] The instrument includes two separate stellar interferometers that have their principal optical axes (nominal target directions) separated by φ, an adjustable angle of about 90 deg. (See Fig. 1.) Since the targets are within a few arcsec of their respective interferometer axes, off-axis distortions and the attendant biases are minimized. In each interferometer, the starlight leaving the beamsplitter is dispersed to form a "channelled spectrum," which gives the instrument an enhanced tolerance of pointing error, especially helpful during target acquisition. A single measurement determines the angular separation of a pair of target stars. Each interferometer has a baseline 2 m long, and two afocal telescopes with 10:1 compression. The two interferometric subapertures of each starlight interferometer are 25 cm in diameter. Our studies of detectors and

mirror coatings show that about 20% of the photons entering the aperture will be detected. We find that the nominal 5 μas measurement uncertainty is reached after about one minute of observing a pair of mag 10 stars. By design, the largest error component is the photon statistics of the starlight. Based on present models of slew, acquisition, and data collecting times, we estimate that POINTS would observe about 350 star pairs per day if the targets were mag 10.

Since the interferometers are mutually perpendicular, the instrument naturally performs global astrometry, which was first practiced by HIPPARCOS, and which provides three advantages: (1) Instrument bias can be routinely determined by 360 deg closure. Thus, for reasonable observing sequences, one obtains a global reference frame that is free of regional biases to the nominal accuracy of the data. (2) Parallax measurements are absolute, not relative. (3) For a given target star, the reference star is chosen from the great-circle band of sky 90 deg away, maximizing the probability of finding a suitable reference. If the relative rotation range of the two interferometers is ±3 deg, this observable band has an area of 2160 square degrees (>5% of the sky) and can be expected to contain about 80 stars as bright as (visual) mag 5; 1200 stars, mag 7.5; and 17,000 stars, mag 10. Thus, the observation time is not dominated by the low photon rate of dim reference stars. Each reference star is a carefully studied target star, chosen from the reference grid described in Section 4.1. Thus the motions of the reference stars are well modelled and do not corrupt the measurements of other stars.

The instrument uses two kinds of metrology systems. The first is the full aperture metrology (FAM), which measures the optical path difference (OPD) in the starlight interferometers. In each interferometer, two laser gauges measure the starlight OPD and hold it fixed with respect to the "pseudobaseline" defined by a pair of "fiducial points." The second system uses these fiducial points to measure the angle between the pseudobaselines of the two starlight interferometers.

In FAM, modulated laser light is injected backward into the starlight optical path and fully illuminates the optical elements that transfer the starlight. The first element that encounters the starlight has a low-amplitude phase-contrast holographic surface. This holographic optical element (HOE) diffracts about 2% of the FAM light, and the samples of FAM light from the two sides of the interferometer are brought together to produce an error signal that drives a null servo. In the process, as discussed below, the "fiducial blocks" are surveyed into position. Each fiducial block contains four truncated retroreflectors, constructed such that their apices coincide with the fiducial point to within a few microns. Knowledge of the six distances defined by these four points determines the angle between the pseudobaselines of the two starlight interferometers.

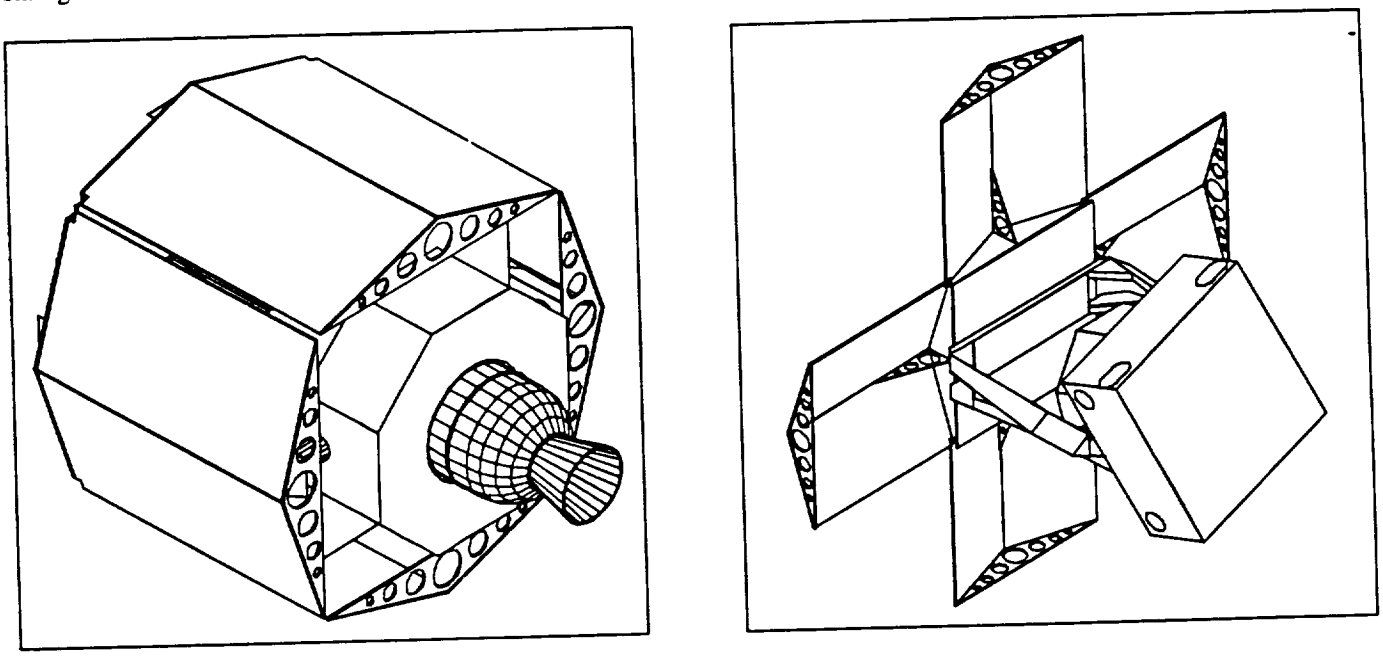

Figure 1. Proposed POINTS configuration. Left, stowed for launch. Right, operating. Not shown are four flexible triangular shields that connect the solar panels to complete the octagonal shield. *Note added in proof:* This version of the spacecraft is no longer under consideration. For the present spacecraft design, see the paper in these proceedings by Schumaker *et al.*[10]

The second kind of metrology system consists of a set of six point-to-point laser gauges that measure those six distances. The angle φ between the real baselines is the quantity of interest; the angle between pseudobaselines is measured. The small difference between these two angles depends in second order on the displacements of the targets from the nominal optical axes of the starlight interferometers and the skew between the baselines and the corresponding pseudobaselines. Thus, the measurement of one angle yields a biased determination of the other. The parameters of the bias are discussed in Section 2.4 and in more detail in the Appendix. The bias is estimated from the closure information in the astrometric data, as discussed in Section 4.

Section 2 contains a description of the instrument. The design of the spacecraft is discussed briefly in Section 3. Mission operations, including the bias determination and correction, are discussed in Section 4. For a brief review of the history of the project, see Reasenberg *et al.*[3] For a discussion of the critical laser gauge technology, see Noecker *et al.*[4] and Reasenberg *et al.*[3]

2. INSTRUMENT DESCRIPTION AND CONCEPT

2.1 Principles of operation

The principal elements of the POINTS instrument are two starlight interferometers, mounted at a nearly right angle, and a metrology system. The instrument determines θ, the angular separation between two widely separated stars, by measuring φ, the angle between the interferometers, and measuring independently δ_1 and δ_2, the offsets of the target stars from their respective interferometer axes. With proper selection of target stars and a small adjustment capability in φ (nominally $87 \leq \varphi \leq 93$ deg), a pair of stars can be brought simultaneously to within less than one arcsec of their respective interferometer axes. Once a target star is in the field of an interferometer, δ is measured through the analysis of the dispersed fringe which forms a channelled spectrum. A central feature of the instrument is the real-time monitoring of the angle between the interferometers and the metrology along the starlight optical path, each of which uses a laser interferometer scheme based on currently or soon-to-be-available technology.

In each of the two interferometers, the afocal telescopes compress samples of the starlight, which are directed toward the fringe-forming and detecting assembly. At the exit ports of the beamsplitter, the light is dispersed and focused onto a pair of linear arrays of detectors. When the star is on axis ($\delta = 0$), the signal at any given wavelength has equal intensity at the two beamsplitter exit ports. When the star is off axis ($\delta \neq 0$), constructive interference for a given wavelength at one port is complemented by destructive interference at the other port. At each port, an alternating pattern of constructive and destructive interference is observed. The resulting complementary channelled spectra form the basis for determining δ. Since the detectors in the array see narrow, contiguous portions of the optical spectrum, there are effectively a large number of narrow-band interferometers that collectively make use of all of the light. Because of their small bandwidths, these interferometers can function when the instrument is pointed several arcsec from the target. However, to keep the fringe visibility high, it is desirable to keep the pointing offset small compared to δ_N, the Nyquist angle, at which there are two detector pixels per fringe.

The channelled-spectrum approach has two distinct advantages over a system in which a single detector measures the white light fringe. In the latter system, the pointing error would have to be under 0.05 arcsec during observations (unless an active system of path compensation were included); white light fringe detection would require an oscillating mirror to modulate the OPD (say at sonic frequency). The fringe visibility would be substantially reduced at 2 arcsec, making the initial acquisition of the fringe more difficult. Thus, the use of the dispersed fringe greatly simplifies the pointing system and removes the need for the motion of major parts (*i.e.*, delay line) during an observation, which would add mass and complexity and reduce reliability. The second advantage of the dispersed fringe approach is that there is additional information available in the channelled spectrum. This information can be used to separate targets that are closely spaced and might otherwise be confused, such as members of a binary system. An instrument utilizing this technique exclusively was proposed by Massa and Endal.[5]

2.2 Detectors and instrument pointing

There are three questions concerning detectors and pointing: (1) How far from the target direction can the instrument point and still detect the target? (2) What is the effect on the information rate of a pointing offset? (3) What is the limiting magnitude of the instrument? As $|\delta|$ is increased from zero, the number of fringes on the detector array increases, and the fringe visibility V decreases because each pixel averages over an increasingly large portion of a fringe.

The information content of the data is monotonic with V, both of which are zero at $\delta=2\delta_N$, where there is one fringe per pixel. The information content falls rapidly with decreasing V near V = 1, so the visibility must be kept high. A prism, like a diffraction grating (but in the opposite sense), provides a nonlinear dispersion so that, if the detector pixels are of uniform width, the number of pixels per cycle of channelled spectrum will vary with color. One solution is to combine a grating and a prism, as is being done for the IOTA ground-based interferometer.[6] An alternative approach, which is adopted for POINTS, is to use only a prism, allowing the pixel width to vary with the color and so avoiding the light loss of the grating. Below, we consider in turn the detectors, the spectrometer, limiting magnitude, and the fine pointing and isolation system.

As discussed below, we have found that the fringes can be held sufficiently stable on the detectors that an integrating detector such as a CCD can be used with little loss of fringe visibility due to motion during the integration period. CCDs offer high quantum efficiency, and there is a wide base of experience of their use in space, as well as continuing development. With a stabilized fringe integrated on the CCD detector, there is an automatic solution to the problem of data compression, which otherwise would require considerable on-board computation.[a] As presently envisioned, the CCD arrays will have 650 cells to cover an optical bandpass from 0.25 to 0.9 μm, and the nominal mirror coating will be aluminum.

The spectrometers, one for each exit beam, must disperse the starlight to produce the channelled spectrum while maintaining high fringe visibility. Three primary effects govern resolution and thus fringe visibility: diffraction, aberration, and detector pixel size. In the dispersion direction, the diffraction-limited spot must be $\lesssim$ 1/30 the spacing of the dispersed fringes in order to maintain high fringe visibility. Additionally, providing spatial resolution in the cross-dispersion direction might allow simultaneous acquisition of data on multiple targets in crowded fields. To improve the performance in crowded fields, a slit could be provided to eliminate light from stars too far off-axis to produce measurable fringes. This would require additional reflections and so reduce the single-star throughput. It has not yet been decided whether to include a slit.

So far, we have considered slitless designs in which the collimated beam from the starlight beamsplitter passes through the prism and is focussed onto the detector by a single off-axis mirror. These designs are characterized by three parameters: focal length, prism deviation range, and pixel size. A range of designs meet the resolution requirement, and we are currently determining what design best meets a range of secondary requirements including Nyquist angle δ_N, cross-dispersion resolution, dark current, sensitivity to detector position, the option to include a polarizing spectrometer, and suppression of scattered metrology light.

Limiting magnitude depends on dark current. We believe that present CCD's impose a limit somewhere between magnitudes 17 and 20. The two important factors for setting the limiting magnitude are detector temperature, currently expected to be around -80° C, and the area of detector in which the stellar spectrum appears.

In the present design, the instrument is connected to the spacecraft scan platform by means of a soft, single-axis pivot with a free swing range of several tens of arcsecs. A flexural pivot that would serve well as the basis for the isolator has been made by the Perkin-Elmer division that is now Hughes-Danbury Optical Systems (HDOS). (The pivot was flown as part of the Apollo Telescope Mount on Skylab, 1973-1974.[7,8]) There are several suitable magnetic actuators to provide fine pointing correction to the isolated instrument. The instrument mounted on the pivot would have a torsional resonance between 1/20 and 1/5 Hz.[b] Given such a soft mount, there would be considerable filtering at the detector sampling rate of 100 Hz, applicable to bright target stars.

---

[a] Consider an observation in which 10^7 photons are collected in 100 batches by one interferometer. Without compression, two numbers (epoch and detector number, about ten digits total) must be transmitted to the ground for each photon. Without stabilization and on-chip integration, the fringe must be rotated and integrated in software, requiring several floating point operations per photon in addition to the real-time filter. With stabilization and on-chip integration, there is little computation required for fringe tracking, and the telecommunication load without explicit compression is 2×10^4 numbers of five digits. It appears that a compression of at least 10 fold will be possible.

[b] There would need to be cables, *etc.* crossing the pivot, and these would add to the stiffness by an as yet undetermined amount; this is the principal uncertainty contributing to the stated possible range of the frequency.

The present scheme requires that at least one target be bright, say mag 10. Initially, a star tracker would be used to find the bright target and the approximate rotation rate of the instrument. This information would be used to reduce the offset and rotation rate to below the threshold for detecting starlight fringes. Once the fringes were found, they would serve as the reference for the fine pointing. On a mag 10 star, with a sample rate of 100 Hz, the samples would have a statistical uncertainty of ≈300 μas. However, the use of one of the interferometers as the angular reference requires real-time data analysis and the corresponding on-board computational capability. The 100 Hz sample rate probably limits to ≈10 Hz the unit-gain frequency of the control loop for the orientation of the instrument.

2.3 Internal measurements and systematic error

The control of systematic error is central to achieving the stated instrument performance and the mission science objectives. We address this problem at three levels: (1) stable materials and thermal control; (2) real-time metrology; and (3) the detection and correction of systematic error in conjunction with the global data analysis. The last of these is addressed in Section 3.4. The best materials fail by orders of magnitude to provide the long-term dimensional stability required to maintain each interferometer's OPD and other critical dimensions, in the absence of other means of control. Stable materials for the structural elements of the instrument serve to limit the dimensional changes that the metrology system must determine, and to control errors that are second order in component displacements. In a few places, we are forced to rely on material stability (over short times). The instrument is designed so that such metering elements are small, and can be thermally isolated and regulated.

For a 2-m baseline, the nominal 5-μas uncertainty corresponds to a displacement of one end of the interferometer toward the source by 0.5Å = 50 pm (picometer = 10^{-12} m). Since similar displacements of internal optical elements are also important, the instrument requires real-time metrology of the entire starlight optical path at the few picometer level. This metrology does not pose an overwhelming problem for two reasons. First, the precision is needed only for averaging times between 1 and 100 minutes. Second, a slowly changing bias in the measurement is acceptable, as discussed in Section 3.4.

The instrument relies on two kinds of laser-driven optical interferometers to determine changes in critical dimensions. New concepts and technology have been required for these interferometers to obtain picometer accuracy. The laser gauges *per se*, a new application for a HOE, and the laser-gauge endpoint assemblies were invented during the development of POINTS. The laser gauges can be grouped according to whether they measure distances internal to a starlight interferometer or distances between starlight interferometers. Below, we consider the former. In the next section, we consider the latter and some related questions of instrument geometry (the relation between the baselines and the pseudobaselines) and measurement bias.

The high-precision star position measurement is made with respect to the optical axis of the interferometer by measuring the difference in the optical paths from the target to the beamsplitter *via* the two sides of the interferometer. In turn, the position of this axis is determined (defined) by the positions of the optical elements used to transfer the starlight. The metrology system must determine, to about 10 pm overall accuracy, the average change in the starlight OPD's induced by all motions and distortions of all optical elements. Our approach is to use FAM, a novel technique discussed below. FAM provides three significant advantages over conventional approaches.

(a) FAM removes complexity. The usual metrology systems use a large number of laser gauges to determine the locations of the elements individually. From these measurements, the optical path through the system is computed. FAM directly measures the optical path through the system.

(b) FAM measures the correct quantity. Because the metrology signal fully illuminates the surface of each optical element that determines the starlight OPD at the beamsplitter, the metrology OPD represents accurately the average starlight OPD through the system.

(c) FAM provides the basis for an operational definition of the direction of the interferometer baseline. It measures the OPD with respect to a pair of fiducial points that define the pseudobaseline, which is located in front of each interferometer and which is held at a small fixed angle (nominally zero) to the real interferometer baselines. These fiducial points are used to determine φ, the angle between the two interferometers' optical axes. (The small bias resulting from the angle between the pseudobaseline and the real baseline is determined routinely as part of the data analysis.)

Figure 2 illustrates the preferred version of the technique. The key element is the set of primary mirrors which have shallow (phase contrast) zone plates on their surfaces: alternate zones are depressed about 100Å. In this HOE, the zones are approximately in the form of Newton's rings; each zone has about the same total area. For the flight hardware, we would manufacture the HOE by a method that would provide the required spatial dependence of diffractive efficiency. The needed binary pattern would be found numerically and used to make a mask such as is used in the manufacture of integrated circuits. The mask could be written on a master plate by an "e-beam machine" or a "laser lathe." Each mirror would be given a thin (ca. 100Å) coating of metal and contact printed using photoresist and metal etching. Finally, the optic would be given a reflective coating. This technique has been used for many years at Hughes-Danbury Optical Systems, Inc. (HDOS) in support of DoD projects.

It is important that the thickness of the metallic layer on the optic match the desired radial profile to perhaps ½%, as the diffractive efficiency is proportional to the square of zone thickness in the intended regime. The radial variation is required to compensate for the intensity variation of the metrology beam, which is roughly Gaussian. To achieve the required accuracy, it may suffice to deposit material under carefully controlled conditions, with masks to achieve the desired radial variation. A densitometer could be used to measure the thickness variations, as the coating will have an optical depth of order 1. It may also be possible to use Plasma-Assisted Chemical Etching, an HDOS process, to correct the profile after deposition.

In the traditional FAM system, modulated laser light is injected backward into the starlight optical path and fully illuminates the optical elements that transfer the starlight. The hologram diffracts about 2% of the FAM light, and the samples of FAM light from the two sides of the interferometer are brought together at the metrology beamsplitter to produce an error signal that drives a null servo. In the process, the fiducial blocks are surveyed into position. Each fiducial block contains four incomplete hollow cornercube retroreflectors, constructed such that their apices coincide at the fiducial point to within a few microns. Knowledge of the six distances defined by these four fiducial points determines the angle between the pseudobaselines of the two starlight interferometers. There is a substantial advantage to making the FAM laser light travel in the same direction as the starlight.[9] We are investigating the principal disadvantage to this variation, that laser light will be scattered into the starlight detectors.

The FAM technique requires two principal servos. The laser beams diffracted from the HOE's in the two arms of the interferometer are recombined at a metrology beam splitter; this is a Mach-Zehnder interferometer configuration, which is sinusoidally sensitive to the length difference from beam splitter to beam splitter *via* the two paths. A servo regulates this path difference to a constant value by moving the starlight beamsplitter assembly. A second laser beam injected into the metrology beam splitter parallel to the FAM beams similarly measures the difference in distances from that beam splitter to each of two corner cube retroreflectors situated in the fiducial blocks; this auxiliary servo regulates that path difference to a constant value by moving the auxiliary beamsplitter assembly. With both servos working, there is a small (under 1 mm) and constant difference between the distances from the starlight beamsplitter to the fiducial points, which are the apices of the retroreflectors inside the fiducial blocks. These servos can have small bandwidths because the time scale for distortion is long compared to a second, and because we require that vibrations of the OPD be small enough that they need not be tracked. Since it is desirable to limit the contamination of the starlight by the laser signal (*e.g., via* scattering from the surfaces of the optical elements), a minimum of laser light is used in the FAM servo.

We have shown that a change in the distance between the telescope primary and the athermal collimating lens has an effect on the FAM OPD that is about 0.7% of the change of distance. For this reason, we introduce a third servo related to FAM that moves one (or both) of the fiducial blocks. (Note that if both fiducial blocks are moved in equal and opposite directions, the two overlapping illuminated regions on the auxiliary beamsplitter move in the same direction.) The sensor for this focus servo is a laser gauge that measures the difference of the distances from the auxiliary beamsplitter to the telescope primary mirrors. With the auxiliary servo working, the focus servo measures the differential distance from the fiducial points to the primary mirrors. Note that the fiducial point is several cm from the athermal lens. This distance, which must be stable to be about 0.1 nm, is metered by the body of the fiducial block, which is quite stable, as discussed below.

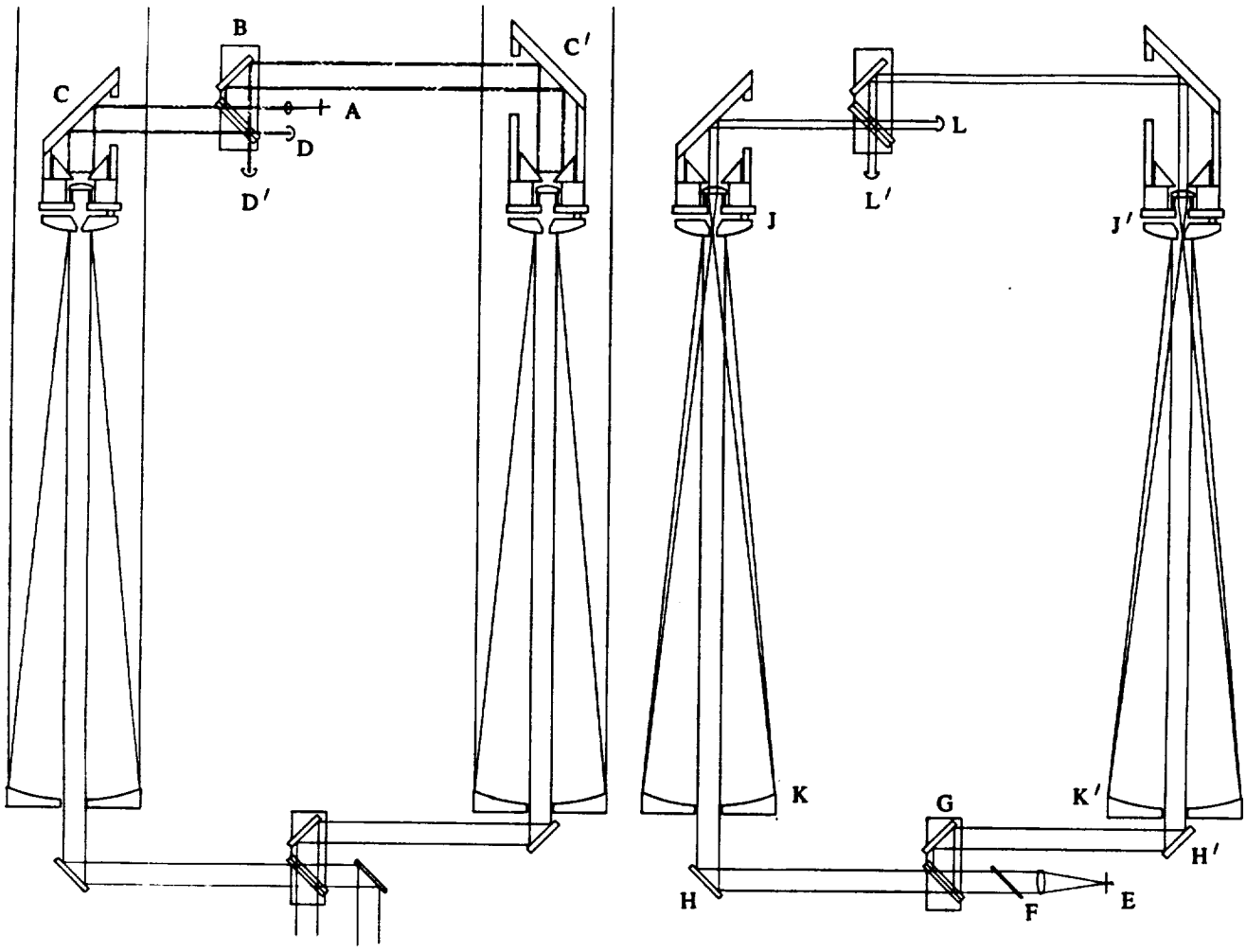

Figure 2. Interferometer optical paths. (left) Starlight and auxiliary null interferometer. For the latter, a laser signal passes through the spatial filter A and is divided by the metrology beamsplitter B to form beams that enter the fiducial blocks C and C′. Within each fiducial block, the beam is deflected by the 45° mirror, retroreflected by the hollow corner cube, and returned toward the metrology beamsplitter by the 45° mirror. The returning signals are combined at the metrology beamsplitter and fall on detectors D and D′. The metrology beamsplitter may thus be referred to the cornercube apices. (right) FAM interferometer. A laser signal passes through the spatial filter E and injection beamsplitter F and is divided by the starlight beamsplitter G. The separated beams are reflected from the tertiary mirrors H and H′ and secondary mirrors J and J′ to fully illuminate the primary mirrors K and K′. The zone plates on the primaries diffract a small proportion of the metrology light to focal points in the holes in the secondaries, and the athermal lenses collimate the diffracted light. Finally, the signals are reflected from the 45° mirrors, are recombined at the metrology beamsplitter, and fall on detectors L and L′. The starlight beamsplitter may thus be referred to the metrology beamsplitter *via* the starlight optics, and thence to the cornercube apices. *Note added in proof:* In the present design, the FAM light is injected at the auxiliary beamsplitter and travels in the same direction as the starlight. See the paper in these proceedings by Noecker *et al.*[4]

The fiducial blocks (Fig. 3) and the metrology beamsplitter assemblies pose the only critical materials problem identified. To minimize changes of the size or shape of either of these, which would cause a corresponding changes in the bias of the metrology system, they will be made of a stable material and kept in a thermally stable environment. For the fiducial blocks, we plan optically contacted Premium ULE®; the beamsplitter material is still under study. The effective separation of metrology links within the fiducial blocks would be under 10 μm, and the temperature would be held stable to 10^{-2} deg C on a time scale of a few hours. The effects of temperature fluctuations on a longer time scale will be routinely removed during the analysis on the ground of the astrometric data. The thermal gradient will be reduced by putting a pair of nested aluminum cylinders with 1.5 mm walls around the fiducial block. We plan to achieve the required thermal stability with active control of the outer skin of the fiducial block enclosure to 10^{-1} deg C (although 10^{-2} deg C does not seem difficult), and with polished facing surfaces on the outside of the inner cylinder and the inside of the outer cylinder. The poor radiative heat exchange between the cylinders, combined with the heat capacity of the fiducial block and inner cylinder, will yield a thermal time constant of about one day. Using Premium ULE®, which has a linear coefficient of thermal expansion $|\alpha| < 5 \times 10^{-9}$/deg C in a range from 5 to 35 deg C, the resulting distance error would be $\leq 10^{-3}$ pm. More important would be the effects of thermal gradients of up to 10^{-3} deg C over the ≈ 5 cm separation of metrology beams where they reflect from the fiducial block mirrored surfaces. Such gradients would produce a measurement bias under 1 pm, again within the required limit.

In the manufacture of the fiducial blocks, the critical concern is for the alignment of the "retrostrips," which are sections of hollow corner-cube retroreflectors. (See Figure 3.) Each fiducial block has four retrostrips, each of which must be assembled onto the main body from three small pieces of glass, using optical contacting, glue a few μm thick, or wetting with a thin layer of indium. Each retro has a symmetry axis that must point in approximately the correct direction and all four apices must be collocated to within a few microns. We now envision a manufacturing jig that manipulates and holds the three small pieces of glass in position on the main body. During assembly, the jig would permit the unit to be rotated on precision bearings, perhaps air bearings. The alignment procedure calls for the retrostrip under assembly to form one part of an interferometer using laser light. Under rotation, the changing fringe pattern would indicate misalignments of the three small pieces of glass. Algorithms have been developed for converting the interferometer fringe pattern into corrections to be made to the positions of the three small pieces of glass. The interferometric measurement is not expected to limit the accuracy of the alignment of the retrostrips. The precision bearings, which should have sub-micron runout, and the devices used to position the small pieces of glass will probably set the limit to the alignment.

2.4 Determination of φ

The angle φ between the pseudobaselines of the two interferometers (*i.e.*, the instrument articulation) is determined by the measurements of the six distances among four fiducial points in the system.

$$\cos\varphi = (d_2^2 + d_3^2 - d_1^2 - d_4^2) / 2b_m b_f$$

Here d_i are the four distances between the fiducial points of one interferometer and the fiducial points of the other and b_m, b_f are the baseline distances for each interferometer, *i.e.*, each is the separation of the fiducial points of one interferometer. Each of the six distances is measured by a laser gauge. (The laser gauges *per se* are discussed by Noecker *et al.*,[4] who note that the techniques we have developed easily extend to an absolute distance gauge.) We have investigated the problems associated with the laser gauges reading the distance correctly except for a fixed bias, as would be the case if an incremental gauge were used and the zero point determined crudely by alternative means (*e.g.*, by an encoder on the articulation axis or from the known positions of bright stars observed by startrackers mounted on the interferometer optical benches.) Under these conditions, there would be an additional five parameters of the system that would need to be determined from the astrometric data each time the laser gauges were turned on. Nominally, this would be at the start of the mission only. Our covariance studies show that estimating these parameters poses no problem even if it were decided to estimate them *ab initio* as often as every day.

The metrology system measures the angle between the pseudobaselines, which are defined by the pairs of fiducial points in the two starlight interferometers. The two (nearly) perpendicular pseudobaselines define the "interferometer plane." For simple analyses, we assume that each starlight interferometer lies in the interferometer plane. However, we have considered the effects of the three small rotations of each of the starlight interferometers: (1) around the perpendicular to the interferometer plane; (2) around the pseudobaseline; and (3) around the starlight interferometer's nominal optical axis. The first type of rotation yields a bias proportional to the difference of the rotation angles. This

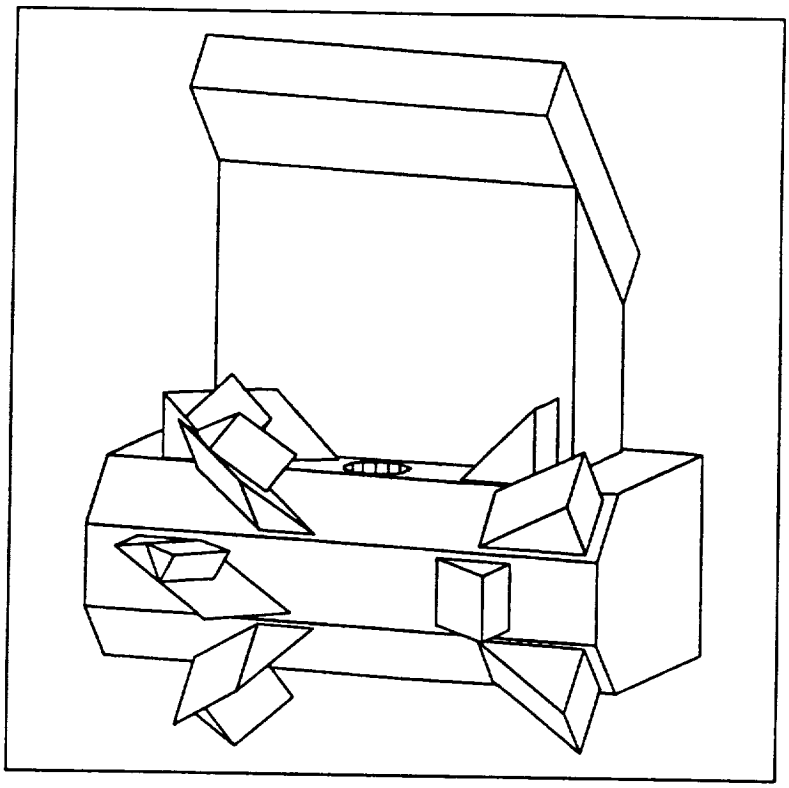

Figure 3. A fiducial block. There are four "retro-strips," each a slice of a truncated cornercube retroreflector, and each to serve as the end point for a laser gauge. The apices of the cornercubes coincide at the fiducial point in this computer-generated engineering sketch.

bias is directly observed and held stable by the laser gauges and then estimated and removed in the data analysis. The other four rotations (two for each starlight interferometer) do not contribute to the measured angle in first order, but do contribute in second order. Thus the latter two types of rotations need to be aligned to somewhat better than an arcsec. - For further discussion, see Appendix. In a related study, we are considering how the above rotations and skews could come about from misalignments of the optical elements of the starlight interferometers.

Although the above described metrology system is capable of providing the required precision, it contains many finite-size optical components, each of which will introduce a bias into the measurement of the angle φ. This bias is likely to be time dependent at the microarcsec level. It is essential that we be able to determine and correct for the instrument bias, preferably without the introduction of additional hardware. Because POINTS, like HIPPARCOS, does global astrometry, that bias determination and correction naturally occur when the observations are combined in a least-squares estimate of the individual stellar coordinates (including proper motion and parallax), instrument model parameters, and the expected biases. In particular, our covariance studies have shown that even without the introduction of a special observing sequence, it is possible to estimate simultaneously the stellar coordinates and tens of instrument bias parameters per day. The stellar coordinate estimate uncertainties increase by a factor of $1+0.003\ N_b$, where N_b is the number of bias parameters to be estimated per day, and $M = 5$. (The redundancy factor, M, is defined in Section 4.1.) Thus, metrology biases and related errors can be allowed to change on a time scale of hours without significantly degrading the performance of the instrument. This result allows us to relax the required stability at time-scales longer than 100 minutes of both the laser used in the metrology and the rest of the instrument. This subject is also discussed in Section 4.

3. SPACECRAFT DESIGN

The POINTS spacecraft will contain the usual set of systems to support the instrument: telecommunications, attitude control, power, and computation. Pointing interferometers at each of two stars requires control of rotation about four axes. One axis is provided by relative articulation of the interferometer axes. The instrument will be articulated

with respect to the solar shield with a two-axis drive. That articulation will be constrained by the requirement that the Sun shield keep the instrument housing (and preferably also the bus) in shadow at all times. The fourth axis is provided by rotating the spacecraft-plus-instrument about a line to the Sun. The spacecraft bus may require an isolator to keep jitter from entering the instrument from the spacecraft. For a more detailed description of the spacecraft see Schumaker *et al.*[10]

Within the instrument, there is an articulation mechanism that sets φ. This mechanism must permit about 0.1 radian of motion and should have a resolution of order 0.1 arcsec: 2×10^5 steps. Of course, during observations, the combination of the articulation pivot and drive must be stiff in all six degrees, especially in the rotation that changes φ.

The instrument is kept behind a solar shield, which is important in permitting large coverage of the sky without exposing the instrument interior to the direct light of the Sun. The solar cell array is mounted on portions of that shield. During launch, portions of the shield are folded along the spacecraft to fit inside the launch shroud. They provide limited power during the 17 hour cruise from parking orbit to the 100,000 km altitude at which the orbit is circularized.

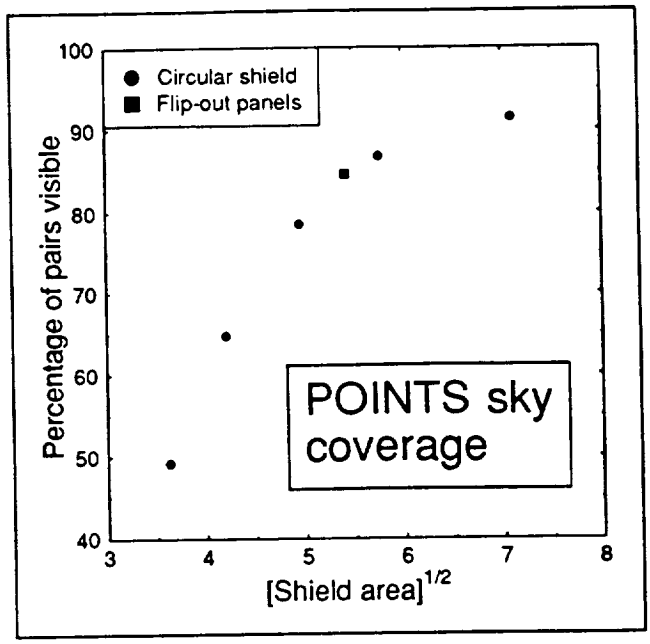

Figure 4. Fraction of star pairs with 90° separation visible to POINTS at any epoch.

The question of sky coverage is normally considered in the context of an instrument with a single pointing direction and exclusion angles for the Sun, Earth, and Moon. For POINTS, the problem is more complicated because the instrument needs to look simultaneously in two directions about 90 deg apart. Thus it takes four angles to describe the phase space of the sky coverage. For the purpose of calculating sky coverage, we constrain the target separation to be 90 deg, reducing the number of independent angles to three. We may neglect both the Earth and Moon exclusions since we are willing to wait a few hours for any particular measurement. (The nominal orbit is circular at 100,000 km, which has a four day period.) Thus we are left considering only the spacecraft and the Sun. The line between them is an axis of symmetry. Rotation about that axis can be neglected in discussion and analysis of sky coverage; there are only two nontrivial angles.

In our sky-coverage study, the first parameter was $\cos(\gamma)$, where γ is the angle between the anti-Sun direction and the first star, as seen from the spacecraft. The second parameter was ω, the Sun-star1-star2 angle on the celestial sphere centered on the spacecraft, *i.e.*, the angle between the planes defined by: (a) spacecraft, Sun, and star1; and (b) spacecraft, star1, and star2. The study maps out the portion of phase space that is accessible. With this choice of parameters, the area in the "$\cos(\gamma)$ - ω plane" is proportional to the volume of phase space. With the nominal configuration, 83% of phase space is accessible at any one time, and stars in 99.1% of the sky can be observed, but some with a limited range of ω. (Stars in 98.5% of the sky can be observed with a cumulative range of ω of at least 180 deg.) In all cases, the stars or star pairs that cannot be seen at a particular time can be seen a few weeks earlier or later.

The original work has been extended to address the relationship between the available volume of phase space and the size of the solar shield. As shown in Fig. 4, increasing the size of the shield increases the sky coverage for shields similar in size to the nominal, which has a 30 m^2 area. However, saturation of sky coverage is found for shields with diameters larger than about 7m.

4. MISSION OPERATIONS

Here we consider five aspects of mission operations: normal operation of the instrument, the effect of a faint companion, data analysis, the search for other planetary systems, and in-orbit testing. We do not discuss detailed target selection since there is an overabundance of interesting targets and the actual selection will depend strongly on which division of NASA/OSS sponsors the mission.

4.1 Normal instrument operations

Our understanding of the characteristics of the instrument's operation is based on a series of covariance studies and simulations. Since POINTS is a "global astrometric instrument," all well-observed objects can and will be made to contribute to the stability of the reference frame used for each observation. In turn, each object that contributes to the reference-frame stability can and will be studied astrometrically and its motions modelled. A small number of observations of quasars will connect the POINTS reference frame to the best available candidate for an inertial frame. Table 1 lists the number of BL-Lac objects, quasars, and Seyfert galaxies of magnitude 15 or brighter from the catalog of Veron-Cetty and Veron.[11] Finally, because of the ≈ 90 deg separation of the target pair, for any target there are always several bright reference stars among the set of well studied objects.

Table 1. Number of reference objects of magnitude m or brighter

m	NUMBER OF OBJECTS		
	BL-Lac	Quasar	Seyfert
10	1	0	0
10.5	1	0	0
11	6	0	0
11.5	9	0	0
12	23	0	0
12.5	38	1	1
13	61	2	1
13.5	99	5	3
14	166	13	5
14.5	266	23	7
15	381	49	15

Our performance analyses assume the target to be an isolated, unresolved point source, *i.e.*, one with no significant structure. In practice, this condition will not always be met. Star spots, flares, *etc.* will set the limit to the accuracy of the astrometric measurement of the center of mass of some targets. We may gain useful information about some stars from the motions of their centers of light. At 10 pc, the Sun has a magnitude of 5. A shift of its center of light by 0.1% of the Sun's diameter, which is the largest one expects from sunspots, would cause an apparent astrometric shift of nearly 0.5 μas. For some active stars, the effect is much larger. The effect of a companion star is addressed in Section 4.2.

When an observation set has sufficient redundancy, it can be analyzed to yield a rigid frame; it serves to determine the angular separation of all pairs of observed stars, even those that were not observed simultaneously. The redundancy is measured by M, the ratio of the number of observations to the number of stars observed, which must be greater than about 3.5 to yield a rigid frame. With moderate redundancy (M=4.2), the uncertainty in the separation of all star pairs (a majority of which could not be observed directly because they are not separated by ≈ 90°), is about equal (on average) to the instrument measurement uncertainty. The grid is free of regional biases and may be further strengthened by additional data obtained when the grid stars are used as reference stars for additional science targets.

If we use 300 grid stars plus a few quasars and take M = 5, then the observation series requires about five days at the nominal rate of 350 observations per day. Such a series could be repeated four times a year to provide not only coordinates but proper motions and parallaxes for the stars. Our Monte Carlo covariance studies show that after ten years the coordinate uncertainties are ~0.6 μas, the proper motion uncertainties are ~0.2 μas per year, and the parallax uncertainties are ~0.4 μas.[12,13] Note that this parallax determination is a factor of 2 better than one would naively calculate from the coordinate uncertainties in a single series. The reason for this enhancement is that the 90 deg nominal angle of POINTS results in direct observations of "absolute parallax."

Recall that in Section 2.4 we noted that instrument biases can be determined from the analysis of an astrometric data set by virtue of the closure information it contains. The analysis would include a time-dependent bias model for each observing sequence such that the residual bias would be small compared to the measurement uncertainty. The appropriate form of the bias model will depend on a detailed understanding of bias mechanisms that we expect to acquire in later stages of design. Exploratory studies during the mission will be aimed at uncovering any bias mechanisms not identified before launch. The operational bias model will be augmented accordingly. All the recorded data from the mission may be re-analyzed at any time using a new bias model.

In other Monte Carlo covariance studies, we investigated the ten-year observing sequence with fewer observations. We found that observations can be deleted from the series by a variety of random or systematic procedures yielding an increase in the mean parameter-estimate uncertainty which depends principally on the square root of the total number of observations. Further, additional stars can be added to the observation sequence with a minimal number of observations (perhaps 20) per star.

4.2 Faint companions and immunity from biasing signals

Some target stars will be undetected binaries. (The statistics of star densities on the sky indicate that accidental companions close enough and bright enough to have a biasing effect are too rare to be of interest except in particularly dense star fields, *e.g.*, globular clusters.) We have shown that: (a) If the separation between the stars is small compared to the resolution of the interferometer baseline ($\lambda/L \sim 0.05$ arcsec), then the instrument tracks the center of light; (b) A well separated companion is ignored. For an unexpected companion one magnitude fainter than the target, at a 1 arcsec separation (in the interferometer plane) the biasing effect is small compared to the nominal measurement accuracy, and; (c) Between these extremes, the offset of the apparent position of the target from its true position varies as a sinusoid (of generally decreasing amplitude) in the star-pair separation.

The above analysis assumed the star and its companion were modelled as a single source, and that they had the same temperature -- a worst case. If the separation is comparable to or greater than the resolution of the interferometer baseline, or if the two stars have known different spectra, then their separation can be determined from the distortion of the channelled spectrum. With measurements of a known binary against several reference stars, the accuracy of the separation measurement is only slightly worse than would be obtained for the position of the dimmer star if the companion were absent. Equally important, the distortion of the channelled spectrum will reveal that the source is a previously unknown binary so that biased measurements can usually be avoided. Finally, we note that if the channelled spectra are preserved and if a previously undetected binary is revealed, the old data can be reanalyzed to removed the bias due to the companion.

4.3 Data analysis, iterative and global nature

Although the mission will support a large and diverse set of science objectives, we picture much of the data analysis as being done centrally because one worker's target is everybody's reference star. The effort required will depend on the degree to which we need to use spacecraft engineering data to help understand systematic errors. In any case, it is not a complex effort nor does it require special computing facilities. If the data were available today, the central analysis could be done on a desk-top workstation. The effort would require a single analyst and would result in a reduced dataset that would be sent to the participating scientists for further analysis leading to publishable results.

Early in the mission, the analysis will be limited to positions determined during observing periods of a few to a few tens of days. Of course, the best *a priori* proper motions and parallaxes will be included in the analysis model although these will have little effect. Timely analysis early in the mission will permit instrument problems to be detected without undue loss of data. At about one year, it will become possible to estimate the full set of five parameters (position [2], proper motion [2], and parallax [1]) for each star. The stability of the solution should increase considerably during the second year.

After about two years of observation, the postfit residuals from the data reduction will be used to investigate irregularities in the motions of individual stars. Their apparent motions will be analyzed both for the intrinsic scientific interest and to improve the stability of the resulting reference frame. Initially, the position of each star will be determined with respect to the mean of the positions of all the stars. After the initial modeling of the irregularities in stellar proper motions, the position of each star will be determined with respect to the nominal modelled reference positions of all the stars. Based on recent Monte Carlo covariance studies, we know that this iterative procedure converges quickly. The global motion of the frame will be measured against the quasars included in the set of observed objects.

4.4 Planetary system detection

If there are Jupiter-size bodies orbiting nearby stars, the astrometric wobble seen from the solar system will be two orders of magnitude larger than the POINTS single-measurement uncertainty. However, the wobble will be distinguishable from proper motion only when the observations span a significant fraction of an orbital period. We performed Monte Carlo mission simulations with single planets around stars of the reference grid. Planets orbiting stars not in the grid should be an easier analysis problem because omitting them from the model will not distort the reference grid solution. Preliminary studies confirm that multiple-planet systems will make greater demands on the observing system and the data analysis. (However, note that observing the solar system from outside, the main signature would be from Jupiter. Saturn's longer period produces a signal similar to proper motion, and the signals from Mars and Earth are too small to detect with POINTS unless the system is both very nearby and heavily-studied.) This subject will require further study.

In the first simulations, it became clear that knowing the right answer made the analyst's task much easier. To make the simulations more realistic, we developed a "double blind" methodology. 100 nearby stars were selected from the catalogs to serve as hosts for the fictitious planets for all simulations. A person other than the analyst would prepare an input file for the simulation program. The file contained a "seed" for the random number generator and ranges for mass, radius, eccentricity, and number of planets. Until a simulation was completed, no one knew how many planets were included or which stars they orbited, and the analyst didn't know what ranges of the parameters were used for the simulation.

Searching for planets is an iterative procedure. The analysis procedure identifies candidates for planet modelling and optimizes parameters to minimize the RMS error. Since this is not a linear system, these two tasks interact. Initially, the model includes only star coordinates, parallaxes, and proper motions. Postfit residuals for observations involving each star are examined for power at a comb of frequencies. The largest signals flag candidates for planet modelling in the next iteration. But, since a star may be measured against one or more stars which have unmodelled companions, power in the residuals does not always correspond to a real planet. Fortunately, the procedure is robust; spurious planet models converge to near zero mass or otherwise reveal themselves as the iterations proceed.

Simulations had a 100-star grid and 20-50 planets with signatures ranging from 0.002 to 1 "Jove"[c] and periods of 1-20 years. A mission lasted 10 years, and all observable star pairs were observed quarterly with the articulation range set to yield M=5. Planets were detected with greater than 90% probability for signatures between 0.01 and 0.05 Jove, and with 100% above 0.05 Jove; sensitivity dropped rapidly below 0.01 Jove. All six orbital elements could be determined in 80% of the cases with signatures larger than 0.01 Jove. Where not all orbital elements could be determined, generally the observing geometry was edge-on or the orbital period was substantially longer than the mission length. Detections were reliable; there were no false alarms in the studies.

4.5 In-orbit testing and performance verification

There are three approaches to the in-orbit evaluation of the instrument. On the shortest time scale, a few pairs of stars will be chosen as calibrators. They will be observed regularly to provide a measure of short-term reproducibility of the measurements. Throughout the mission, the instrument bias will be estimated. The history of the estimated bias will be compared to pre-flight engineering estimates of its characteristics. Additional least-squares solutions for astrometric parameters and biases will be obtained with an enlarged bias set as a means of uncovering unexpected instrument behavior. Finally, the postfit residuals from the analysis will be a measure of the performance of the instrument. Astrometrically uninteresting, isolated stars will be important in understanding the instrument performance.

5. ACKNOWLEDGEMENTS

The development of POINTS has been supported by NASA through Innovative Research Program Grants NSG 7176 and NAGW 1647 from OSSA and Grants NAGW 1355 and NAGW 2497 from the Solar System Exploration Division of OSSA. It has also been supported by the Smithsonian Institution both directly and through its Scholarly Studies Program. During the past few years, there has been a team working on POINTS under the leadership of B.L.

[c] A Jove is the astrometric wobble of the Sun due to Jupiter as seen from 10 pc.

Schumaker at the Jet Propulsion Laboratory. The JPL team has contributed in many ways to our understanding of POINTS and thus to the description in this paper. The authors gratefully acknowledge the careful preparation of the camera-ready text by S.A. Silas.

6. APPENDIX: HIGHER ORDER RELATIONSHIP OF MEASUREMENTS TO STAR-PAIR SEPARATION.

Each of the two POINTS starlight interferometers measures the offset δ of a target star from the interferometer's optical axis. In the simplest description, the separation θ of the targets is related to the separation φ of the optical axes of the starlight interferometers by those offsets δ_i, where i = 1,2.

$$\theta = \varphi - \delta_1 + \delta_2 \tag{A1}$$

By design, $\varphi = \pi/2 + \Delta$, where the absolute value of the articulation angle Δ is up to 3 deg. Here we develop the next level of approximation to θ, taking into consideration the effect of transverse instrument pointing errors and the differences between the orientations of the baselines and the corresponding pseudobaselines.

Each POINTS starlight interferometer has a pair of fiducial blocks, which serve to connect the end points of a set of laser gauges. In particular, each laser gauge ends in a hollow retroreflector on the fiducial block. The fiducial block design has the apices of the retroreflectors coinciding (to within a few microns) at the fiducial point. A fiducial point serves as a surrogate for the corresponding aperture; the pair of fiducial points in a single starlight interferometer define a pseudobaseline that by construction is very nearly the same as the real baseline, except for a translation, which is mainly in the direction of the interferometer's optical axis.

Let P_i (i = 1,2) be the pseudobaselines and $\hat{Z}_o$ the direction perpendicular to the "instrument plane" defined by

$$\hat{Z}_o = P_1 \times P_2/|P_1 \times P_2| \tag{A2}$$

The corresponding interferometer axes (pseudo-optical axes) are

$$\hat{A}_i = \hat{P}_i \times \hat{Z}_0 \tag{A3}$$

for i = 1, 2. The articulation angle φ is the angle between the unit vectors $\hat{A}_1$ and $\hat{A}_2$, both of which are in the instrument plane.

The real baseline B can be rotated from the pseudobaseline P as shown in Fig. A1, where ζ is the baseline rotation around the Z_o axis and ξ is the baseline skew toward the Z_o axis. For each starlight interferometer, we define an "interferometer plane." The interferometer axis Q is perpendicular to the true baseline. Since this leaves an unconstrained degree of freedom, we require the interferometer axis to be in the instrument plane. Then the interferometer plane is defined to contain both the interferometer axis and true baseline. The perpendicular to interferometer plane i has a direction $Z_i = Q_i \times B_i$.

Shown in Fig. A1 is the target-axis offset. The target is at T, and is related to the coordinate frames by the following arc lengths: β = UD, δ = QD, ε = DT, and ν = VT. The offset is described as an in-plane displacement δ, which is the quantity that the starlight interferometer measures, and ε, the displacement of the target T from the interferometer plane, which must be measured by other means. (The subscripts are dropped where it will cause no confusion.) The displacement of T from A can more simply be described by the spherical coordinates μ = AV and ν = VT. Below, μ and ν are found as functions of the small angles ζ, ξ, δ, and ε. In turn, θ is found as a function of φ, μ, and ν.

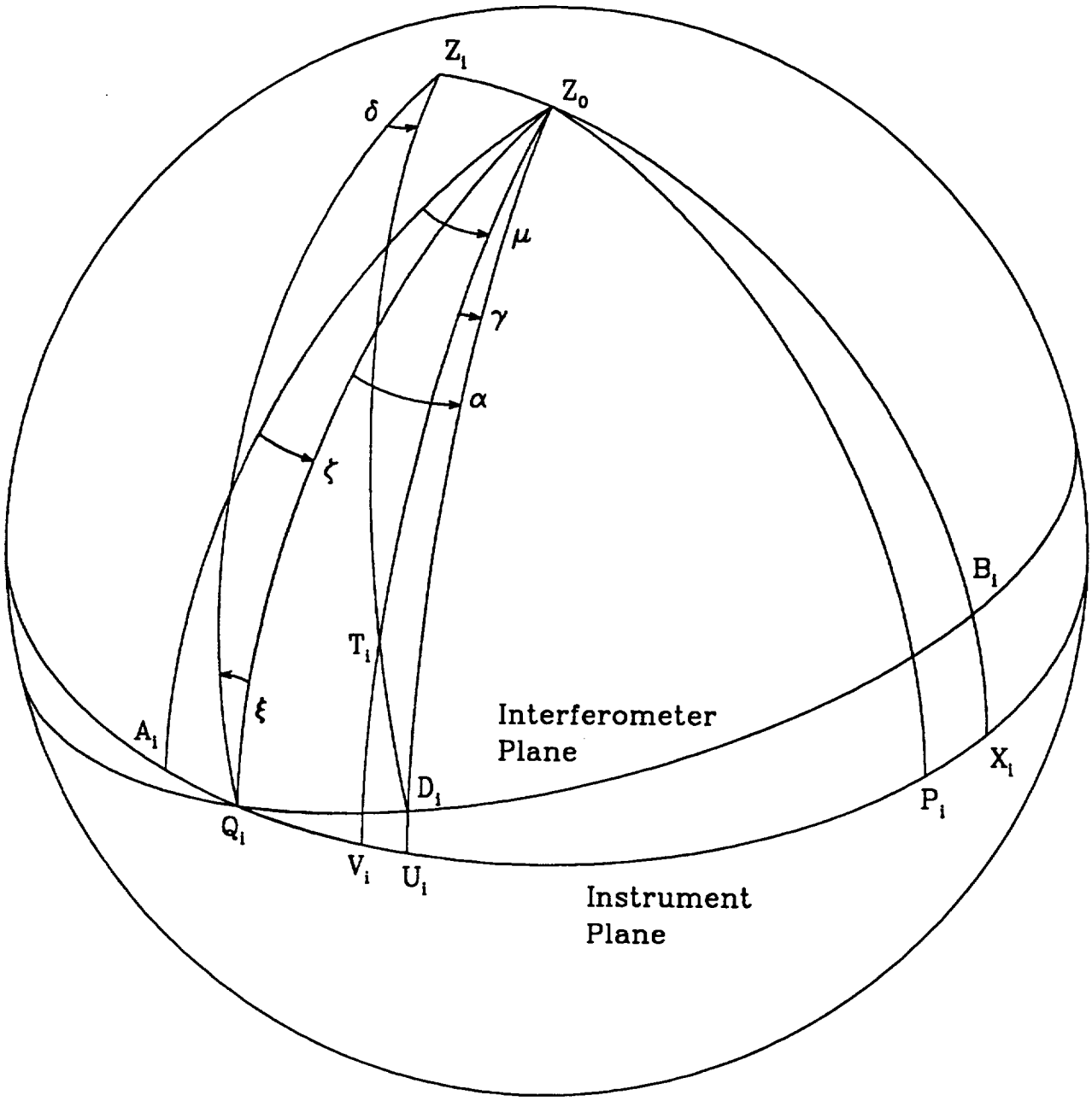

Figure A1. Spherical triangles. The target is at T, and is related to the coordinate frames by the following arc lengths: β = UD, δ = QD, ε = DT, and ν = VT.

In Triangle QUD, the required relations are:

$$\sin\beta = \sin\delta \sin\xi \qquad \text{(A4)}$$

$$\sin\alpha = \tan\beta \,/\, \tan\xi \qquad \text{(A5)}$$

$$\cos\kappa = \sin\xi \cos\alpha \qquad \text{(A6)}$$

where κ = QDU and ξ = DQU. In triangle Z_0TD, the required relations are:

$$\sin\nu = \cos\varepsilon \sin\beta + \sin\varepsilon \cos\beta \sin\kappa \tag{A7}$$

$$\sin\gamma = \sin\varepsilon \cos\kappa / \cos\nu \tag{A8}$$

We next replace the above expressions with the corresponding series expansions in the small quantities δ, ξ, and ε, to obtain expressions for μ and ν. From Equ. A4:

$$\sin\beta = \delta\xi ; \quad \cos\beta = 1 - \frac{\xi^2\delta^2}{2} \tag{A9}$$

From Eqs. A5 and A9:

$$\cos\alpha = 1 - \frac{\delta^2}{2} ; \quad \alpha = \delta - \frac{\delta\xi^2}{2} \tag{A10}$$

From Eqs. A6 and A10:

$$\cos\kappa = \xi - \frac{\xi\delta^2}{2} - \frac{\xi^3}{6} ; \quad \sin\kappa = 1 - \frac{\xi^2}{2} \tag{A11}$$

From Eqs. A7, A9, and A11:

$$\cos\nu = 1 - \frac{\varepsilon^2}{2} - \varepsilon\delta\xi ; \quad \nu = \varepsilon + \delta\xi - \frac{\varepsilon\xi^2}{2} \tag{A12}$$

From Eqs. A8, A11, and A12:

$$\gamma = \varepsilon\xi \tag{A13}$$

We can now find $\mu = AV = \zeta + \alpha - \gamma$ from Eqs. A10 and A13:

$$\mu = \zeta + \delta - \xi\varepsilon - \frac{\delta\xi^2}{2} \tag{A14}$$

We next consider the angular separation θ of the target stars and find an expression that is more accurate than Equ. A1. Figure A2 shows the geometry. We consider spherical triangle $Z_0\ T_1\ T_2$, for which

$$\cos\theta = \sin\nu_1 \sin\nu_2 - \cos\nu_1 \cos\nu_2 \sin u \tag{A15}$$

where $u = \eta - \pi/2$. Note that u is about the same as Δ, the deviation from $\pi/2$ of the separation of the interferometer pointing directions. Thus, with the present instrument nominal specifications, $|u| \leq 3$ deg. We introduce $\rho = \theta - \eta$, which we expect to be a very small quantity (*i.e.*, measured in microarcseconds), and obtain

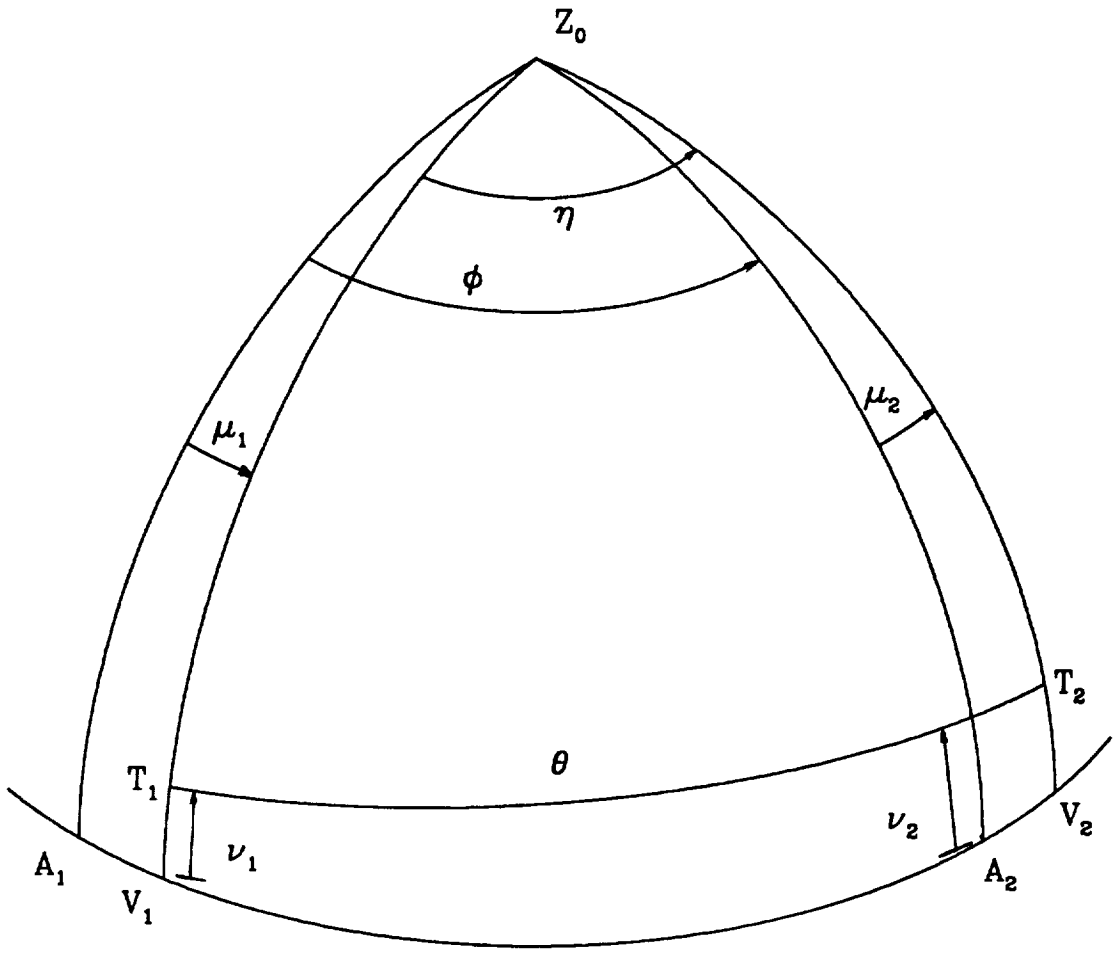

Figure A2. Separation of targets.

$$\cos\theta = -\sin(u+\rho) = -\sin u\cos\rho - \cos u\sin\rho \tag{A16}$$

By combining Eqs. A15 and A16 and neglecting terms of order ν^4, we obtain

$$\rho = -\frac{\nu_1\nu_2}{\cos u} - \frac{\nu_1^2+\nu_2^2}{2}\tan u \tag{A17}$$

We are now in a position to find $\theta = \varphi - \mu_1 + \mu_2 + \rho$ to second order in small quantities.

$$\theta - \varphi = D + E + F \tag{A18}$$

where

$$D = \delta_2 - \delta_1 \tag{A19}$$

$$E = \zeta_2 - \zeta_1 \tag{A20}$$

$$F = \xi_1\varepsilon_1 - \xi_2\varepsilon_2 - \frac{\varepsilon_1\varepsilon_2+(\varepsilon_1^2+\varepsilon_2^2)\sin u}{\cos u} \tag{A21}$$

In Equ. A18, the first term (D) is the principal interferometric measurement. The second term (E) is a simple, fixed bias related to the rotations of the baselines with respect to the pseudobaselines. This quantity is held fixed by the null servos of the FAM system. The third term (F) is a complex bias, further complicated by the realistic assumption that the measured value of ε_i will have a bias that we will need to estimate. It appears that by making a string of astrometric measurements with a range of values for ε_1, ε_2, and u, it should be possible to determine ξ_1, ξ_2, and the biases in ε_1 and ε_2. This is more readily seen if one assumes that several measurements are made of a single pair of stars, but the conclusion does not depend on that assumption. Finally, we note that the third order terms in θ-φ, which were excluded from Eqs. A19-21, are negligible.

7. REFERENCES

1. Reasenberg, R.D., "Microarcsecond Astrometric Interferometry," in *Proceedings of the Workshop on High Angular Resolution Optical Interferometry from Space*, (Baltimore, 13 June 1984), Ed. by P.B. Boyce and R.D. Reasenberg, *BAAS*, **16**, pp. 758-766, 1984.

2. Reasenberg, R.D., R.W. Babcock, J.F. Chandler, M.V. Gorenstein, J.P. Huchra, M.R. Pearlman, I.I. Shapiro, R.S. Taylor, P. Bender, A. Buffington, B. Carney, J.A. Hughes, K.J. Johnston, B.F. Jones, and L.E. Matson, "Microarcsecond Optical Astrometry: An Instrument and Its Astrophysical Applications," *Astron. J.*, **32**, pp. 1731-1745, 1988.

3. R.D. Reasenberg, R.W. Babcock, M.C. Noecker, and J.D. Phillips, "POINTS: The Precision Optical INTerferometer in Space." To appear in *Remote Sensing Reviews* (Special Issue Highlighting the Innovative Research Program of NASA/OSSA), Guest Editor: Joseph Alexander, 1993.

4. M.C. Noecker, J.D. Phillips, R.W. Babcock, and R.D. Reasenberg, "Internal laser metrology for POINTS," in *The Proceedings of the SPIE Conference # 1947, OE/Aerospace Science and Sensing '93*, Orlando, FL, April 14-16, 1993.

5. D. Massa and A.S. Endal, "An Instrument for Optimizing a Spaceborne Interferometer: Application to Calibrating the Cepheid Distance Scale," *Astron. J.*, 93(3), p. 760, 1987.

6. W.A. Traub, "Constant-dispersion grism spectrometer for channelled spectra," *Opt. Soc. Am. A.*, vol. 7, no. 9, p. 1779, 1990.

7. A. Wissinger, private communication, Hughes Danbury Optical Systems, Inc. 1993.

8. J.A. Eddy, *A New Sun: The Solar Results from Skylab*, NASA SP-402, NASA, Washington, DC, p. 47, 1979.

9. M.C. Noecker, M.A. Murison, and R.D. Reasenberg, "Optic-misalignment tolerances for the POINTS interferometers," in *The Proceedings of the SPIE Conference # 1947, OE/Aerospace Science and Sensing '93*, Orlando, FL, April 14-16, 1993.

10. B.L. Schumaker, M. Agronin, G.-S. Chen, W. Ledeboer, J. Melody, D. Noon, J. Ulvestad, "Spacecraft and mission design for the precision optical interferometer in space (POINTS)" in *The Proceedings of the SPIE Conference # 1947, OE/Aerospace Science and Sensing '93*, Orlando, FL, April 14-16, 1993.

11. M.P. Veron-Cetty and P. Veron, "A Catalogue of Quasars and Active Nuclei," 5th Edition, *E.S.O. Sci. Rep.*, 10, 1991.

12. R.D. Reasenberg, "Microarcsecond Astrometric Interferometry," in *Proceedings of IAU Symposium 109, Astrometric Techniques* (Gainesville, 9-12 January 1984), Ed. by H.K. Eichorn and R.J. Leacock, pp. 321-330 (Reidel, Dordrecht), 1986.

13. R.D. Reasenberg, "Precision Optical Interferometry in Space," in *Proceedings of The First William Fairbank Meeting on Relativistic Gravitational Experiments in Space*, (Rome, September 10-14, 1990), 1991.

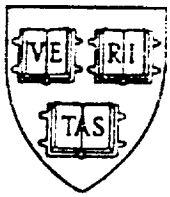

Harvard-Smithsonian Center for Astrophysics

Preprint Series

No. 3602
(Received March 29, 1993)

POINTS: The Precision Optical INTerferometer in Space

R.D. Reasenberg, R.W. Babcock, M.C. Noecker, and J.D. Phillips
Harvard-Smithsonian Center for Astrophysics

Invited paper

To appear in
Remote Sensing Reviews
(Special Issue Highlighting the Innovative Research
Program of NASA/OSSA)
(Guest Editor: Joseph Alexander)

Center for Astrophysics
Preprint Series No. 3602

POINTS: The Precision Optical INTerferometer in Space

R.D. Reasenberg, R.W. Babcock, M.C. Noecker, and J.D. Phillips
Harvard-Smithsonian Center for Astrophysics

POINTS: The Precision Optical INTerferometer in Space

R.D. Reasenberg, R.W. Babcock, M.C. Noecker, and J.D. Phillips
Smithsonian Astrophysical Observatory
Harvard-Smithsonian Center for Astrophysics

ABSTRACT

POINTS, an astrometric optical interferometer with a nominal measurement accuracy of 5 microarcseconds for the angle between a pair of stars separated by about 90 deg, is presently under consideration by two divisions of NASA-OSSA. It will be a powerful new multi-disciplinary tool for astronomical research. If chosen as the TOPS-1 (Toward Other Planetary Systems) instrument by the Solar-System Exploration Division, it will perform a definitive search for extra-solar planetary systems, either finding and characterizing a large number of them or showing that they are far less numerous than now believed. If chosen as the AIM (Astrometric Interferometry Mission) by the Astrophysics Division, POINTS will open new areas of astrophysical research and change the nature of the questions being asked in some old areas. In either case, it will be the first of a new class of powerful instruments in space and will prove the technology for the larger members of that class to follow. Based on a preliminary indication of the observational needs of the two missions, we find that a single POINTS mission will meet the science objectives of both TOPS-1 and AIM.

The instrument detects a dispersed fringe (channelled spectrum) and therefore can tolerate large pointing errors. In operation, the difficult problem of measuring the angular separation of widely spaced star pairs is reduced to two less difficult problems: that of measuring the angle between the two interferometers and that of measuring interferometrically the small offset of each star from the corresponding interferometer axis. The question of systematic error is the central theme of the instrument architecture and the data-analysis methods. Stable materials, precise thermal control, and continuous precise metrology are fundamental to the design of the instrument. A preliminary version of the required picometer laser metrology has been demonstrated in the laboratory. Post-measurement detection and correction of time-dependent bias are the essential elements in data analysis. In that post-measurement analysis, individual star-pair separations are combined to determine both the relative positions of all observed stars and several instrument parameters including overall time-dependent measurement bias. The resulting stellar separation estimates are both global and bias-free at the level of the uncertainty in the reduced (*i.e.*, combined and analyzed) measurements.

1 INTRODUCTION

Astronomical optical interferometry was first practiced by Michelson, who added a pair of translatable, fixed-angle siderostats to a large telescope so that he could measure the fringe visibility of stars as a function of interferometer baseline length. In 1920, he formally announced his determination of the diameter of Betelgeuse, to much public excitement. Each

of his measurements was a *tour de force*, and the technique fell into disuse for decades. (For a review of Michelson's life and work, see Physics Today, 40(5), 1987.) More recently, new technologies have made possible construction of ground-based optical interferometers that could make routine observations of high scientific value. Early versions of these instruments are now working or near completion. Mariotti (1993) lists 17 ground-based interferometers, more than half of which are working. However, ground-based interferometers and telescopes jointly suffer two classes of restrictions: (1) Observations are made through a turbulent atmosphere with limited windows of visibility; and (2) The platform (Earth) rotates slowly, necessitating compensatory pointing, restricting the portion of the sky that can be observed at one time, and setting the time between observations of points well separated on the sky. These restrictions are removed when the observations are made from space.

Eventually several optical interferometers can be expected in space. Support for this assertion comes from the report of the Astronomy and Astrophysics Survey Committee (AASC), established by the National Research Council under the chairmanship of John Bahcall to set the priorities for astronomy and astrophysics in the US during the 1990's, and from the more detailed discussion of the future of optical interferometry contained in the report of the Interferometry Panel of the AASC (National Academy of Sciences 1991). Further support comes from a rapidly growing community of scientists and technologists interested in optical interferometry. We expect that most of the starlight interferometers in space will be imaging devices on a grand scale, with corresponding price tags. Because they represent a new and complex technology, these "greater observatory" class instruments are not likely to be flown without the benefit of a smaller, less expensive precursor instrument such as POINTS.

POINTS, a space-based astrometric optical interferometer with a nominal measurement accuracy of 5 microarcseconds (μas), will be a powerful new multi-disciplinary tool for astronomical research (Reasenberg 1984; Reasenberg *et al.* 1988). The instrument includes two separate stellar interferometers that have their principal optical axes (nominal target directions) separated by φ, an adjustable angle of about 90 deg. (See Fig. 1.) Since the targets are within a few arcsec of their respective interferometer axes, off-axis distortions and the attendant biases are minimized. In each interferometer, the starlight leaving the beamsplitter is dispersed to form a "channelled spectrum," which gives the instrument an enhanced tolerance of pointing error, especially during target acquisition. A single measurement determines the angular separation of a pair of target stars. Each interferometer has a baseline 2 m long, and two afocal telescopes with 10:1 compression. The two interferometric subapertures of each starlight interferometer are 25 cm in diameter. Our studies of detectors and mirror coatings show that 20% of the photons entering the aperture will be detected. We find that the nominal 5 μas measurement uncertainty is reached after about one minute of observing a pair of mag 10 stars. The largest error component is the photon statistics of the starlight. Based on present models of slew, acquisition, and data collecting times, we estimate that POINTS would observe about 350 star pairs per day if the targets were mag 10.

Since the interferometers are mutually perpendicular, the instrument naturally performs global astrometry, which was first practiced by HIPPARCOS, and provides three advantages: (1) Instrument bias can be routinely determined by 360 deg closure. Thus, for reasonable observing sequences, one obtains a global reference frame that is free of regional biases to the nominal accuracy of the data. (2) Parallax measurements are absolute, not relative. (3) For a given target star, the reference star is chosen from the great-circle band of sky 90 deg away, maximizing the probability of finding a suitable reference. If the relative rotation range of the two interferometers is ±3 deg, this observable band has an area of 2160 square degrees (>5% of the sky) and can be expected to contain about 80 stars as bright as (visual) mag 5; 1200 stars, mag 7.5; and 17,000 stars, mag 10. Thus, the observation time is not dominated by the low photon rate of dim reference stars. Each reference star is a carefully studied target star, chosen from the reference grid described in Section 6.1. Thus the motions of the reference stars are well modelled and do not corrupt the measurements of other stars.

The instrument uses two kinds of metrology systems. The first is the Full Aperture Metrology (FAM), which measures the Optical Path Difference (OPD) in the starlight interferometers. In each interferometer, two laser gauges measure the starlight OPD and hold it fixed with respect to the "pseudobaseline" defined by a pair of "fiducial points." The second system uses these fiducial points to measure the angle between the pseudobaselines of the two starlight interferometers.

In FAM, modulated laser light is injected backward into the starlight optical path and fully illuminates the optical elements that transfer the starlight. The first element that encounters the starlight has a low-amplitude phase-contrast holographic surface. This

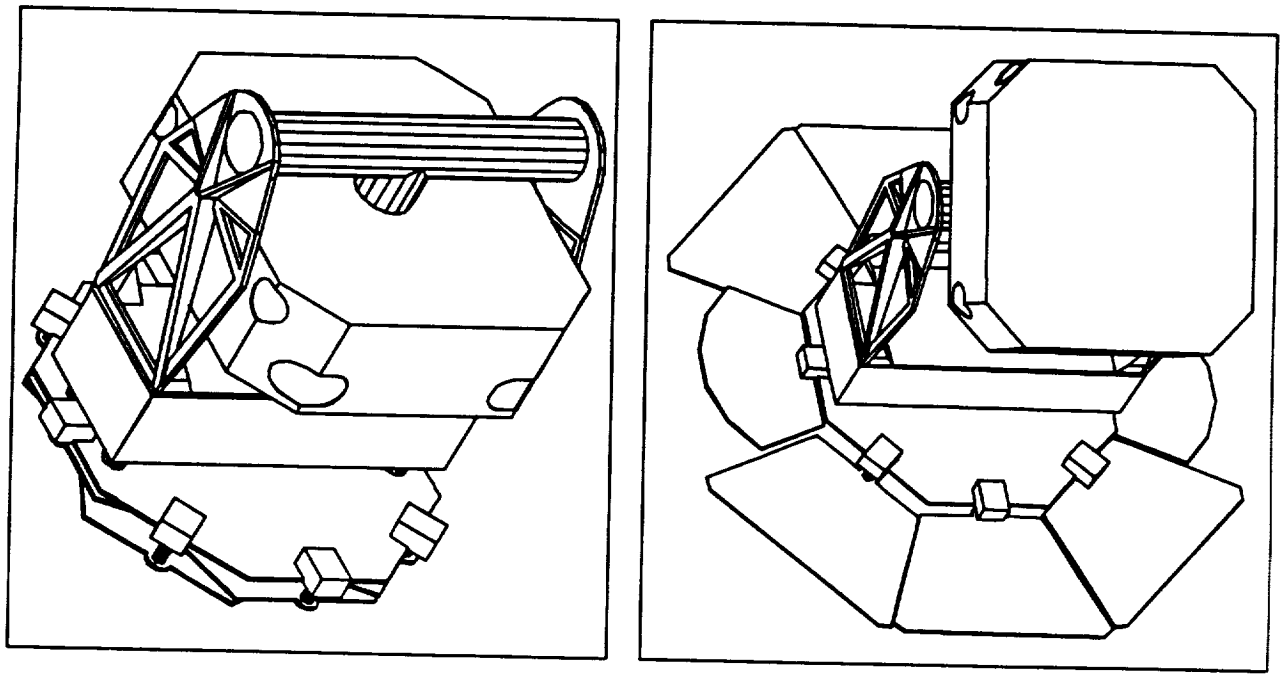

Figure 1. Proposed POINTS configuration. Left, stowed for launch. Right, operating.

holographic optical element (HOE) diffracts about 2% of the FAM light, and the samples of FAM light from the two sides of the interferometer are brought together to produce an error signal that drives a null servo. In the process, as discussed below, the "fiducial blocks" are surveyed into position. Each fiducial block contains four incomplete retroreflectors, constructed such that their apices coincide with the fiducial point to within a few microns. Knowledge of the six distances defined by these four points determines the angle between the pseudobaselines of the two starlight interferometers.

The second kind of metrology system consists of a set of six point-to-point laser gauges that measure those six distances. The angle φ between the real baselines is the quantity of interest; the angle between pseudobaselines is measured. Since these two angles differ by a small constant, the measurement of one yields a biased determination of the other. The bias is estimated from the closure information in the astrometric data, as discussed in Section 6.

In section 2, there is a brief history of POINTS. Section 3 contains a description of the instrument. A central aspect of the instrument, the laser gauge is discussed in section 4. The design of the spacecraft is discussed briefly in Section 5. Mission operations, including the bias determination and correction, are discussed in Section 6.

2 BRIEF HISTORY

The POINTS concept can be traced to 1974 when I.I. Shapiro was asked to provide ideas for NASA missions in the distant future. Among the concepts he offered was optical interferometry in space, and his proposed applications included a second-order deflection test of general relativity. A few years later, after completing some preliminary analysis of a design that included two articulated starlight interferometers pointed in opposite directions, Reasenberg established a collaborative effort with K. Soosaar *et al.* at the C.S. Draper Laboratory, Cambridge, Massachusetts.

For the Draper studies, each of two interferometers had a nominal baseline length of 20 to 25 m and a pair of subapertures of from 0.5 to 1.0 m diameter. These studies yielded three major conclusions. (1) A right angle separation of the starlight interferometers would be an important improvement. This design to use widely separated targets predated the development of HIPPARCOS, which has become the first spacecraft to perform global astrometry.[1] (2) With modest thermal insulation, thermal time constants of major components would be hours to days. (3) Adding imaging capability would be exciting, but would add considerable complexity and cost and appeared inconsistent with the dimensional precision needed for the astrometry. The imaging capability required rotatable siderostat mirrors and the ability to observe with the baseline far from perpendicular to the line of sight, which required using an auxiliary delay line to compensate for the extra path to one of the mirrors.

[1] Kovalevsky (1980) defines five types of astrometry from very narrow field to global, depending on the scale of the target separation. He notes that HIPPARCOS is the first instrument able to do global astrometry at high accuracy.

In the late 70's, the drawings of POINTS explicitly showed a long boom supporting the solar occulters that were needed for the light-deflection test of general relativity. Reasenberg presented the use of POINTS for a search for extra-solar planets at the AAS/DPS Meeting #11, Clayton, Missouri, October 1979. (Reasenberg and Shapiro 1979) That year, a spherical enclosure, as shown in Fig. 2, was added to reduce the variation of temperature with instrument orientation, and to decrease the radiation temperature anisotropy, which would distort the precision structure. (Reasenberg 1980, 1982) It was not realized until 1991 that the occulter intended for the deflection test could be made large enough to put the entire instrument in a permanent shadow, thus making the enclosure unnecessary.

By 1978, the baseline and aperture had shrunk to 10 m and 0.5 m, respectively. (Reasenberg and Shapiro 1982) However, it was not until 1983 that they reached their current nominal dimensions of 2 m and 0.25 m, respectively. This shrinking reflected a growing realization of the close connection between the cost of a mission and the size and *a fortiori* the mass of the spacecraft. Of course, were there an opportunity to build the instrument with larger baselines or larger apertures, we would be pleased. However, for now we seek to use technology in place of size to achieve the desired accuracy.

At the beginning of 1983, Shapiro and Reasenberg moved to the Center for Astrophysics, and shortly thereafter the first POINTS laboratory was established. From 1985 to 1990, POINTS received support from the Smithsonian Institution through its Scholarly Studies Program. From 1985 to 1989, POINTS (along with a few other projects) received

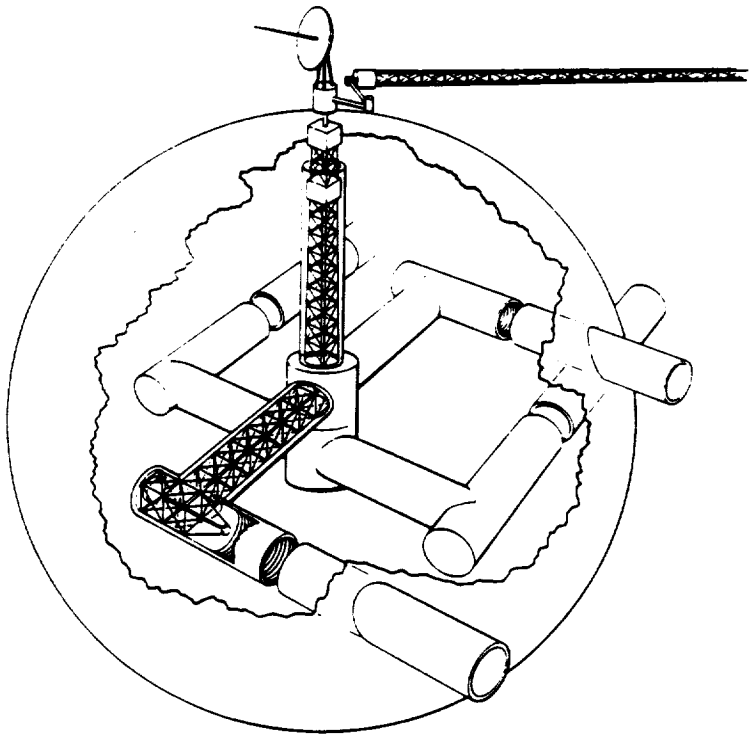

Figure 2. POINTS with spherical enclosure, as envisioned in 1979.

modest funding through a CfA-wide grant from the Innovative Research Program (IRP) of NASA's Office of Space Science and Applications (OSSA). For the three years starting early in 1989, POINTS was supported directly by the IRP. It was the work done under the Scholarly Studies Program and early IRP funding that developed the concept to a level that was attractive to the Solar System Exploration Division (SSED) of OSSA. The more substantial IRP support during the last three years permitted rapid progress in developing both the concept and critical technology.

In 1988, the Solar-System Exploration Division (SSED) began to fund the development of POINTS under the Planetary Instrumentation Definition and Development Program (PIDDP). PIDDP has continued to fund the development as an instrument to search for and characterize extra-solar planetary systems, and perform additional solar-system research. That year, the SSED established the Planetary System Science Working Group (PSSWG) under the chairmanship of B. Burke (MIT). The PSSWG was to investigate opportunities for advancing planetary science by observing stellar environments and to recommend strategies to pursue these opportunities. An outgrowth of that SWG's activities was the establishment by the SSED of the TOPS (Toward Other Planetary Systems) program. The program has three phases including TOPS-1, a space-based survey to find extra-solar planetary systems. The development of POINTS has been aimed at meeting the evolving requirements of the TOPS-1 mission, including that it meet the restrictions of a NASA Moderate Mission (for which the cost at launch + 30 days must be under $400M not including the cost of launch *per se*.)

The TOPSSWG (formerly PSSWG) has recommended a set of requirements for a TOPS-1 search, which are included in the report "TOPS: Toward Other Planetary Systems" issued by the SSED during the last quarter of 1992. In discussing the TOPS-1 search for extra-solar planetary systems, the report states that (1) a negative result must be "a fundamental advance in our knowledge," and (2) "the search should encompass a sufficient population of target stars, ultimately exceeding 100 to 1000 stars of solar type, and ... extend to distances between 15 and 30 pc." (p. 18) Independently, the POINTS team has proposed a distribution of targets: 200 F, 400 G, 200 K, and 200 M stars not known to be in multiple-star systems plus a few hundred special stars, including binaries. Excluding those known to be binary and those for which there is insufficient information, we find that the faintest of the basic {F, G, K, M} set will be $m_b \approx 9.6$. The most difficult astrometric signatures, based on a Uranus mass planet at Jovian distance (5.2 AU) from the star, range from 4μas for F stars (mag 6) to 50 μas for M stars (mag 9.6). In a POINTS mission concentrated on the search for extra-solar planetary systems, the targets would be bright and the required measurement correspondingly quick. A subset of easily observed targets (*e.g.*, near) would be observed far more closely than the others to extract additional information in case they should have planets.

In the past four years, there have been valuable contributions to POINTS by students working on the project. Two students have come to the project as fellows under the Summer Undergraduate Fellowships in Science program of the New England Consortium for Under-

graduate Science Education (NECUSE). That program, which places students in research situations outside their home institutions, has funded a major part of their stipends. Others have worked as laboratory assistants and in undergraduate honors thesis work.

Patrick Morrissey began working with us through the NECUSE program while a junior at Brown University. He later did his senior honors thesis on some error sources in the POINTS distance gauges. Patrick measured the polarization-dependent phase shift of the mirrors that make up the laser gauge endpoint cornercubes, showing that the phase differences were large, and that there were large variations from mirror to mirror (25° to 45°), but that they were very nearly constant with position on the mirror, and with rotation of the mirror about its normal. Patrick did a significant amount of the work needed to commission the laser gauges, including careful identification of the causes of stray light in the laser modulator, and suppression of the stray light. He also showed that the sensitivity of the quad cells we were using was very nearly constant over the surface, set up other optics, and built and debugged electronics. Patrick is now a graduate student in astronomy at Johns Hopkins University.

Andrew Gerber worked with us for two summers, one as a NECUSE fellow. The first summer, he wrote a multi-channel data acquisition program for our laboratory PC. His program acquires the data, displays it graphically, and allows changing parameters and writing comments into the file without disturbing the data acquisition. The second summer, Andrew worked on an analytic ray tracing method, the forerunner of a system that we have used for the analysis of the POINTS high precision optics. Andrew wrote analytical ray tracing routines using algebra software running on machines of the IBM PC family and identified the size of the expressions as the main problem that needed to be addressed. Andrew is now a fourth year student in physics at Yale.

Harvard undergraduates Gordon Fauth and Tom Killian have worked as lab assistants on the picometer distance gauges. A large part of their work was building electronic equipment to our designs. They also worked with us testing the electronic systems that are used the by the gauge, and analyzing the test results.

3 INSTRUMENT DESCRIPTION AND CONCEPT

3.1 Principles of Operation

The principal elements of the POINTS instrument are two starlight interferometers, mounted at a nearly right angle, and a metrology system. The instrument determines θ, the angular separation between two widely separated stars, by measuring φ, the angle between the interferometers, and measuring independently δ_1 and δ_2, the offsets of the target stars from their respective interferometer axes. With proper selection of target stars and a small adjustment capability in φ (nominally $87 \leq \varphi \leq 93$ deg), a pair of stars can be brought simultaneously to within less than one arcsec of their respective interferometer axes. Once a target star is in the field of an interferometer, δ is measured through the analysis of the

dispersed fringe which forms a channelled spectrum. A central feature of the instrument is the real-time monitoring of the angle between the interferometers and the metrology along the starlight optical path, each of which uses a laser interferometer scheme based on currently or soon-to-be available technology.

In each of the two interferometers, the afocal telescopes compress samples of the starlight, which are directed toward the fringe-forming and detecting assembly. At the exit ports of the beamsplitter, the light is dispersed and focused onto a pair of linear arrays of detectors. When the star is on axis ($\delta = 0$), the signal at any given wavelength has equal intensity at the two beamsplitter exit ports. When the star is off axis ($\delta \neq 0$), constructive interference for a given wavelength at one port is complemented by destructive interference at the other port. At each port, an alternating pattern of constructive and destructive interference is observed. The resulting complementary channelled spectra form the basis for determining δ. Since the detectors in the array see narrow, contiguous portions of the optical spectrum, there are effectively a large number of narrow-band interferometers that collectively make use of all of the light. Because of their small bandwidths, these interferometers can function when the instrument is pointed several arcsec from the target. However, to keep the fringe visibility high, it is desirable to keep the pointing offset small compared to δ_N, the Nyquist angle, at which there are two detector pixels per fringe.

The channelled-spectrum approach has two distinct advantages over a system in which a single detector measures the white light fringe. In the latter system, the pointing error would have to be under 0.05 arcsec during observations (unless an active system of path compensation were included); white light fringe detection would require an oscillating mirror to modulate (say at sonic frequency) the OPD. The fringe visibility would be substantially reduced at 2 arcsec, making the initial acquisition of the fringe more difficult. Thus, the use of the dispersed fringe greatly simplifies the pointing system and removes the need for the motion of major parts (*i.e.*, delay line) during an observation, which would add mass and complexity and reduce reliability. The second advantage of the dispersed fringe approach is that there is additional information available in the channelled spectrum. This information can be used to separate targets that are closely spaced and might otherwise be confused, such as members of a binary system. An instrument utilizing this technique exclusively was proposed by Massa and Endal (1987).

There were two principal contenders for the coatings on the mirrors that transfer the starlight to the beamsplitter: silver and aluminum. Thus far, we have not considered complex coatings out of concern that they may have temperature-dependent phase shifts. Silver has higher reflectivity at the longer wavelengths, but is not useful at wavelengths shorter than about 0.4 micron. (The nominal bandpass for POINTS is from 0.9 microns to 0.25 microns.) In order to assess the relative merits of these two coatings and of various detectors, we developed a computer code that calculates the astrometric precision of one starlight interferometer by numerically integrating over a specified portion of the optical spectrum. This code can use various source spectra including a black-body spectrum (of specified temperature), a smoothed solar spectrum, and smoothed spectra of various types of stars.

These spectra are modified by the wavelength-dependent reflectivity of the assumed mirrors and the wavelength-dependent sensitivity of the assumed detectors to yield the detected spectrum. The study showed that to maximize the measurement rate for a TOPS-1 mission, which would look at Sun-like stars, we should use silver coatings and neglect the light at wavelengths shorter than 0.4 micron; for an AIM mission we should use aluminum and observe the shorter wave lengths. However, we have more recently learned that silver mirrors, even with protective coatings, have a history of visible deterioration before launch. Therefore, the nominal mirror coating is aluminum.

3.2 Detectors and Instrument Pointing

There are three questions concerning detectors and pointing: (1) How far from the target direction can the instrument point and still detect the target? (2) What is the effect on the information rate of a pointing offset? (3) What is the limiting magnitude of the instrument? As $|\delta|$ is increased from zero, the number of fringes on the detector array increases, and the fringe visibility V decreases because each pixel averages over an increasingly large portion of a fringe. The information content of the data is monotonic with V, which is zero at $\delta=2\delta_N$, where there is one fringe per pixel. The information content falls rapidly with decreasing V near V = 1, so the visibility must be kept high. A prism, like a diffraction grating (but in the opposite sense), provides a nonlinear dispersion so that, if the detector pixels are of uniform width, the number of pixels per cycle of channelled spectrum will vary with color. One solution is to combine a grating and a prism, as is being done for the IOTA ground-based interferometer (Traub, 1990). An alternative approach, which is adopted for POINTS, is to use only a prism, allowing the pixel width to vary with the color and so avoiding the light loss of the grating. Below, we consider in turn the detectors, the spectrometer, limiting magnitude, and the fine pointing and isolation system.

For many years, the nominal detector had been a set of photon-counting avalanche photodiodes. Such detectors permit a fringe to be observed in the presence of a high fringe rate, *i.e.*, when the instrument is rotating. However, as discussed below, we have found that the fringes can be held sufficiently stable on the detectors that an integrating detector such as a CCD can be used with little loss of fringe visibility due to motion during the integration period. CCDs offer high quantum efficiency, and there is a wide base of experience of their use in space, as well as continuing development. Among the instruments that have flown with CCD's or for which they are being developed are the Wide Field/Planetary Camera I and II and the Space Telescope Imaging Spectrometer for Hubble Space Telescope, the Solid State Imaging camera aboard Galileo, and the imaging cameras and the Visual and Infrared Mapping Spectrometer for Cassini. Since the spectrum is dispersed along the array, a tapered anti-reflection coating can be used, offering a further increase in quantum efficiency. With a

stabilized fringe integrated on the CCD detector, there is an automatic solution to the problem of data compression, which otherwise would require considerable on-board computation.[2] As presently envisioned, the CCD arrays will have 650 cells to cover an optical bandpass from 0.25 to 0.9 μm.

The spectrometers, one for each exit beam, must disperse the starlight to produce the channelled spectrum while maintaining high fringe visibility. Three primary effects govern resolution and thus fringe visibility: diffraction, aberration, and detector pixel size. In the dispersion direction, the diffraction-limited spot must be $\lesssim$ 1/20 the spacing of the dispersed fringes in order to maintain high fringe visibility. Additionally, providing spatial resolution in the cross-dispersion direction allows simultaneous acquisition of data on multiple targets in crowded fields. With this capability, the scientific throughput on stars in globular clusters may be as much as two orders greater than on isolated targets. In the cross-dispersion direction, the limit to resolution is the diffraction limit of the subapertures. Both the requirement for high visibility and for resolution in the cross-dispersion direction dictate that the aberration-limited spot and the size of the pixels should be less than the Airy disk, *i.e.* the system should be diffraction-limited.

The current design meets the above requirements. It employs a prism followed by an off-axis section of a paraboloidal mirror (f/40). The prism provides adequate dispersion with an apex angle as small as 10 deg. The nominal prism material is fused silica, because of the need for high transmission over the bandwidth from 0.9 μm to 0.25 μm.

At one time, the limiting magnitude was set by the requirement that the interferometer collect enough photons to determine the fringe phase before the unmodelled part of the fringe drift smeared the fringe. The current design, however, calls for the fringes to be held sufficiently stable to allow on-chip integration, with duration limited only by the frequency with which instrument biases must be recalibrated. In this mode, limiting magnitude depends on dark current. We believe that present CCD's impose a limit somewhere between magnitude 17 and 20. The two important factors for setting the limiting magnitude are detector temperature and total size.

In the present design, the instrument is connected to the spacecraft scan platform by means of a soft, single-axis pivot with a free swing range of several tens of arcsecs. A flexural pivot that would serve well as the basis for the isolator has been made by the Perkin-Elmer division that is now Hughes-Danbury Optical Systems (HDOS). (The pivot was flown as part of the Apollo Telescope Mount on Skylab, 1973-1974. A. Wissinger, HDOS, private

---

[2] Consider an observation in which 10^7 photons are collected in 100 batches by one interferometer. Without compression, two numbers (epoch and detector number, about ten digits total) must be transmitted to the ground for each photon. Without stabilization and on-chip integration, the fringe must be rotated and integrated in software, requiring several floating point operations per photon in addition to the real-time filter. With stabilization and on-chip integration, there is little computation required for fringe tracking, and the telecommunication load without explicit compression is 2 10^4 numbers of five digits. It appears that a compression of at least 10 fold will be possible.

communication; Eddy 1979.) There are several suitable magnetic actuators to provide fine pointing correction to the isolated instrument. The instrument mounted on the pivot would have a torsional resonance between 1/20 and 1/5 Hz[3]. Given such a soft mount, there would be considerable filtering at the detector sampling rate of 100 Hz, applicable to bright target stars.

The present scheme requires that at least one target be bright, say mag 10. Initially, a star tracker would be used to find the bright target and the approximate rotation rate of the instrument. This information would be used to reduce the offset and rotation rate to below the threshold for detecting starlight fringes. Once the fringes were found, they would serve as the reference for the fine pointing. On a mag 10 star, with a sample rate of 100 Hz, the samples would have a statistical uncertainty of ≈250 μas. However, the use of one of the interferometers as the angular reference requires real-time data analysis and the corresponding on-board computational capability. The 100 Hz sample rate probably limits to ≈10 Hz the unit-gain frequency of the control loop for the orientation of the instrument.

3.3 Internal Measurements and Systematic Error

The control of systematic error is central to achieving the stated instrument performance and the mission science objectives. We address this problem at three levels: (1) stable materials and thermal control; (2) real-time metrology; and (3) the detection and correction of systematic error in conjunction with the global data analysis. The last of these is addressed in Section 3.4. The best materials fail by orders of magnitude to provide the long-term dimensional stability required for each interferometer's Optical Path Difference (OPD) and other critical dimensions, in the absence of other means of control. Stable materials for the structural elements of the instrument serve to limit the dimensional changes that the metrology system must determine, and to control errors that are second order in component displacements. In a few places, we are forced to rely on material stability (over short times). The instrument is designed so that such metering elements are small, and can be thermally isolated and regulated.

For a 2-m baseline, the nominal 5-μas uncertainty corresponds to a displacement of one end of the interferometer toward the source by 0.5Å = 50 pm (picometer = 10^{-12} m). Since similar displacements of internal optical elements are also important, the instrument requires real-time metrology of the entire starlight optical path at the few picometer level. This metrology does not pose an overwhelming problem for two reasons. First, the precision is needed only for averaging times between 1 and 100 minutes. Second, a slowly changing bias in the measurement is acceptable, as discussed in Section 3.4.

The instrument relies on two kinds of laser-driven optical interferometers to determine changes in critical dimensions. New concepts and technology have been required for the on-

[3] There would need to be cables, *etc.* crossing the pivot, and these would add to the stiffness by an as yet undetermined amount, which is a contributor to the stated possible range of the frequency.

board measurements to picometer accuracy. The laser gauges *per se*, a new application for a holographic optical element (HOE), and the laser-gauge endpoint assemblies were invented during the development of POINTS. The laser gauges can be grouped according to whether they measure distances internal to a starlight interferometer or distances between starlight interferometers. Below, we consider the former. In the next section, we consider the latter and some related questions of instrument geometry (the relation between the baselines and the pseudobaselines) and measurement bias.

The high-precision star position measurement is made with respect to the optical axis of the interferometer by measuring the difference in the optical paths from the target to the beamsplitter *via* the two sides of the interferometer. In turn, the position of this axis is determined (defined) by the positions of the optical elements used to transfer the starlight. The metrology system must determine, to about 10 pm overall accuracy, the average change in the starlight optical path differences (OPD) induced by all motions and distortions of all optical elements. Our approach is to use Full-Aperture Metrology (FAM), a novel technique discussed below. The roots of the FAM system in POINTS are in the workshops held in 1980 and 1981 by D. Black of NASA-ARC, and can be traced *via* D. Staelin of MIT to concepts developed for large DoD optical systems. FAM provides three significant advantages over conventional approaches.

(a) FAM removes complexity. The usual metrology systems use a large number of laser gauges to determine the locations of the elements individually. From these measurements, the optical path through the system is computed. FAM directly measures the optical path through the system.

(b) FAM measures the correct quantity. Because the metrology signal fully illuminates the surface of each optical element that determines the starlight OPD at the beamsplitter, the metrology OPD represents accurately the average starlight OPD through the system.

(c) FAM provides the basis for an operational definition of the direction of the interferometer baseline. It measures the OPD with respect to a pair of fiducial points that define the pseudobaseline, which is located in front of each interferometer and which is held at a small fixed angle (nominally zero) to the real interferometer baselines. These fiducial points are used to determine φ, the angle between the two interferometers' optical axes. (The small bias resulting from the angle between the pseudobaseline and the real baseline is determined routinely as part of the data analysis.)

Figure 3 illustrates the preferred version of the technique. The key element is the set of primary mirrors which have shallow (phase contrast) zone plates on their surfaces: alternate zones are depressed about 100Å. In this holographic optical element (HOE), the zones are approximately in the form of Newton's rings; each zone has about the same total area. We have shown that the required Zone-Plate Mirror (ZPM) can be made holographically such that the diffractive spherical aberration is zero. Since the system functions essentially on axis, there are therefore no Seidel (*i.e.*, third order) aberrations in the diffractive focus.

In FAM, modulated laser light is injected backward into the starlight optical path and fully illuminates the optical elements that transfer the starlight. The hologram diffracts about 2% of the FAM light, and the samples of FAM light from the two sides of the interferometer are brought together at the metrology beamsplitter to produce an error signal that drives a null servo. In the process, the fiducial blocks are surveyed into position. Each fiducial block contains four incomplete hollow cornercube retroreflectors, constructed such that their apices coincide at the fiducial point to within a few microns. Knowledge of the six distances defined by these four fiducial points determines the angle between the pseudobaselines of the two starlight interferometers.

For the flight hardware, we would manufacture the holographic optical element (HOE) by a method that would provide the required spatial dependence of diffractive efficiency. The needed pattern would be found numerically and used to make a mask such as is used in the manufacture of integrated circuits. The mask could be written on a master plate by an "e-beam machine" or a "laser lathe." Each mirror would be given a thin (ca. 100Å) coating of metal and contact printed using photoresist and metal etching. Finally, the optic would be given a reflective coating. This technique has been used for many years at Hughes-Danbury Optical Systems, Inc. (HDOS) in support of DoD projects.

It is important that the uniformity of the thickness of the metallic layer on the optic be of controlled to about 1%, as the diffractive efficiency is proportional to zone thickness in the intended regime. We propose the following three-step process: (1) Normal sputtering. (2) Evaluation with a densitometer. The coating of interest will be about one optical depth. (3) Correction with Plasma Assisted Chemical Etching. With this technique, it would be possible to achieve a controlled non-uniformity to compensate for the (nearly Gaussian) profile of the laser light used to illuminate the ZPM. Senior engineers at HDOS have reviewed this plan and opined that it will work. Other approaches are being considered.

The FAM technique requires two principal servos. The laser beams diffracted from the HOE's in the two arms of the interferometer are recombined at a metrology beam splitter; this is a Mach-Zehnder interferometer configuration, which is sinusoidally sensitive to the length difference from beam splitter to beam splitter *via* the two paths. A servo regulates this path difference to a constant value by moving the starlight beamsplitter assembly. A second laser beam injected into the metrology beam splitter parallel to the FAM beams similarly measures the difference in distances from that beam splitter to each of two corner cube retro-reflectors situated in the fiducial blocks; a second servo regulates that path difference to a constant value by moving the auxiliary beamsplitter assembly. With both servos working, there is a small (under 1 mm) and constant difference between the distances from the starlight beamsplitter to the fiducial points, which are the apices of the retroreflectors inside the fiducial blocks. These servos can have small bandwidths because the time scale for distortion is long compared to a second, and because we require that vibrations of the OPD be small enough that they need not be tracked. Since it is desirable to limit the contamination of the starlight by the laser signal (*e.g., via* scattering from the surfaces of the optical elements), a minimum of laser light is used in the FAM servo.

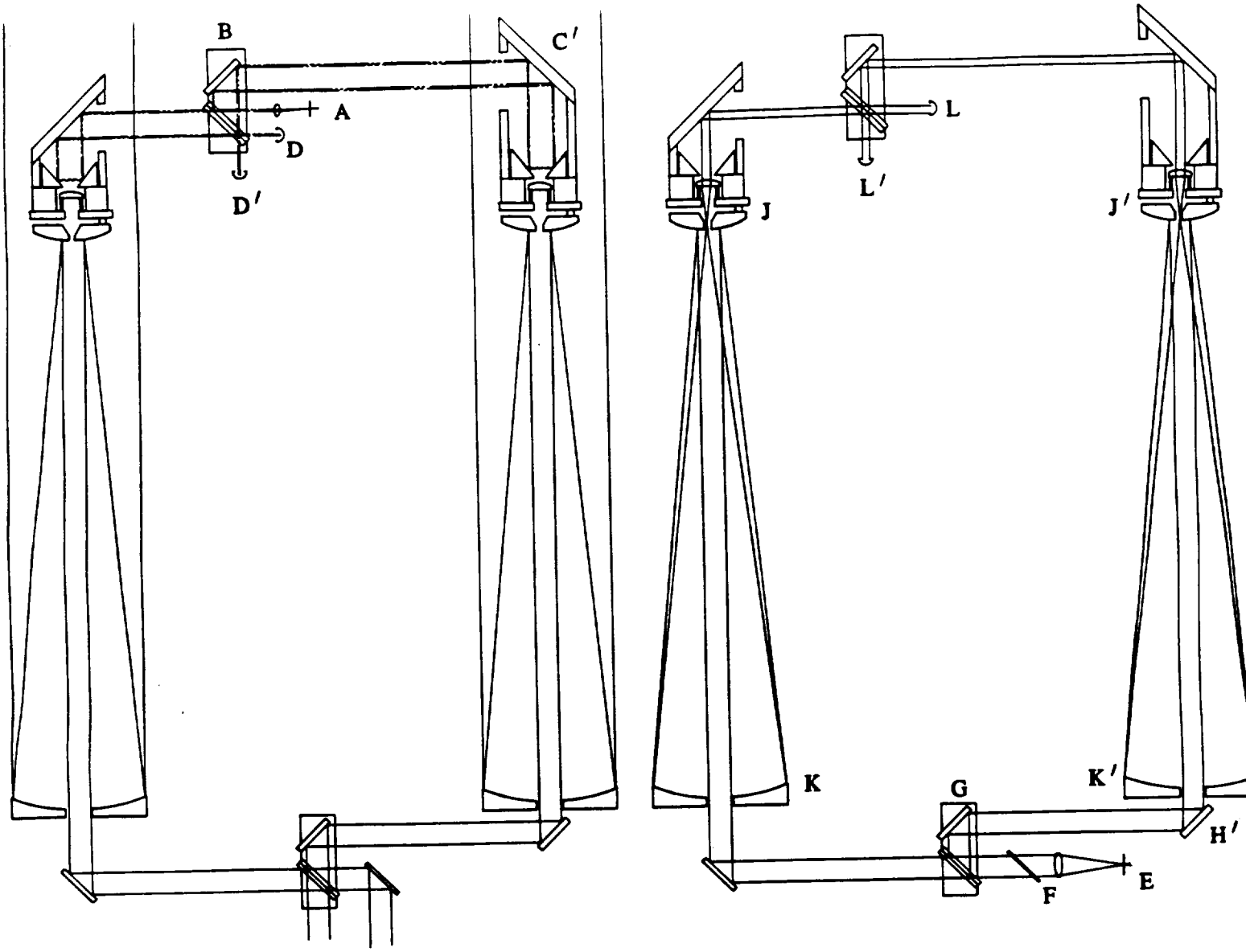

Figure 3. Interferometer optical paths. (left) Starlight and auxiliary null interferometer. For the latter, a laser signal passes through the spatial filter A and is divided by the metrology beamsplitter B to form beams that enter the fiducial blocks C and C′. Within each fiducial block, the beam is deflected by the 45° mirror, retroreflected by the hollow corner cube, and returned toward the metrology beamsplitter by the 45° mirror. The returning signals are combined at the metrology beamsplitter and fall on detectors D and D′. (right) FAM interferometer. A laser signal passes through the spatial filter E and injection beamsplitter F and is divided by the starlight beamsplitter G. The separated beams are reflected from the tertiary mirrors H and H′ and secondary mirrors J and J′ to fully illuminate the primary mirrors K and K′. The zone plates on the primaries diffract the signal to focal points in the holes in the secondaries and the athermal lenses collimate the diffracted light. Finally, the signals are reflected from the 45° mirror, are recombined at the metrology beamsplitter, and fall on detectors L and L′.

In an alternative and earlier approach to FAM (Reasenberg 1981; Reasenberg *et al.* 1993), the HOE is on a large folding flat (*i.e.*, fixed siderostat) which is the first element encountered by starlight. The two beam compressors (telescopes) in each of the starlight interferometers are mounted along the baseline, "looking" in opposite directions. In this arrangement, the fiducial block is located toward the target star from the folding flat, and is not associated with the telescope secondary. The primary disadvantages to this scheme are (1) the asymmetry of the geometry at the HOE, and (2) the need for an extra large optical element for each telescope -- a total of four for the instrument. For a large scale instrument, the extra weight would clearly be important; for a small instrument like POINTS, the case is less clear. There are two advantages to this scheme. (1) The HOE is external to and independent of the telescope. Thus the behavior of the diffractive optics is not complicated by the problems of telescope alignment. (2) The telescopes are "buried" deep inside the instrument, which makes them less susceptible to heating by stray light.

The fiducial blocks (Fig. 4) and the metrology beamsplitter assemblies pose the only critical materials problem identified. To minimize changes of the size or shape of either of these, which would cause a corresponding changes in the bias of the metrology system, they will be made of a stable material and kept in a thermally stable environment. For the fiducial blocks, we plan optically contacted Premium ULE®; the beamsplitter material is still under study. The effective separation of metrology links within the fiducial blocks would be under 10 μm, and the temperature would be held stable to 10^{-2} deg C on a time scale of a few hours. The effects of temperature fluctuations on a longer time scale will be routinely removed during the analysis on the ground of the data. The thermal gradient will be reduced by putting an aluminum cylinder with 0.5 cm walls around the fiducial block. We plan to achieve the required thermal stability with active control of the outer skin of the fiducial block enclosure to 10^{-1} deg C (although achieving a factor of ten better does not seem difficult) and a layer of insulation between the outer skin and the aluminum cylinder. The insulation, combined with the heat capacity of the fiducial block and aluminum cylinder, will yield a thermal time constant of about one day. Using Premium ULE®, which has a linear coefficient of thermal expansion $|\alpha| < 5 \times 10\text{-}9$/deg C in a range from 5 to 35 deg C, the resulting distance error would be $\leq 10^{-3}$ pm. More important would be the effects of thermal gradients of up to 10^{-3} deg C over the $\approx$ 5 cm separation of metrology beams where they reflect from the fiducial block mirrored surfaces. Such gradients would produce a measurement bias under 1 pm, again within the required limit.

In the manufacture of the fiducial blocks, the critical concern is for the alignment of the "retrostrips," which are sections of hollow corner-cube retroreflectors. Each fiducial block has four retrostrips, each of which must be assembled onto the main body from three small pieces of glass. Each retro has a symmetry axis that must point in approximately the correct direction and all four apices must be colocated to within a few microns.

We now envision a manufacturing jig that manipulates and holds the three small pieces of glass in position on the main body. During assembly, the jig would permit the unit to be rotated on precision bearings, perhaps air bearings. The alignment procedure calls for

the retrostrip under assembly to form one part of an interferometer; laser light would be used. Under rotation, the changing fringe pattern would indicate misalignments of the three small pieces of glass. Algorithms have been developed for converting the interferometer fringe pattern into corrections to be made to the positions of the three small pieces of glass. The interferometric measurement is not expected to limit the accuracy of the alignment of the retrostrips. The precision bearings, which should have sub-micron runout, and the devices used to position the small pieces of glass will probably set the limit to the alignment.

3.4 Determination of φ

The angle φ between the baselines of the two interferometers (*i.e.*, the instrument articulation) is determined by the measurements of the six distances among four fiducial points in the system.

$$\cos\varphi = (d_2^2 + d_3^2 - d_1^2 - d_4^2) / 2b_m b_f$$

Here d_i are the four distances between the fiducial points of one interferometer and the fiducial points of the other and b_m, b_f are the baseline distances for each interferometer, *i.e.*,

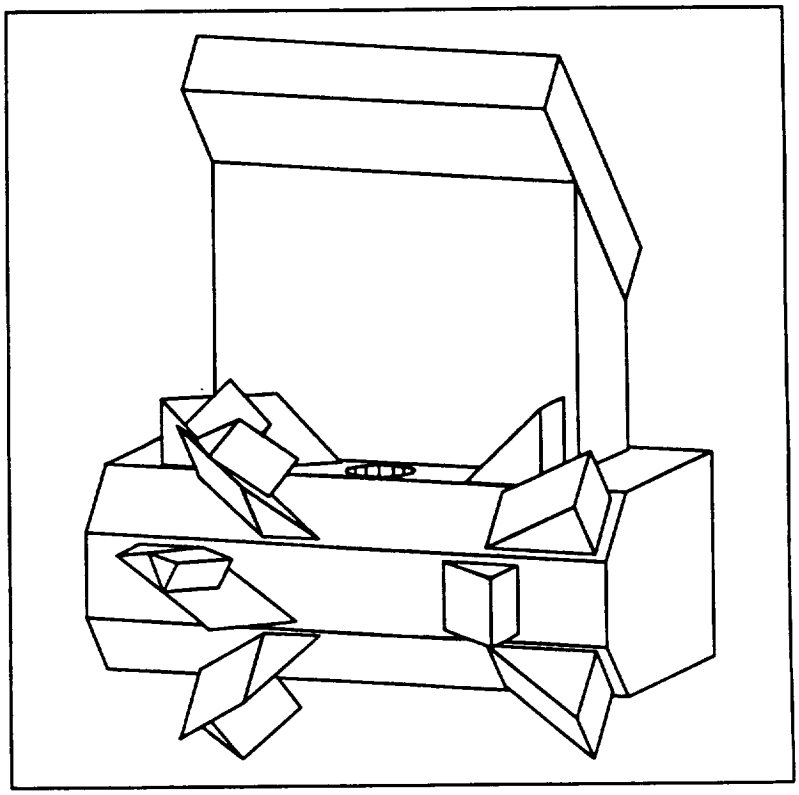

Figure 4. A fiducial block. There are four "retro-strips," each a slice of a truncated cornercube retroreflector, and each to serve as the end point for a laser gauge. The apices of the cornercubes coincide at the fiducial point in this computer-generated engineering sketch.

each is the separation of the fiducial points of one interferometer. Each of the six distances is measured by a laser gauge. (The laser gauges *per se* are discussed in Section 4, where we note that the techniques we have developed easily extend to an absolute distance gauge.) We have investigated the problems associated with the laser gauges reading the distance correctly except for a fixed bias, as would be the case if an incremental gauge were used and the zero point determined crudely by alternative means (*e.g.*, by an encoder on the articulation axis or from the known positions of bright stars observed by startrackers mounted on the interferometer optical benches.) Under these conditions, there would be an additional five parameters of the system that would need to be determined from the astrometric data each time the laser gauges were turned on. Nominally, this would be at the start of the mission only. Our covariance studies show that estimating these parameters poses no problem even if it were decided to estimate them *ab initio* as often as every day.

The metrology system measures the angle between the pseudo-baselines, which are defined by the pairs of fiducial points in the two starlight interferometers. The two (nearly) perpendicular pseudo-baselines define the "interferometer plane." For simple analyses, we assume that each starlight interferometer lies in the interferometer plane. However, we have considered the effects of the following small rotations of each of the starlight interferometers: (1) around the perpendicular to the interferometer plane; (2) around the pseudo-baseline; and (3) around the starlight interferometer's nominal optical axis. The first of these types of rotations yields a bias proportional to the difference of the rotation angles. The other four rotations (two for each starlight interferometer) do not contribute to the measured angle in first order, but do contribute in second order. Thus the latter two types of rotations need to be aligned to somewhat better than an arcsec. In a related study, we are considering how the above rotations and skews could come about from misalignments of the optical elements of the starlight interferometers.

Although the above described metrology system is capable of providing the required precision, it contains many finite-size optical components, each of which will introduce a bias into the measurement of the angle φ. This bias is likely to be time dependent at the microarcsec level. It is essential that we be able to determine and correct for the instrument bias, preferably without the introduction of additional hardware. Because POINTS, like HIPPARCOS, does global astrometry, that bias determination and correction naturally occur when the observations are combined in a least-squares estimate of the individual stellar coordinates (including proper motion and parallax), instrument model parameters, and the expected biases. In particular, our covariance studies have shown that even without the introduction of a special observing sequence, it is possible to estimate simultaneously the stellar coordinates and tens of instrument bias parameters per day. The stellar coordinate estimate uncertainties increase by a factor of $1+0.003\ N_b$, where N_b is the number of bias parameters to be estimated per day, and $M = 5$. (The redundancy factor, M, is defined in Section 6.1.) Thus, metrology biases and related errors can be allowed to change on a time scale of hours without significantly degrading the performance of the instrument. This result allows us to relax the required stability at time-scales longer than 100 minutes of both the

laser used in the metrology and the rest of the instrument. This subject is also discussed in Section 6.

4.0 Laser Gauges

There are several standard means of using laser interferometry to measure distance. The European and American gravity-wave interferometer groups (Man *et al.* 1990, Shoemaker *et al.* 1991) have demonstrated Michelson laser gauges with more than 3 orders of magnitude higher precision than we need, but only for measurements of ultrasonic-frequency vibration. Salomon, Hils, and Hall (1988) have demonstrated DC performance about 5 orders of magnitude better than our requirement, but they used two-mirror cavity interferometers (not corner cubes) with very high quality mirrors. Commercial heterodyne distance gauges using corner cube endpoints (Hewlett Packard Model 5527A, Zygo AXIOM 2/20^{TM}) quote resolution no better than 1.25 nanometers, with systematic errors known to be much larger. Further, with the exception of a few complex and bulky devices, all of the laser gauges provide incremental distance from an initial epoch, not absolute distance.

We have built a research prototype of one of the laser gauges we need using relatively crude interferometer optics and simple, inexpensive equipment. This gauge has met our nominal accuracy requirement for the flight instrument: 2 pm for averaging times from 1 to 100 minutes. The "deviation" plotted in Fig. 5 is a root two-point variance directly analogous to the Allan variance which is used to characterize clock stability[4]. The laser gauge is the subject of a patent application filed 8 May 1992.

Some of the POINTS laser gauges are intended to operate between corner-cube retroreflectors. If the laser beam makes an angle α with the line between the apices of the retros of such a gauge, the measurement is subject to a fractional error of 1-cos(α). Although this error is proportional to α^2, for few-picometer gauge accuracy we require half-arcsec

---

[4] One useful measure of gauge performance is an adaptation of the Allan variance used to characterize clock stability. For each averaging time τ, the Allan variance is defined to be:

$$\sigma_y^2(\tau) \equiv \frac{1}{2(m-1)} \sum_{k=1}^{m-1} (y_{k+1} - y_k)^2$$

where y_k are the frequency-offset averages scaled to the clock frequency. We use the term "deviation" to mean the square root of the analogous variance without scaling:

$$\text{deviation} \equiv \sqrt{\frac{1}{2(m-1)} \sum_{k=1}^{m-1} (L_{k+1} - L_k)^2} = L\sigma_y(\tau)$$

where L is the length being measured and L_k are a set of such measurements averaged over interval τ. This measures the predictability of drifting measurements as a function of the averaging and observation time scale τ.

alignment stability. This can be achieved by a beam-position servo deriving its error signal from a quad cell behind a partially transmitting mirror in the retro.

An enhancement to the performance of the laser gauge comes from operating the pair of retros as a cavity. This configuration permits the removal from the measured path of all the glass (with its temperature-dependent contribution to optical path.) For the cavity to be optically stable, which is desirable but not essential for the gauge to work, there must be some focusing power in at least one of the mirrors that form the retroreflectors. In a recently completed study, we showed that such cavities significantly reduce the effect of misalignment provided that the fringe-detecting photodiode has uniform sensitivity across its face.

We have considered the use of two gauging systems for each measured distance, both to offer redundancy in the picometer-resolution incremental gauging and to enable absolute distance gauging. In particular, reducing the uncertainty in absolute distance to less than the optical wavelength would permit connection with the picometer incremental measurements. This would simplify recovery from a loss of fringe count and would obviate the question of fringe slipping. The repeatable and unambiguous resolution of the integer order of the interferometer requires much higher gauge performance than otherwise needed. However, even significantly less accuracy in the absolute distance measurement would be of value.

POINTS does not require extraordinary laser wavelength stability. Of the nominal measurement uncertainty, 25 picoradians, we assign 5 picoradians to the laser (in a quadrature-sum sense). Fortunately, this does not require correspondingly high laser stability. In the determination of φ, we depend on the ratio of laser-determined distances and therefore

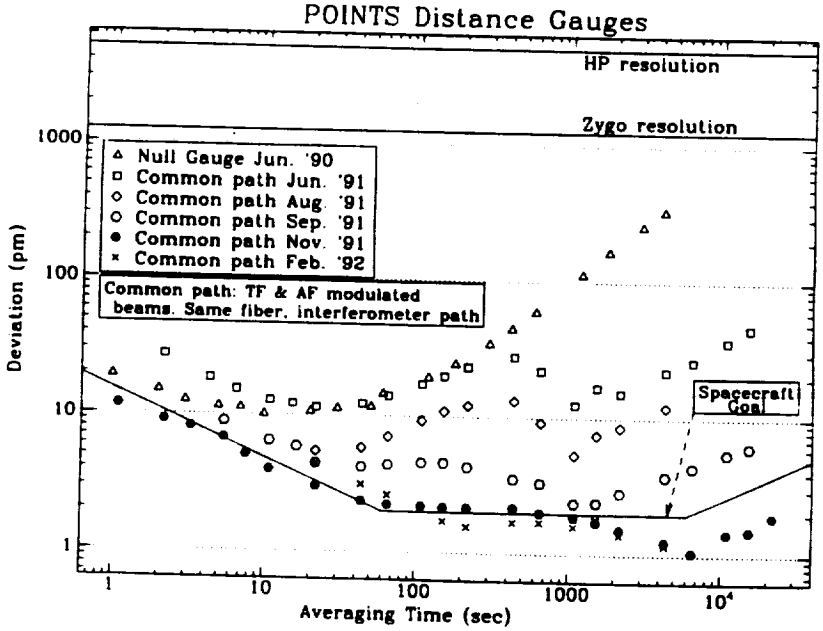

Figure 5. Deviation of the distance measured by the laboratory laser gauge.

laser frequency shifts cancel. (Secondary effects limit this cancellation at about the 10^{-3} level.) In the FAM system, the quantity being measured (with 10 pm accuracy) is the difference between two nominally equal paths, which should be under 1 mm, and laser frequency shifts would affect only this difference. Thus, the stability in either system need not be better than 10^{-9}, and that stability is required only for time scales from 1 to 100 minutes.

Recently there has been a rapid evolution of the technology of lasers suitable for space missions of several years duration. There are at least two solid-state laser technologies which can meet the POINTS requirement: external-cavity diode lasers (Harrison and Mooradian 1986), and diode-laser-pumped solid-state lasers (Byer 1988). The former have already demonstrated both drift over one hour and linewidth of under 100 kHz, which is a little better than required by POINTS. The latter have demonstrated sub-Hz linewidth when locked to a reference cavity. In either case, to achieve the required long term stability, it may be helpful to make the cavity of a stable material such as Premium ULE®, which has a thermal expansion coefficient $|\alpha|$ 5 $\times$ 10^{-9} / deg C; its temperature would be held stable over a period of hours to better than 10^{-2} K.

In diode-laser-pumped solid-state lasers, the pump diode can be made multiply redundant by coupling diodes to each of several facets of the lasing crystal. Even with multiple pump sources, diode lasers with a long life will be required. Units with 28 and 100 mW output, amply sufficient for POINTS, have already been space qualified for two missions, with a specified Mean Time To Failure (in one of the missions) of 250,000 hrs (>25 yrs). They are available from Spectra Diode Labs, Mountain View, CA.

4.1 Spacecraft Gauge Design Considerations

There were several architectural considerations in the design of laser gauges for the POINTS instrument. Both path-difference and point-to-point distance measurements are needed in the spacecraft. The fiducial blocks are designed around hollow corned cubes for three reasons. (1) The corner cube properly returns the beam even under rotations around its apex, as will occur during articulation. (2) A uniform thermal expansion of the glass does not change the measured distance. (3) The corner cube apex provides a well-defined endpoint of the measured length. In the design we use, the corner cubes form cavities, and there is no need to place glass in the optical path under measurement. The light is injected and extracted through partially reflecting mirrors.

Distance measurements need to be made to 10^{-5} λ. Such a measurement would be much more difficult if it needed to determine directly an arbitrary fraction of a wavelength than if it were locked to a convenient phase and used a null technique. We therefore extended our earlier successful work with the alternating frequency null gauge to the tracking frequency gauge described below.

It is advantageous to use modulation techniques to lock to a minimum or maximum in the transmitted intensity: DC drift can be quite small, and the modulation frequency may be chosen in a region of low photodiode and amplifier noise. For modulation, dithering the interferometer length is a poor choice since the actuator that imposes it may add serious DC drift and synchronously-varying misalignment, and the optic that is shaken may be too delicate or heavy for rapid modulation. Thus the natural choice is frequency modulation (Drever 1983). In turn, this demands that the interferometer output be sensitive to the laser frequency (implying an OPD of many centimeters in a Michelson). Thus the interferometer outputs must be periodic in both the length and the optical frequency. The period in optical frequency (c/OPD for a Michelson or c/2L for a cavity) is known as the free spectral range (FSR). To maintain the intensity minimum, the servo may either adjust the measured distance with an actuator or retune the laser to track the distance change. In the latter tracking-frequency approach, we measure the frequency offset needed to stay at the minimum; this is proportional to the distance change.

4.2 Laboratory Apparatus and Results

Our prototype Michelson system incorporates both the distance actuator and tracking frequency approaches. Light from a single laser supplies two separate distance gauging systems; both systems measure the same OPD. The signal from the first gauge is used to servo the interferometer OPD to be a constant multiple of the laser wavelength λ. The signal from the second gauge is used to regulate the frequency offset $\delta\nu$ required to reach an adjacent interferometer null. Since the interferometer length is controlled to be an integer number of wavelengths, this frequency offset is expected to be constant. Any variations in that offset may be attributed to noise and systematic errors in one or both of the gauges and to the failure of the OPD servo (*e.g.*, from insufficient gain) to remove the OPD fluctuations. This comparison technique, common in tests of clock and laser stability, allows us to test the gauge performance with picometer resolution despite micron-scale length variations due to air turbulence and the supporting structure.

The first of the two gauge systems was based on an older design using 5 kHz toggling of the laser frequency. A portion of the light from a commercial Zeeman-stabilized HeNe laser is sent through a double-pass acousto-optic frequency shifter, which shifts the optical frequency by Bragg diffraction from a moving RF acoustic wave in a crystal. The RF drive for the acousto-optic modulator toggles at 5 kHz between two crystal-controlled frequencies, 32 and 40 MHz. The emerging laser beam likewise toggles at 5 kHz between two frequencies, 64 MHz and 80 MHz away from the frequency of the HeNe laser. The beam passes through a single-mode polarization-preserving optical fiber and a linear polarizer, and enters the Michelson interferometer. The interferometer has an OPD near 1 m, yielding an FSR of about 300 MHz. The physical structure is approximately temperature-compensated ($\approx$200 nm/deg C) such that the temperature coefficient of OPD due to air dominates. The two alternating frequencies of the injected laser beam land to either side of the intensity minimum to which we are locking. A photodiode detects the 5 kHz square-wave variations at the output of the Michelson interferometer due to detuning of the average optical frequency from

this minimum. A lock-in amplifier demodulates the signal at 5 kHz and feeds it to a servo filter. A high-voltage amplifier boosts this signal to drive a piezo-electric crystal, which pushes one of the interferometer endpoints. A second photodiode records the AM present on the beam at the input of the interferometer. This signal is demodulated in another lock-in amplifier and fed back to control the RF power that drives the acousto-optic device; this regulates the AM on the injected beam to essentially zero. The OPD measurements were made in air, and thus required considerable gain in the servo to remove the effects of air turbulence and temperature fluctuations, neither of which is a consideration in the performance of the gauge in the spacecraft.

With the interferometer OPD thus fixed (as a multiple of the laser wavelength), we remeasure the OPD using the tracking frequency method. A second portion of the light from the HeNe laser passes through a second double-pass acousto-optic frequency shifter driven by a voltage-controlled oscillator (VCO) at about 138 MHz; this system shifts the laser frequency by a slowly varying amount. The beam passes through an electro-optic crystal, where it acquires phase modulation at 8 MHz with modulation index of order 1. This beam is combined with the first at a beamsplitter before entering the optical fiber; thus the two beams exit the fiber and enter the interferometer very precisely overlapped. The second beam (about 300 MHz away from the first) interrogates the interferometer fringe one FSR away from the first. The two forms of modulated light are detected by the same photodiodes, but the 8 MHz AM signals are separately amplified and sent to RF mixers for phase-sensitive detection. The demodulated signal from the second light modulator is filtered and sent to the frequency-control input of the VCO to keep the second beam tuned to the intensity minimum. The frequency of the VCO is monitored as an indication of the distance measurement errors, which may originate in either the alternating-frequency system or the tracking frequency system. The demodulated signal from the other photodiode is either monitored as an indication of the AM on the injected beam or used in a servo to control the 8 MHz AM (Wong and Hall 1985).

Figure 5, which resulted from the recent work with this gauge, shows the deviation falling to around 2 pm for averaging times between 44 seconds and 6 hours. Note that this data record extended for more than 90 hours. This meets or exceeds the spacecraft requirements as presently understood.

The apparatus presently contains only commercially-available equipment and some ordinary mechanical and electronic devices made at SAO. Systematic error sources that were controlled to the required level include electronic effects such as RF pickup and nonlinearities, and AM resulting from interferences within the optical fiber. However, because the beams from the two gauge systems overlapped so precisely in the interferometer, many systematic effects were suppressed; they include beam motion across the endpoint mirror surfaces, thermal gradients in the interferometer optics, differential cosine errors, and polarization variations.

5 SPACECRAFT DESIGN

The POINTS spacecraft will contain the usual set of systems to support the instrument: telecommunications, attitude control, power, and computation. The spacecraft bus will be equipped with a single axis scan platform for the instrument, and may require an isolator to keep jitter from entering the instrument from the spacecraft. The other two degrees of rotational freedom will be provided by rotating the bus in inertial space. That rotation will be constrained by the requirement that the Sun shield keep the bus and instrument housing in shadow at all times. The bus' degrees of rotational freedom are thus around the pivot that joins it to the Sun shield and (with the shield) around the direction to the Sun. A paper describing the spacecraft is in preparation by Schumaker *et al.* (1993).

Within the instrument, there is an articulation mechanism that sets φ. This mechanism must permit about 0.1 radian of motion and should have a resolution of order 0.1 arcsec: 2 10^5 steps. Of course, during observations, the combination of the articulation pivot and drive must be stiff in all six degrees, especially in the rotation that changes φ.

The solar cell array is mounted on a set of "flip-out" panels that form a skirt around the Sun-facing end of the spacecraft. See Fig. 1. As discussed below, this shield is important in permitting large coverage of the sky while not violating the requirement that the instrument enclosure be shielded at all times from the direct light of the Sun.

The question of sky coverage is normally considered in the context of an instrument with a single pointing direction and exclusion angles for the Sun, Earth, and Moon. For POINTS, the problem is more complicated because the instrument needs to look simultaneously in two directions about 90 deg apart. Thus it takes four angles to describe the phase space of the sky coverage. For the purpose of calculating sky coverage, we constrain the target separation to be 90 deg, reducing the number of independent angles to three. We may neglect both the Earth and Moon exclusions since we are willing to wait a few hours for any particular measurement. (The nominal orbit is circular at 100,000 km, which has a four day period.) Thus we are left considering only the spacecraft and the Sun. The line between them is an axis of symmetry. Rotation about that axis can be neglected in discussion and analysis of sky coverage; there are only two nontrivial angles.

In our sky-coverage study, the first parameter was $\cos(\gamma)$, where γ is the angle between the anti-Sun direction and the first star, as seen from the spacecraft. The second parameter was ω, the Sun-star1-star2 angle on the celestial sphere centered on the spacecraft, *i.e.*, the angle between the planes defined by: (a) spacecraft, Sun, and star1; and (b) spacecraft, star1, and star2. The study maps out the portion of phase space that is accessible. With this choice of parameters, the area in the "$\cos(\gamma)$ - ω plane" is proportional to the volume of phase space. With the nominal configuration, 83% of phase space is accessible at any one time, and stars in 99.1% of the sky can be observed, but some with a limited range of ω. (Stars in 98.5% of the sky can be observed with a cumulative range of ω of at least 180 deg.) In all cases, the

stars or star pairs that cannot be seen at a particular time can be seen a few weeks earlier or later.

The original work has been extended to address the relationship between the available volume of phase space and the size of the solar shield. Increasing the size of the shield increases the sky coverage for shields similar in size to the nominal, which has a 30 m^2 area. However, saturation of sky coverage is found for shields with diameters larger than about 7m.

6 MISSION OPERATIONS

Here we consider five aspects of mission operations: normal operation of the instrument, the effect of a faint companion, data analysis, the search for other planetary systems, and in-orbit testing. We do not discuss detailed target selection since there is an overabundance of interesting targets and the actual selection will depend strongly on which division of OSSA sponsors the mission.

6.1 Normal Instrument Operations

Our understanding of the characteristics of the instrument's operation is based on a series of covariance studies and simulations. Since POINTS is a "global astrometric instrument," all well-observed objects can and will be made to contribute to the stability of the reference frame used for each observation. In turn, each object that contributes to the reference-frame stability can and will be studied astrometrically and its motions modelled. A small number of observations of quasars will connect the POINTS reference frame to the best available candidate for an inertial frame. Table 1 lists the number of BL-Lac objects, quasars, and Seyfert galaxies of magnitude 15 or brighter from the catalog of Veron-Cetty and Veron (1991). Finally, because of the ≈ 90 deg separation of the target pair, for any target, there is always a large number of bright reference stars among the set of well studied objects.

Our performance analyses assume the target to be an isolated, unresolved point source, *i.e.*, one with no significant structure. In practice, this condition will not always be met. Star spots, flares, *etc.* will set the limit to the accuracy of the astrometric measurement of the center of mass of some targets. We may gain useful information about some stars from the motions of their centers of light. At 10 pc, the Sun has a magnitude of 5. A shift of its center of light by 0.1% of the Sun's diameter, which is the largest one expects from sunspots, would cause an apparent astrometric shift of nearly 0.5 μas. For some active stars, the effect is much larger. The effect of a companion star is addressed in Section 6.2.

When an observation set has sufficient redundancy, it can be analyzed to yield a rigid frame; it serves to determine the angular separation of all pairs of observed stars, even those that were not observed simultaneously. The redundancy is measured by M, the ratio of the number of observations to the number of stars observed, which must be greater than about 3.5 to yield a rigid frame. With moderate redundancy (M=4.2), the uncertainty in the separation of all star pairs (a majority of which could not be observed directly because they

Table 1. Number of reference objects of magnitude m or brighter			
m	NUMBER OF OBJECTS		
	BL-Lac	Quasar	Seyfert
10	1	0	0
10.5	1	0	0
11	6	0	0
11.5	9	0	0
12	23	0	0
12.5	38	1	1
13	61	2	1
13.5	99	5	3
14	166	13	5
14.5	266	23	7
15	381	49	15

are not separated by $\approx 90°$), is about equal (on average) to the instrument measurement uncertainty. The grid is free of regional biases and may be further strengthened by additional data obtained when the grid stars are used as reference stars for additional science targets.

If we use 300 grid stars plus a few quasars and take M = 5, then the observation series requires about five days at the nominal rate of 350 observations per day. Such a series could be repeated four times a year to provide not only coordinates but proper motions and parallaxes for the stars. Our Monte Carlo covariance studies show that after ten years the coordinate uncertainties are ~0.6 μas, the proper motion uncertainties are ~0.2 μas per year, and the parallax uncertainties are ~0.4 μas (Reasenberg 1986; Reasenberg, 1991.) Note that this parallax determination is a factor of 2 better than one would naively calculate from the coordinate uncertainties in a single series. The reason for this enhancement is that the 90 deg nominal angle of POINTS results in direct observations of "absolute parallax."

Recall that in Section 3.4 we noted that instrument biases can be determined from the analysis of an astrometric data set by virtue of the closure information it contains. The analysis would include a time-dependent bias model for each observing sequence such that the residual bias would be small compared to the measurement uncertainty. The appropriate form of the bias model will depend on a detailed understanding of bias mechanisms that we expect to acquire in later stages of design. Exploratory studies during the mission will be aimed at uncovering bias mechanisms not identified before launch. The operational bias model will be augmented accordingly.

In other Monte Carlo covariance studies, we investigated the ten-year observing sequence with fewer observations. We found that observations can be deleted from the series by a variety of random or systematic procedures yielding an increase in the mean parameter-estimate uncertainty which depends principally on the square root of the total number of observations. Further, additional stars can be added to the observation sequence with a minimal number of observations (perhaps 20) per star.

6.2 Faint companions and immunity from biasing signals

Some target stars will be undetected binaries. (The statistics of star densities on the sky indicate that accidental companions close enough and bright enough to have a biasing effect are too rare to be of interest except in particularly dense star fields, *e.g.*, globular clusters.) We have shown that: (a) If the separation between the stars is small compared to the resolution of the interferometer baseline ($\lambda/L \sim 0.05$ arcsec), then the instrument tracks the center of light; (b) A well separated companion is ignored. For an unexpected companion one magnitude fainter than the target, at a 1 arcsec separation (in the interferometer plane) the biasing effect is small compared to the nominal measurement accuracy, and; (c) Between these extremes, the offset of the apparent position of the target from its true position varies as a sinusoid (of generally decreasing amplitude) in the star-pair separation.

The above analysis assumed the star and its companion were modelled as a single source, and that they had the same temperature -- a worst case. If the separation is comparable to or greater than the resolution of the interferometer baseline, or if the two stars have known different spectra, then their separation can be determined from the distortion of the channelled spectrum. With measurements of a known binary against several reference stars, the accuracy of the separation measurement is only slightly worse than would be obtained for the position of the dimmer star if the companion were absent. Equally important, the distortion of the channelled spectrum will reveal that the source is a previously unknown binary so that biased measurements can usually be avoided. Finally, we note that if the channelled spectra are preserved and if a previously undetected binary is revealed, the old data can be reanalyzed to removed the bias due to the companion.

6.3 Data analysis, iterative and global nature

Although the mission will support a large and diverse set of science objectives, we picture much of the data analysis as being done centrally because one worker's target is everybody's reference star. The effort required will depend on the degree to which we need to use spacecraft engineering data to help understand systematic errors. In any case, it is not a complex effort nor does it require special computing facilities. If the data were available today, the central analysis could be done on a desk-top workstation. The effort would require a single analyst and would result in a reduced dataset that would be sent to the participating scientists for further analysis leading to publishable results.

Early in the mission, the analysis will be limited to positions determined during observing periods of a few to a few tens of days. Of course, the best *a priori* proper motions and parallaxes will be included in the analysis model although these will have little effect. Timely analysis early in the mission will permit instrument problems to be detected without undue loss of data. At about one year, it will become possible to estimate the full set of five parameters (position [2], proper motion [2], and parallax [1]) for each star. The stability of the solution should increase considerably during the second year.

After about two years of observation, the postfit residuals from the data reduction will be used to investigate irregularities in the motions of individual stars. Their apparent motions will be analyzed both for the intrinsic scientific interest and to improve the stability of the resulting reference frame. Initially, the position of each star will be determined with respect to the mean of the positions of all the stars. After the initial modeling of the irregularities in stellar proper motions, the position of each star will be determined with respect to the nominal modelled reference positions of all the stars. Based on recent Monte Carlo covariance studies, we know that this iterative procedure converges quickly. The global motion of the frame will be controlled by the quasars included in the set of observed objects.

6.4 Planetary system detection

If there are Jupiter-size bodies orbiting nearby stars, the astrometric wobble seen from the solar system will be two orders of magnitude larger than the POINTS single-measurement uncertainty. However, the wobble will be distinguishable from proper motion only when the observations span a significant fraction of an orbital period. We performed Monte Carlo mission simulations with single planets around stars of the reference grid. Planets orbiting stars not in the grid should be an easier analysis problem because omitting them from the model will not distort the reference grid solution. Preliminary studies confirm that multiple-planet systems will make greater demands on the observing system and the data analysis. This subject will require further study.

In the first simulations, it became clear that knowing the right answer made the analyst's task much easier. To make the simulations more realistic, we developed a "double blind" methodology. A person other than the analyst would prepare an input file for the simulation program. The file contained a "seed" for the random number generator and ranges for mass, radius, eccentricity and number of planets. Until a simulation was completed, no one knew how many planets were included or which stars they orbited, and the analyst didn't know what ranges of the parameters were used for the simulation.

Searching for planets is an iterative procedure. The analysis procedure identifies candidates for planet modelling and optimizes parameters to minimize the RMS error. Since this is not a linear system, these two tasks interact. Initially, the model includes only star coordinates, parallaxes, and proper motions. Postfit residuals for observations involving each star are examined for power at a comb of frequencies. The largest signals flag candidates for planet modelling in the next iteration. But, since a star may be measured against one or more stars which have unmodelled companions, power in the residuals does not always correspond to a real planet. Fortunately, the procedure is robust; spurious planet models converge to near zero mass or otherwise reveal themselves as the iterations proceed.

Simulations had a 100-star grid and 20-50 planets with signatures ranging from 0.002 to 1 Jove and periods of 1-20 years. A mission lasted 10 years, and all observable star pairs were observed quarterly with the articulation range set to yield M=5. Planets were detected with greater than 90% probability for signatures between 0.01 and 0.05 Jove, and with 100%

above 0.05 Jove; sensitivity dropped rapidly below 0.01 Jove. All six orbital elements could be determined in 80% of the cases with signatures larger than 0.01 Jove. Where not all orbital elements could be determined, generally edge-on observing geometry or orbital periods substantially longer than the mission length were found. Detections were reliable; there were no false alarms in the studies.

6.5 In-orbit Testing and Performance Verification

There are three approaches to the in-orbit evaluation of the instrument. On the shortest time scale, a few pairs of stars will be chosen as calibrators. They will be observed regularly to provide a measure of short-term reproducibility of the measurements. Throughout the mission, the instrument bias will be estimated. The history of the estimated bias will be compared to pre-flight engineering estimates of its characteristics. Additional least-squares solutions for astrometric parameters and biases will be obtained with an enlarged bias set as a means of uncovering unexpected instrument behavior. Finally, the postfit residuals from the analysis will be a measure of the performance of the instrument. Astrometrically uninteresting, isolated stars will be important in understanding the instrument performance.

7 ACKNOWLEDGEMENT

The development of POINTS has been supported by NASA through Innovative Research Program Grants NSG 7176 and NAGW 1647 from OSSA and Grants NAGW 1355 and NAGW 2497 from the Solar System Exploration Division of OSSA. It has also been supported by the Smithsonian Institution both directly and through it's Scholarly Studies Program. During the past two years, there has been a team working on POINTS under the leadership of B.L. Schumaker at the Jet Propulsion Laboratory. The JPL team has contributed in many ways to our understanding of POINTS and thus to the description in this paper.

8 REFERENCES

Babcock, R.W., H.W. Marshall, R.D. Reasenberg, and S. Reasenberg, 1988. "Full Aperture Metrology for High Precision Astrometry," in Topical Meeting on Space Optics for Astrophysics and Earth and Planetary Remote Sensing, (Falmouth, MA, 27-29 September 1988), 1988 Technical Digest Series, Vol. 10 , pp. 25-27, Optical Society of America, Washington, DC.

Byer, R.L. 1988. "Diode Laser-Pumped Solid State Lasers," Science, 239, 742-7.

Drever, R.W.P., Hall, J.L, Kowalski, F.V., Hough, J., Ford, G.M., Munely, A.J., and Ward, H., 1983. "Laser Phase and Frequency Stabilization Using an Optical Resonator," Appl. Phys. B, 31, 97.

Eddy, J.A. 1979. A New Sun: The Solar Results from Skylab, NASA SP-402, NASA, Washington, DC, p. 47.

Harrison, J. and A. Mooradian, 1986. Methods of Spectroscopy, Yehiam Prior *et al.* Eds., p. 133 (Plenum Publishing).

Hils, D., and J.L. Hall, 1990. "Improved Kennedy-Thorndike Experiment to Test Special Relativity," Phys. Rev. Lett., 64, 15, p. 1697.

Kovalevsky J., 1984. "Prospects for Space Stellar Astrometry," Space Sci. Rev., 39, 1, D. Reidel Publishing Co., Dordrecht/Boston, pp. 1-63.

Man, C.N., D. Shoemaker, M. Pham Tu and D. Dewey, 1990. "External modulation technique for sensitive interferometric detection of displacements," Phys. Lett. A, 148, 1, 8.

Mariotti, J.M. (in press 1993). To appear in The Proceedings of the Colloquium on Targets for Space-Based Interferometry, European Space Agency (ESA) Meeting, Beaulieu-sur-Mer, France, 13-16 October 1992.

Massa, D., and A.S. Endal, 1987. "An Instrument for Optimizing a Spaceborne Interferometer: Application to Calibrating the Cepheid Distance Scale," Astron. J., 93(3), 760.

National Academy of Sciences, 1991a. The Decade of Discovery in Astronomy and Astrophysics, National Academy Press, Washington, DC.
— 1991b. Working Papers, Astronomy and Astrophysics Panel Reports, National Academy Press, Washington, DC.

Reasenberg, R.D., 1980. "Experimental Gravitation with Measurements Made Within a Planetary System," in Proceedings of the Sixth Course of the International School of Cosmology and Gravitation, (a series of four lectures presented at the Ettore Majorana Center for Scientific Culture, International School of Cosmology and Gravitation, Sixth Course: Spin, Torsion, Rotation and Supergravity, 6-18 May 1979) Ed. by P. Bergmann and V. deSabbata, pp. 317-357, Plenum Press, New York.

Reasenberg, R.D., 1981. "Astrometric Instruments in Space," Technical Memorandum 81-4 to D.C. Black. See esp. pp 10-12.

Reasenberg, R.D., 1982. "The Solar System: A Cluttered Laboratory for Gravity Research," in Proceedings of the Second Marcel Grossmann Meeting on General Relativity, (International Centre for Theoretical Physics, Trieste, Italy, July 1979), Ed. by R. Ruffini, pp. 1019-1038, North-Holland Publishing.

Reasenberg, R.D., 1984. Microarcsecond Astrometric Interferometry, in Proceedings of the Workshop on High Angular Resolution Optical Interferometry from Space, (Baltimore, 13 June 1984), Ed. by P.B. Boyce and R.D. Reasenberg, BAAS, 16, 758-766.

Reasenberg, R.D., 1986. Microarcsecond Astrometric Interferometry, in Proceedings of IAU Symposium 109, Astrometric Techniques (Gainesville, 9-12 January 1984), Ed. by H.K. Eichorn and R.J. Leacock, pp. 321-330 (Reidel, Dordrecht).

Reasenberg, R.D., 1991. Precession Optical Interferometry in Space, in Proceedings of The First William Fairbank Meeting on Relativistic Gravitational Experiments in Space, Rome, September 10-14, 1990.

Reasenberg, R.D. and I.I. Shapiro, 1979. "POINTS, the Planet Finder," BAAS, 11, 554. Presented at the AAS/DPS Meeting 11, Clayton, Missouri, 23-26 October 1979.

Reasenberg, R.D. and I.I. Shapiro, 1982. "An Optical Interferometer in Earth Orbit for Testing General Relativity," in Space Relativity -- Acta Astronautica, 9, (Proceedings of the 5th International Symposium on Space Relativity, Dubrovnik, Oct. 78), Ed. by W. Wrigley, 103-106.

Reasenberg, R.D., R.W. Babcock, J.F. Chandler, M.V. Gorenstein, J.P. Huchra, M.R. Pearlman, I.I. Shapiro, R.S. Taylor, P. Bender, A. Buffington, B. Carney, J.A. Hughes, K.J. Johnston, B.F. Jones, and L.E. Matson, 1988. "Microarcsecond Optical Astrometry: An Instrument and Its Astrophysical Applications," Astron. J., 32, 1731-1745.

Reasenberg, R.D., R.W. Babcock, J.D. Phillips, M.C. Noecker, (in press 1993) "Space-Based Astrometric Optical Interferometry with POINTS." To appear in The Proceedings of the Colloquium on Targets for Space-Based Interferometry, European Space Agency (ESA) Meeting, Beaulieu-sur-Mer, France, 13-16 October 1992.

Salomon, Ch., D. Hils, and J.L. Hall, 1988. "Laser stabilization at the millihertz level," J. Opt. Soc. Am. B, 5, 8, 1576.

Shoemaker, D., P. Fritschel, J. Giaime, N. Christensen, R. Weiss, 1991. "Prototype Michelson interferometer with Fabry-Perot cavities," Appl. Opt., 30, 22, 3133.

Traub, W.A., 1990. "Constant-dispersion grism spectrometer for channelled spectra," Opt. Soc. Am. A., 7, 9, p. 1779.

Veron-Cetty, M.P. and P. Veron, 1991. A Catalogue of Quasars and Active Nuclei, 5th Edition, E.S.O. Sci. Rep., 10.

Wong, M.C., and J.L. Hall, 1985. "Servo control of amplitude modulation in frequency-modulation spectroscopy: demonstration of shot-noise-limited detection," J. Opt. Soc. Am. B, 2, 9, 15271.

Technical Program

SPIE's

OE/Aerospace and Remote Sensing

1993 International Symposium and Exhibition on Optical Engineering and Photonics in Aerospace and Remote Sensing

12–16 April 1993
Marriott's Orlando World Center
Resort and Convention Center
Orlando, Florida USA

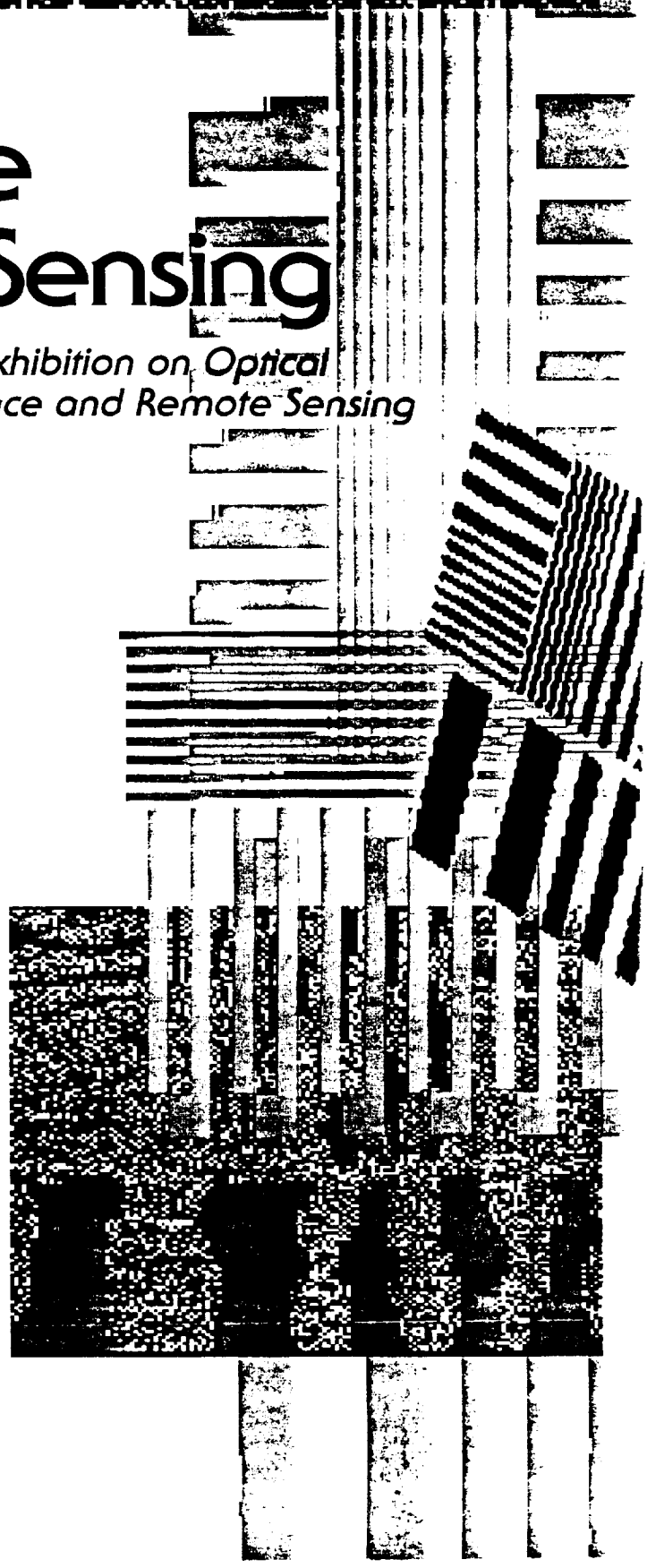

Technical Conferences
Educational Short Courses
On-Site Employment Center

Technical Exhibition
Coordination and Promotion by
PHOTONICS SPECTRA

Symposium Chair:
Philip N. Slater,
Optical Sciences Ctr./Univ. of Arizona

Sponsored by
SPIE—The International Society for Optical Engineering

Two Days ■ Thursday–Friday 15–16 April 1993 ■ SPIE Proceedings Vol. 1947

Spaceborne Interferometry

Conference Chair: **Robert D. Reasenberg,** Smithsonian Astrophysical Observatory
Cochairs: **Robert A. Laskin,** Jet Propulsion Lab.; **M. Charles Noecker,** Smithsonian Astrophysical Observatory; **Stuart B. Shaklan,** Jet Propulsion Lab.; **Wesley A. Traub,** Smithsonian Astrophysical Observatory

Thursday 15 April

OPENING REMARKS

Crystal B ..... **Thurs. 8:15 am**

Robert D. Reasenberg, Smithsonian Astrophysical Observatory

SESSION 1

Crystal B ..... **Thurs. 8:20 am**

Chair: **F. Peter Schloerb,** Univ. of Massachusetts/Amherst

8:20 am: **Scientific support for an astrometric interferometry mission** *(Invited Paper),* S. T. Ridgway, Kitt Peak National Observatory ..... [1947-01]

9:05 am: **POINTS: the first small step** *(Invited Paper),* R. D. Reasenberg, R. W. Babcock, M. C. Noecker, J. D. Phillips, Smithsonian Astrophysical Observatory ..... [1947-02]

9:50 am: **Fringe tracking filters for space-based interferometers,** C. E. Padilla, H. M. Chun, L. E. Matson, Photon Research Associates, Inc.; R. D. Reasenberg, Smithsonian Astrophysical Observatory ..... [1947-03]

Coffee Break ..... 10:10 to 10:45 am

10:45 am: **Analysis of structural and optical interactions of the precision optical interferometer in space (POINTS),** J. W. Melody, H. C. Briggs, Jet Propulsion Lab. ..... [1947-04]

11:05 am: **Spacecraft and mission design for the precision optical interferometer in space (POINTS),** B. Schumaker, A. Agronin, G. Chen, W. Ledeboer, J. Melody, D. Noon, J. Ulvestadt, Jet Propulsion Lab. ..... [1947-21]

11:25 am: **SISTERS: a space interferometer for the search for terrestrial exo-planets by rotation shearing,** P. Y. Bely, C. J. Burrows, Space Telescope Science Institute; F. J. Roddier, Univ. of Hawaii/Manoa; G. Weigelt, Max-Planck-Institut für Radioastronomie (FRG); M. Bernasconi, Ours Foundation (Switzerland); ..... [1947-05]

11:45 am: **Simulated images from rotating tethered interferometers in earth orbit,** A. B. DeCou, Northern Arizona Univ. ..... [1947-06]

Lunch/Exhibit Break ..... 12:05 to 1:45 pm

SESSION 2

Crystal B ..... **Thurs. 1:45 pm**

Chair: **M. Charles Noecker,** Smithsonian Astrophysical Observatory

1:45 pm: **HARDI-II: a high angular resolution deployable interferometer for UV observations of nearby stars** *(Invited Paper),* P. Y. Bely, C. J. Burrows, Space Telescope Science Institute; H. J. Lamers, SRON Lab. for Space Research (Netherlands); F. J. Roddier, Univ. of Hawaii/Manoa; G. Weigelt, Max-Planck-Institut für Radioastronomie (FRG) ..... [1947-07]

2:30 pm: **Orbiting stellar interferometer (OSI)** *(Invited Paper),* M. Shao, Jet Propulsion Lab. ..... [1947-08]

3:15 pm: **Micro-precision interferometer testbed: system integration of control structure interaction technologies,** G. W. Neat, L. F. Sword, B. E. Hines, R. Calvet, Jet Propulsion Lab. ..... [1947-09]

Coffee Break ..... 3:35 to 4:05 pm

4:05 pm: **Design and fabrication of precision truss structures: application to the micro-precision interferometer testbed,** L. F. Sword, Jet Propulsion Lab.; T. G. Carne, Sandia National Labs. ..... [1947-10]

4:25 pm: **Optical design issues for the micro-precision interferometer testbed for space-based interferometry,** B. E. Hines, Jet Propulsion Lab. ..... [1947-11]

4:50 pm: **Application of an integrated modeling tool to address control system design issues on the micro-precision interferometer testbed,** J. W. Melody, G. W. Neat, H. C. Briggs, Jet Propulsion Lab. ..... [1947-12]

Continued

Conference 1947 ■ Crystal Ballroom, Salon B

Friday 16 April

OPENING REMARKS

Crystal B ..... **Fri. 8:20 am**

Robert D. Reasenberg, Smithsonian Astrophysical Observatory

SESSION 3

Crystal B ..... **Fri. 8:30 am**

Chair: **Robert D. Reasenberg,** Smithsonian Astrophysical Observatory

8:30 am: **Precision mechanisms for space interferometers** *(Invited Paper),* M. L. Agronin, Jet Propulsion Lab. .... [1947-13]

9:00 am: **Actively cophased interferometry with Sun/Simuris** *(Invited Paper),* L. Dame, Service d'Aeronomie CNRS (France) ..... [1947-14]

9:40 am: **Internal laser metrology for POINTS,** M. C. Noecker, J. D. Phillips, R. W. Babcock, R. D. Reasenberg, Smithsonian Astrophysical Observatory ..... [1947-22]

10:00 am: **Laser metrology gauges for OSI,** Y. Gursel, Jet Propulsion Lab..... [1947-15]

Coffee Break ..... 10:20 to 11:00 am

11:00 am: **Optical truss and retroreflector modeling for picometer laser metrology,** B. E. Hines, J. K. Wallace, Jet Propulsion Lab..... [1947-16]

11:20 am: **Optic-misalignment tolerances for the POINTS interferometers,** M. C. Noecker, M. A. Murison, R. D. Reasenberg, Smithsonian Astrophysical Observatory .. [1947-23]

11:40 am: **High-precision astrometry of crowded fields by interferometry,** J. W. Yu, S. B. Shaklan, Jet Propulsion Lab. ..... [1947-17]

Lunch Break ..... Noon to 1:30 pm

SESSION 4

Crystal B ..... **Fri. 1:30 pm**

Chair: **Michael L. Agronin,** Jet Propulsion Lab.

1:30 pm: **Materials for space interferometers** *(Invited Paper),* B. P. Dolgin, Jet Propulsion Lab..... [1947-19]

2:10 pm: **Imaging interferometry lessons from the ground** *(Invited Paper),* F. P. Schloerb, Univ. of Massachusetts/ Amherst ..... [1947-20]

2:50 pm: **Point design for the orbiting stellar interferometer,** J. W. Yu, M. Shao, M. M. Colavita, M. D. Rayman, R. Mostert, Jet Propulsion Lab..... [1947-18]

3:10 pm: **Newcomb, a precursor mission with scientific capability,** R. D. Reasenberg, R. W. Babcock, Smithsonian Astrophysical Observatory; K. J. Johnston, Naval Research Lab.; J. D. Phillips, Smithsonian Astrophysical Observatory; R. S. Simon, Naval Research Lab..... [1947-24]

3:30 pm: **Newcomb, the spacecraft and mission,** R. S. Simon, M. A. Brown, A. Clegg, N. Davinic, M. Fisher, K. J. Johnston, M. Levenson, Naval Research Lab.; R. D. Reasenberg, Smithsonian Astrophysical Observatory ..... [1947-25]

Journal Papers, Proceedings Papers, and Published Reports

1. J.F. Chandler and R.D. Reasenberg, "POINTS: A Global Reference Frame Opportunity," in Inertial Coordinate System on the Sky, J.H. Lieske and V.I. Abalakin, eds. Kluwer Academic Publisher, Dordrecht, pp. 217-227, 1990.

2. J.D. Phillips, R.D. Reasenberg, and M.C. Noecker, "Progress Report on a Picometer Null-Sensing Distance Gauge," in the Proceedings of the JPL Workshop on Technologies for Optical Interferometry in Space (30 April-2 May 1990), Astrotech 21 Workshops Series II, Mission Concepts and Technology Requirements, JPLD-8541, Vol. 1, S.P. Synnott, Ed., 15 September 1991.

3. R.D. Reasenberg, "POINTS: A Small Astrometric Interferometer," in Proceedings of the JPL Workshop on Science Objectives and Architectures for Optical Interferometry in Space, (Pasadena, 12-13 March 1990), M. Shao, S. Kulkarni, and D. Jones, eds. Astrotech 21 Workshops, vol. 1, no. 1, 15 May 1991.

4. R.D. Reasenberg, R.W. Babcock, M.C. Noecker, and J.D. Phillips, "POINTS: The Precision Optical INTerferometer in Space," The Proceedings of the ESA Colloquium on Targets for Space-Based Interferometry, European Space Agency, Beaulieu-sur-Mer, France, 13-16 October 1992, ESA Publications Division, Noordwijk, The Netherlands, ESA-SP-345, December 1992.

5. R.D. Reasenberg, "Precision Optical Interferometry in Space," in Proceedings of The First William Fairbank Meeting on "Relativistic Gravitational Experiments in Space," Rome, 10-14 September 1990, in press.

6. R.D. Reasenberg, R.W. Babcock, M.C. Noecker, and J.D. Phillips, "POINTS: The Precision Optical INTerferometer in Space, in Remote Sensing Reviews (Special Issue Highlighting the Innovative Research Program of NASA/OSSA), Guest Editor: Joseph Alexander, 1993, in press.

7. R.D. Reasenberg, R.W. Babcock, M.C. Noecker, and J.D. Phillips, "POINTS: The Precision Optical INTerferometer in Space," in The Proceedings of the SPIE Conference # 1947, OE/Aerospace Science and Sensing '93, Orlando, FL, April 14-16, 1993, in press.

8. M.C. Noecker, J.D. Phillips, R.W. Babcock, R.D. Reasenberg, "Internal laser metrology for POINTS," in The Proceedings of the SPIE Conference # 1947, OE/Aerospace Science and Sensing '93, Orlando, FL, April 14-16, 1993, in press.

9. M.C. Noecker, M.A. Murison, R.D. Reasenberg, "Optic-misalignment tolerances for the POINTS interferometers," in The Proceedings of the SPIE Conference # 1947, OE/Aerospace Science and Sensing '93, Orlando, FL, April 14-16, 1993, in press.

Abstracts

1. R.D. Reasenberg, R.W. Babcock, and J.F. Chandler, "POINTS, the Planet Finder, II," BAAS, 21, 972, 1989. Presented at the AAS/DPS Meeting 21, Providence, Rhode Island, 31 October-3 November 1989.

2. R.D. Reasenberg, R.W. Babcock, and J.F. Chandler, "Prospects for a Deflection Test with Space-Borne Astrometric Optical Interferometry," at XXVI COSPAR Meeting, Espoo, Finland, 18-29 July 1988, R.D. Reasenberg and R.F.C. Vessot, eds., pp. 71-74, 1989.

3. R.W. Babcock, J.F. Chandler, and R.D. Reasenberg, "Searching for Planets around Nearby Stars with POINTS," BAAS, 22, 949, 1990. Presented at AAS Division on Dynamical Astronomy, Austin, TX April 25-27, 1990.

4. R.D. Reasenberg, "Space Optical Interferometry, a 21st Century Revolution," BAAS, 23(4), 1447, 1991. Presented at the 179th AAS Meeting, Atlanta, GA, 12-16 January 1991.

5. J.D. Phillips, M.C. Noecker, and R.D. Reasenberg, "Tracking Frequency Laser Gauge," Program and Abstracts, National Radio Science Meeting, U.S. National Committee for the International Union of Radio Science (URSI), (5-8 January 1993, Boulder, CO), USCN/URSI, National Academy of Sciences, Washington, DC, 1993.

6. J.D. Phillips, R.W. Babcock, J.F. Chandler, M.C. Noecker, and R.D. Reasenberg, "Precision Optical Interferometer in Space (POINTS)," Program and Abstracts, National Radio Science Meeting, U.S. National Committee for the International Union of Radio Science (URSI), (5-8 January 1993, Boulder, CO), USCN/URSI, National Academy of Sciences, Washington, DC, 1993.

7. M.C. Noecker, R.W. Babcock, J.D. Phillips, and R.D. Reasenberg, "Picometer Distance Gauges for POINTS," presented at the Optical Society of America 1992 Annual Meeting, 1992 Technical Digest Series, vol. 23, p. 75, (Albuquerque, NM, 20-25 September 1992).

8. M.C. Noecker, R.W. Babcock, J.F. Chandler, J.D. Phillips, and R.D. Reasenberg, "POINTS: Micro-arcsecond Optical Astrometry in Space," presented at the Optical Society of America 1992 Annual Meeting, 1992 Technical Digest Series, vol. 23, p. 168, (Albuquerque, NM, 20-25 September 1992).

9. M.C. Noecker, R.W. Babcock, J.D. Phillips, and R.D. Reasenberg, "POINTS: Technology for Micro-arcsecond Optical Astrometry," presented at the Optical Society of America 1992 Annual Meeting, 1992 Technical Digest Series, vol. 23, p. 211, (Albuquerque, NM, 20-25 September 1992).

Techical Memorandum

1. TM89-2: R. D. Reasenberg, Effect of a Uniform Expansion on the Characteristics of a Zone-Plate Mirror.

2. TM90-1: R. D. Reasenberg and J. D. Phillips, Patent Disclosure for a New Laser Gauge.

3. TM90-3: J. D. Phillips, Permissible Amplitude of Coherent Spurious Beams in Distance Gauges.

4. TM90-4: M. C. Noecker, Optical Fiber Corruption and Dipole Gradient Forces.

5. TM90-7: M. C. Noecker, Deflection of the Beam Emerging from an Imperfect Corner Cube.

6. TM90-8: R. D. Reasenberg, False alarms in experiments that search for rare events.

7. TM91-1: R. D. Reasenberg, Absolute laser gauging and the effect of biased distance measurements on POINTS angle determinations

8. TM91-2: M. C. Noecker, AM produced by birefringence in an optical fiber

9. TM91-3: J. D. Phillips, Distance to and size of the waist of a Gaussian Beam having a known radius and radius of curvature

10. TM91-4: R. W. Babcock and R. D. Reasenberg, Simulations of planet searches using POINTS.

11. TM91-8: R.D. Reasenberg, The fiducial block and the opening in its insutlation required permit FAM light to enter.

12. TM91-9: J.D. Phillips, Thermal distorion of a plate and of clamped parallel rods.

13. TM91-10: R.W. Babcock, POINTS and the traveling salesman problem.

14. TM91-11: J.D. Phillips, Measurement Strategy for Faint Objects.

15. TM92-01: M.C. Noecker, AM produced using HV DC on the EO.

16. TM92-02: J.D. Phillips, Blackbody Spectra.

17. TM92-03: J.D. Phillips, POINTS Starlight Beamwalk

18. TM92-04: M.C. Noecker, Optical Path through the imperfect corner cube

19. TM92-05: R.W. Babcock, POINTS Astrometric Sensitivity

Newcomb, a POINTS precursor mission with scientific capacity

Robert D. Reasenberg, Robert W. Babcock, and James D. Phillips

Smithsonian Astrophysical Observatory
Harvard-Smithsonian Center for Astrophysics
60 Garden Street, Cambridge, MA 02138

Kenneth J. Johnston and Richard S. Simon

Naval Research Laboratory
Remote Sensing Division
4555 Overlook Avenue, S.W., Washington, DC 20375

ABSTRACT

Newcomb is a design concept for an astrometric optical interferometer with nominal single-measurement accuracy of 100 microseconds of arc (μas). In a three-year mission life, it will make scientifically interesting measurements of O-star, RR Lyrae, and Cepheid distances, establish a reference grid with internal consistency better than 100 μas, and lay groundwork for the larger optical interferometers that are expected to produce a profusion of scientific results during the next century. With an extended mission life, Newcomb could do a useful search for other planetary systems.

The instrument is a highly simplified variant of POINTS. It has three (or four) interferometers stacked one above the other. All three (four) optical axes lie on a great circle, which is also the nominal direction of astrometric sensitivity. The second and third axes are separated from the first by fixed "observation angles" of 40.91 and 60.51 deg. The fourth axis would be at either 70.77 or 78.60 deg from the first. Each interferometer detects a dispersed fringe (channeled spectrum), which falls on a CCD detector array nominally 8k elements long and a small number of elements wide. With a nominal baseline length of 30 cm and optical passband from 0.9 to 0.3 microns, the Nyquist limit is reached by a star ±21 arcmin from the optical axis. The instrument will be constructed of stable materials such as ULE glass, and have neither internal moving parts nor laser metrology.

A reference frame can be constructed using stars located in a regular pattern on the sky. We start with the 60 points that are vertices of the regular truncated icosahedron. The instrument axis separations are chosen as separation angles of the figure such that for each point there are four other points at the chosen angle. (There is no angle offering higher multiplicity.) To the original set of 60 points, we add two additional such sets by rotating the figure ±20.82 deg, which provides 40 interconnections among the three sets of 60 points. With such a grid of 180 stars, we have shown POINTS-like grid lock-up even with large Sun-exclusion angles (of up to 75 deg). In the covariance studies, we assumed nine quarterly observation series and five bias parameters per series per observation angle; we estimated position, proper motion, and parallax for each star. In an extension of the study, we eliminated stars at random from the set and found that there was stable behavior with as few as half the stars in the grid. Further, with 120 stars in the grid, the statistical uncertainty of star position increased by only 35% due to degeneracy (*i.e.*, with constant number of observations.)

As with POINTS, additional stars can be observed with respect to the grid. With three interferometers and a full grid and without exceeding the Nyquist limit, the region accessible for observing with respect to at least two grid stars is over 50% of the sky outside of the Sun exclusion zone. This observable region can be enlarged by either including more sets of 60 points in the reference star grid, or adding the fourth interferometer, or increasing the number of elements in the detector arrays, or by limiting the passband with the same number of elements.

1. INTRODUCTION AND HISTORY

Newcomb is a design concept for an astrometric optical interferometer with nominal single-measurement accuracy of 100 microseconds of arc (μas). It is a low-cost derivative of POINTS (Reasenberg, *et al.* in these proceedings) intended for early demonstration of some interferometer technology and a reduced (from the POINTS goals) but significant scientific program in addition to the principal goal of establishing a high precision reference grid.

The concept was first documented in a letter to M.S. Kaplan (NASA, Astrophysics) from R.D. Reasenberg on 11 December 1992, describing a suggestion made by the latter in response to a concern raised by K.J. Johnston during a phone conversation of 10 December. There quickly ensued a collaboration between SAO and NRL to develop Newcomb for the Navy's Space Test Program (STP). The plan was to use a standard spacecraft bus such as STEP (made by TRW), which could be put into Earth orbit by a launcher commonly used by the STP. The instrument would be kept simple and the mission, low cost and of short duration for an astrometric investigation, say 27 months.

No detailed study has yet been made of systematic error in Newcomb. However, the plan to dispense with the metrology is plausible. If the instrument is constructed of solid ULE with expansion coefficient 1×10^{-8}/K (in a worst case we may assume that this varies by 100% across the instrument) and thermal expansion of the 0.3 m dimensions must contribute no more than 30 microarcsec to the instrument bias, then the instrument average temperature and temperature gradients must be held constant to within ~0.015 K over the recalibration timescale (several hours). Our thermal studies of POINTS have shown that this level of control is likely to be achievable, even accounting for the variation in thermal input from the warm spacecraft.

2. INSTRUMENT DESIGN

The nominal instrument comprises three or four Michelson stellar interferometers, each with a dispersed-fringe detection system. Each interferometer baseline will be parallel to the instrument's "principal plane." As we picture the construction, there will be a stack of parallel plates with an interferometer assembled between each pair of adjacent plates. The nominal baseline length is 30 cm and the nominal aperture is 5 cm. Figure 1 shows the optical plan for one of the interferometers.

Starlight from folding flats M_1 and M_1' in each interferometer combines at beamsplitter BS. A beam from each beamsplitter exit port is directed into a spectrometer. The usual beam-compressing telescopes are absent, which reduces the number of components, the light loss in reflections, and beamwalk on M_1 and M_1'. The spectrometers employ prisms instead of gratings because of the light loss of the latter, which would be especially severe over the Newcomb optical passband (nominally 0.9 to 0.3 μm). The high loss would have contributions from the blazing, which could not be optimum over the whole passband, and from the filters needed to defeat the response at undesired grating orders. Given specifications for the prism, focussing optics, and detector, the range of optical frequencies $\delta\nu_p$ corresponding to each pixel may be calculated. The blur due to the combined effects of diffraction and geometrical aberration expressed in terms of optical frequency must be less than $\delta\nu_p$ at most or all pixels. This resolution can be provided by a prism with a 68 deg apex angle.

The detector has 8192 pixels of 7.5 μm width for a total length of 6 cm, and the prism deviation range is 4.1 deg. The camera focal length of 85 cm matches the prism deviation range to the length of the detector. A single mirror design would provide the greatest throughput, but would require excessive length and would have unacceptable geometrical aberration over the range of angles produced by the prism. A two-mirror design was adopted. The camera is similar to the standard Ritchey-Chretien telescope, which is a Cassegrain with conic constants adjusted to cancel coma in leading order.[1] Dimensional stability of the camera will not be as much of a problem in this application as in ordinary telescopes as both the mirrors and their spacers can be made of ULE glass. A secondary magnification factor of 3 was chosen. A design with higher magnification would be more compact, but might have larger aberration and tighter tolerances. The conic constants were further optimized using the numerical ray trace program Zemax [FocuSoft, Inc., Pleasanton, CA].

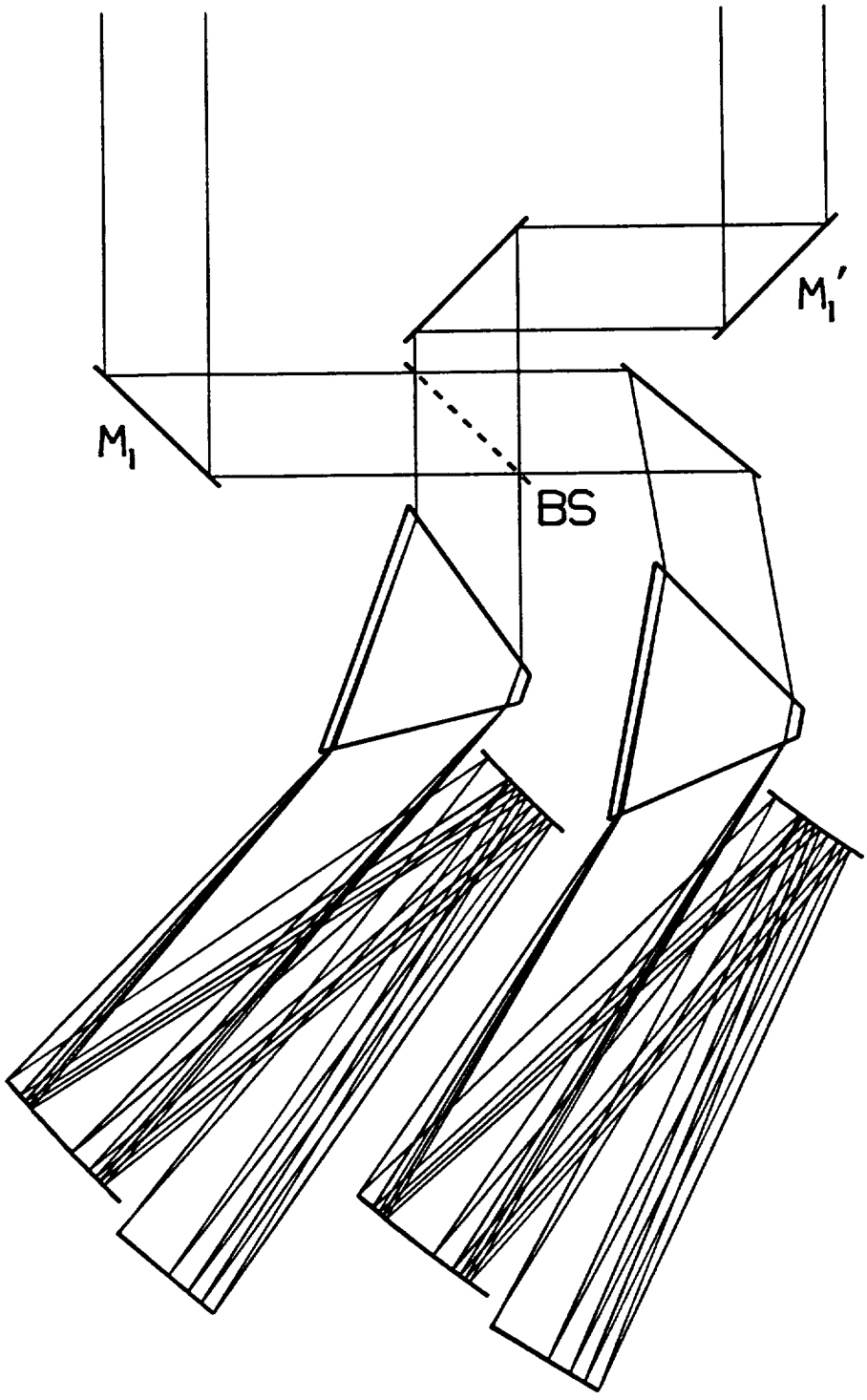

Figure 1. Optical plan for one Newcomb interferometer: starlight folding flats, beamsplitter, prism dispersers, two-mirror cameras, and detectors. The five sets of rays bound optical frequency regions which each contain one quarter of the information $\int_{\nu_1}^{\nu_2} I(\nu)\ \nu\ d\nu$, where $I(\nu)$ is the detected intensity per unit frequency.

As shown, the camera has a geometrical blur a factor of several greater than the diffractive blur at some wavelengths. Some of the options for further improvement are: additional aspheric terms in the shape of the mirrors (the present mirrors are hyperboloids of revolution about a common center line), an aspheric corrector plate, and reducing the deviation range (trading increased diffractive blur for reduced geometric). The optimization has not yet been performed, as it involves the dependence on optical frequency of all of the following quantities: the dispersion (*i.e.*, the deviation angle per unit optical frequency), the diffractive blur, the photon rate from a typical star, the angular information in a single photon, and the photon detection probability.

The starlight optics operate at non-normal incidence, and most mirrors exhibit a difference in phase delay for light polarized perpendicular and parallel to the plane of incidence (s and p polarizations). This implies that fringes in s and p polarized light will be formed in different places on the detector. The detector will record the sum of the two fringe patterns, so will see fringes of lowered visibility. The reflection phase difference will be minimized to the extent possible through coating design, but it might be necessary to have polarizing beamsplitters, and separate detectors for the two polarizations.

Each of Newcomb's 3 or 4 interferometers requires two of these spectrometers, one at each beamsplitter exit port. Figure 1 shows how two spectrometers might be arranged in relation to the interferometer optics. To make the design more compact, a secondary magnification factor higher than 3 could be used, or it might be advantageous to rearrange the components, reversing one or both prisms, and placing one or both secondaries on the side towards the star of the line from M_1 to BS, and from M_1' to BS.

3. THE STAR-GRID PROBLEM

The mission concept for Newcomb relies on a reference grid of stars and a redundant set of intra-grid observations that permit the grid star positions to form a tightly connected system. This aspect of a Newcomb mission resembles a POINTS mission[2,3,4] for which the critical quantity is the redundancy factor:

$$M = \frac{\text{number of observations}}{\text{number of stars in the grid}} \tag{1}$$

From our studies of POINTS, we know that when $M > M_0$, where M_0 is about 3.5, the grid "locks up" such that the angle between any pair of stars can be determined by the analysis of the data, even when the pair of interest cannot be directly observed. For POINTS, we normally assume M = 5 in studies of the mission. In the nominal POINTS architecture, the angle between a pair of stars to be observed must be $\phi = \phi_o + \Delta$, $|\Delta| \le \Delta_o$, where ϕ_o = 90 deg and Δ_o is the one sided articulation range. If POINTS observes all of the star pairs within its articulation range, then

$$N^* = \frac{114\ M}{\Delta_O \sin\phi_o} \tag{2}$$

where N^* is the number of stars in the grid. For POINTS, with the nominal parameters of M=5, Δ_o=3 deg, and ϕ=90 deg, we find that N^*=190.

For Newcomb, if we were to have two interferometers at ϕ_o=90 deg, and if we assumed M=5 and Δ_o= 21 min., then we would find that N^* = 1629. If the instrument can make D observations per day, the time needed to make a complete set of grid-star observations is $M \times N^*/D$. Since D is of order 200, it would require 41 days to complete one observation cycle of the grid. This is clearly not acceptable.

3.1. A sparse and regular star grid

An alternative to the random grid of stars is a regular pattern that defines special angles, which are each the exact separations of a large number of star pairs. Such a "crystal on the sky" could be based on one of the semi-regular polyhedra. We selected one of the biggest of these, the truncated regular icosahedron (a.k.a. buckyball) as the starting

point. We have not yet tested several other semi-regular polyhedra that might form the basis of a reference grid. These include the snub icosidodecahedron, rhombicosidodecahedron, truncated dodecahedron, and truncated icosidodecahedron. Some of the dual polyhedra, which have vertices above the centers of the faces of the semi-regular polyhedra, also look promising.

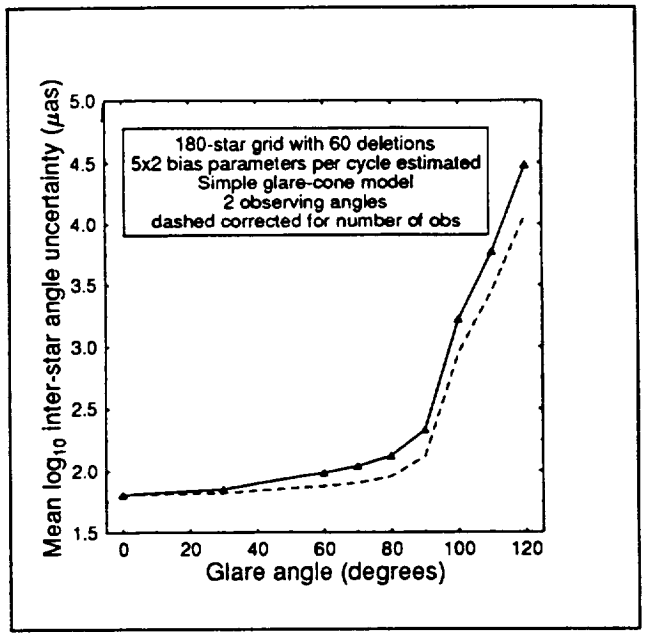

Figure 2. Degradation of star coordinate uncertainty with increasing solar glare exclusion angle. Dashed curve assumes that with fewer observations possible, correspondingly more time can be spent on each one.

The truncated regular icosahedron has 60 vertices, 90 sides, and 32 surfaces: 12 pentagons plus 20 hexagons. It is the pattern on the familiar soccer ball and the geometry of the nearly spherical C_{60} molecule known as a buckyball. Each vertex can be mapped into each other vertex by a (possibly improper) rotation. Of the 59 angles from a given vertex to the other vertices, the following repeat four times: 40.91, 60.51, 70.77, 78.60, 101.40, 109.23, 119.49, and 139.09 deg. No angle repeats more than four times. Observation angles near 90 deg provide maximum sky area in which to find target stars, but smaller observation angles are expected to be required for solar-glare isolation. A measurement grid must meet three increasingly stringent requirements: (1) it must lock up when a complete set of data are analyzed, (2) it must remain locked up when biases are estimated, and (3) it must be robust against deleting a moderate fraction of the stars. Grids were tested using the POINTS simulation program [TM81-6]. In a typical simulation, all observable star pairs were measured each quarter year for 9 quarters. Stars within a cone of adjustable size near the Sun were not observed. Five star parameters (two positions, parallax, and two proper motions) were estimated, as well as a variable number of Fourier bias parameters for each observation angle. Star positions were given a weak *a priori* estimate to break the overall rotational degeneracy, and all measurements were assumed to have 100 μas precision.

A simple measure of grid robustness is the distribution of $\log_{10}$(inter-star angle uncertainty) for all star pairs. We prefer the mean of this to be somewhat smaller than $\log_{10}$ (single measurement uncertainty), and that the distribution have few if any outliers. The 60-star grid is rigid with a single measurement angle of either 40.91 or 60.51 deg, but if even a single bias parameter is estimated each quarter, the bias uncertainty is large and the grid falls apart. Since M is only 2.0, the fragility of the 60-star grid is not surprising.

A more robust system was assembled by using three sets of 60 stars and two measurement angles, 40.91 and 60.51 deg. The second and third sets of stars are rotated from the first around an axis through the centers of opposing pentagonal faces by ± 20.82 deg to yield M = 4.22. (No intra-grid observation is possible at the 19.60 deg difference angle, but this angle can be used to observe non-grid stars.) The grid is robust against deletion of roughly one third of the stars, even if biases are estimated and near-Sun observations are excluded. Figure 2 shows the behavior of the 180-star grid, with 60 randomly-selected stars deleted, which reduces M to 2.85. Mean inter-star angle uncertainty increases slowly as the glare cone angle is increased to nearly 90° (keeping constant the total number of observations). Actually, insensitivity to solar glare was a general feature of all grids tested. If the grid were rigid, adding a glare exclusion cone merely increased slightly the uncertainty of the inter-star angle unless the cone angle was $\gtrsim$90 deg, in which case some pairs were never observable and the grid unlocked.

Sensitivity to missing stars was tested by making multiple runs with randomly selected stars deleted from the grid. When the grid is incomplete, some stars may become "orphans," that is, they do not have the minimum of three reference stars required for them to contribute to the information that locks the rest of the grid. Figure 3 shows scatter plots of uncertainties in inter-star angle for orphan, normal, and all pairs as a function of the number of stars in the grid. In selecting a set of real stars, we are free to try a large number of cases and pick the most favorable. Therefore, we take

Delete random points from 180 star grid

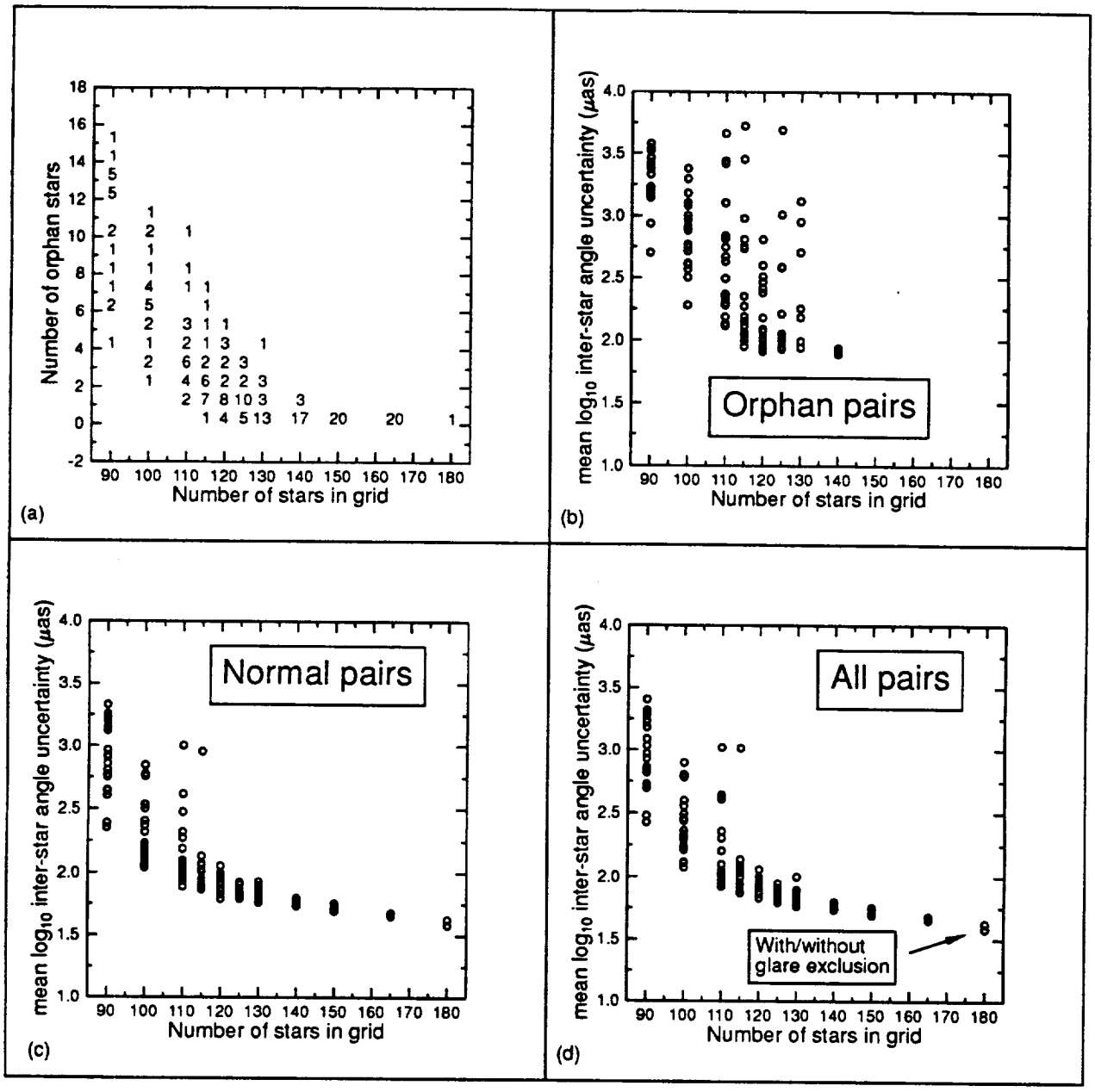

Figure 3. Results from simulations in which randomly selected stars are deleted from 180-star Newcomb grid. 20 runs were made for each grid size. (a) Distribution of numbers of orphan pairs encountered versus number of stars in grid. Numbers shown in the plot are the number of cases (max of 20) for which a particular number of orphaned stars was found. (b-d) Uncertainties in inter-star angles for orphan, normal, and all pairs. (An orphan pair is one which includes an orphan star. Orphan stars were not excluded when counting reference stars to determine whether another star is an orphan.)

the bottom of each vertical distribution as indicative of the results we expect from a formal search process. It appears that at least one third of the grid stars can be deleted without greatly increasing the angle uncertainties, more with selected matchings of the grid to the sky.

3.2. Finding stars in the patches

In the preceding section, we were concerned with the star grid as an abstract construct. Here we address the characteristics of a star grid based on real stars. When we select specific stars to form a grid on the sky, we require that both interferometers work within the Nyquist limit for all intra-grid observations. The simplest way of assuring this is to require that each grid star be within the Nyquist angle of the nominal position, *i.e.*, to require that each selected star be within a circular patch with a radius equal to the Nyquist angle, and centered on the nominal position. Ideally, stars should be more accurately positioned than this to get a higher information rate, but if we are unlucky, it may sometimes be necessary to observe well off axis with both interferometers. We can estimate how faint the grid stars might be from the average density of stars and the area of sky seen by each interferometer. If each star must be within 21 arcmin of the nominal position, then each grid star must be located within a circular patch of area 0.38 sq. deg.

If the density of stars is ρ, and the sky area within the Nyquist angle is A, then the average number of stars in a patch is ρA. Assuming Poisson statistics, the probability that a patch is empty is $P_0=e^{-\rho A}$, and the probability that a patch is occupied is $1 - e^{-\rho A}$. Since the number of occupied patches has a Binomial distribution, the probability of having exactly m out of n patches occupied is

$$C(n,m)\ (1-e^{-\rho A})^m\ (e^{-\rho A})^{n-m} \qquad (3)$$

where $C(n,m)$ is the number of combinations of n things taken m at a time. The probability of k or more occupied patches is obtained by summing Eq. 3 over the range $m=k$ to n. The result of this sum is shown in Fig. 4; we want to operate at $P_0<1/3$, which implies $\rho A>1.1$. Table I gives the average density of stars on the sky as a function of visual magnitude.[5] Note that the star density is roughly a factor of two higher than tabulated near the galactic plane, and a factor of two lower near the galactic pole. From the table, we see that if stars were uniformly distributed, the grid stars would only have tc be as faint as m=9. The uneven distribution will require accepting fainter stars. However, as previously noted, we have the option to

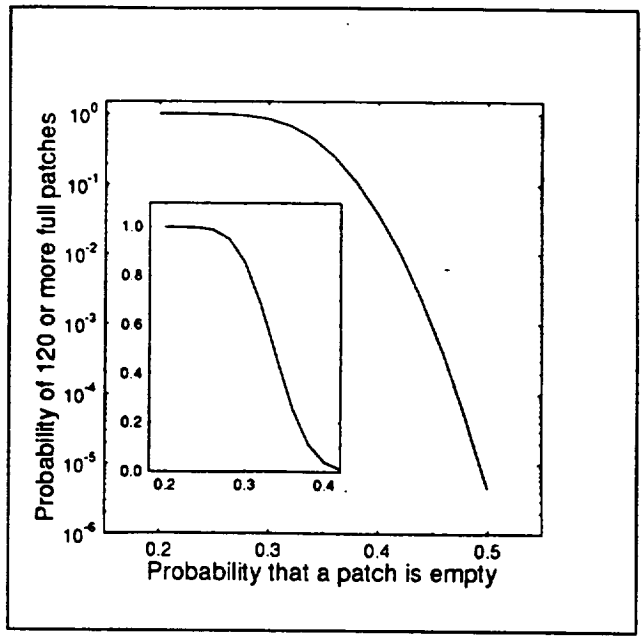

Figure 4. Probability that 120 or more of 180 possible patches of sky contain a grid star as a function of the probability that any single patch is empty. Insert is a blowup of the high-probability region on a linear scale.

Table I - Density of stars

m_{vis}	Stars/ 0.38 sq. deg	Expected no. of occupied patches
5	0.015	2.7
6	0.046	8.1
7	0.13	22
8	0.38	57
9	1.1	120
10	3.1	172
11	8.4	180
12	22	180
13	56	180
14	138	180

pick the best orientation of the set of patches on the sky and, by Monte Carlo methods, we can have a large number of cases from which to make the selection.

3.3. Sky coverage

A multitude of small patches of sky are observable relative to the reference grid. The centers of these patches are at $\hat{P}_k$ which are the solutions of

$$\begin{aligned} \hat{P}_i \cdot \hat{P}_k &= \cos\theta_m \\ \hat{P}_j \cdot P_k &= \cos\theta_n \end{aligned} \qquad (4)$$

where $\hat{P}_i, \hat{P}_j$ are unit vectors pointing at appropriate combinations of grid stars and θ_m, θ_n are all possible combinations of observation angles. Physically, each measurement angle generates a band, bounded by a pair of small circles, surrounding each grid star, and the intersections of these with the bands of another grid star are observable patches. The corners of the approximately rhomboidal observable patches could be found by solving Eqs. 4 with θ_i offset by the maximum off-axis angle. We took another approach. Sections of the sky were covered with a 0.1×0.1° lattice and the number of references stars visible from the center of each lattice box was tabulated. (Because of the symmetry of the 180-star grid, the study region needed only cover 36 deg of longitude and from the equator to one pole.)

Figures 5a and 5b show the fraction of the sky visible against the nominal 180-star grid as a function of the inter-star angle tolerance. More than 30% of the sky can be observed with respect to at least the minimum of three references stars that are needed to estimate star-specific biases. Additional coverage could be obtained with additional 60-star sub-grids. It might also be useful to put grid stars in the patches that can be seen from at least six of the grid stars. (Starting with a 60- or 120-star grid and adding stars at high-redundancy patches is an alternative way of building a grid, which has not yet been explored.)

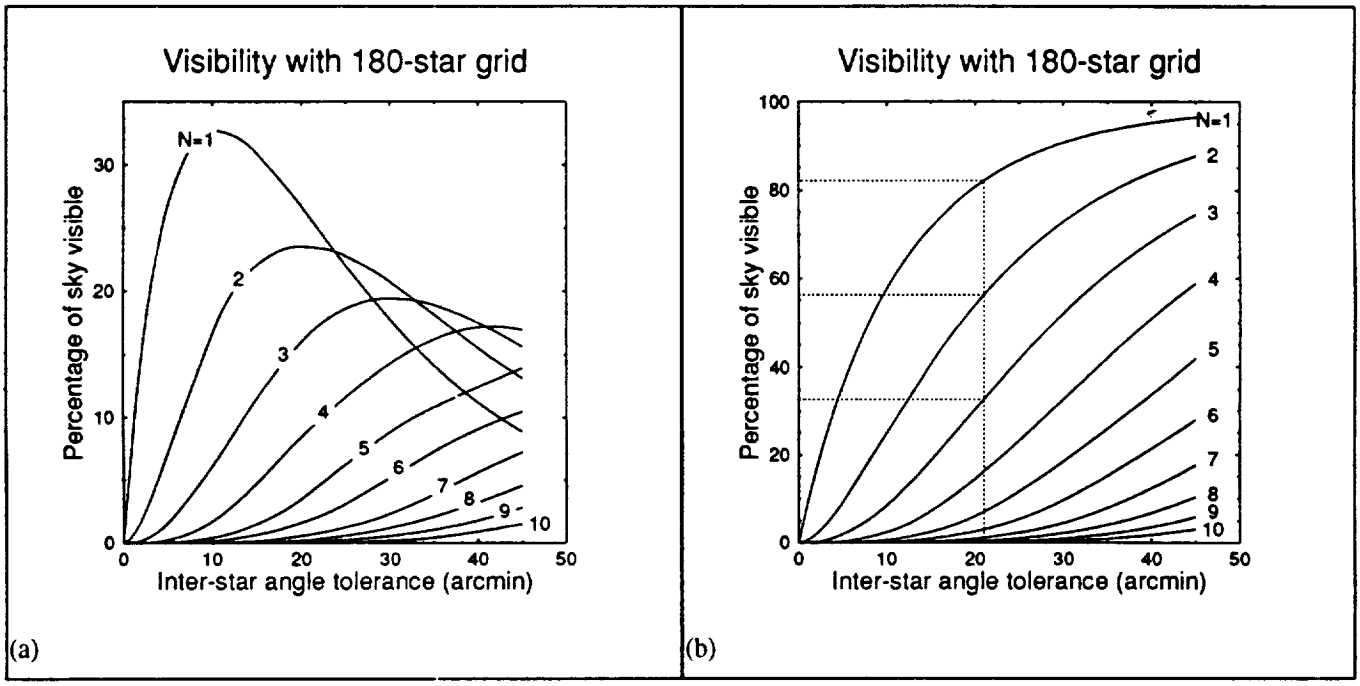

Figure 5. Fraction of sky observable against the 180-star Newcomb grid. The inter-star angle is 19.6, 40.91, or 60.51 deg, with a tolerance of ± 21 arcmin. Curves are labeled with N, (a) with exactly N reference stars and (b) with N or more reference stars. (Note that the 180 patches containing reference stars cover about 1/6% of the sky.)

4. APPLICATIONS

Newcomb would establish a precise reference frame that would be accessible to optical and infrared sensors. This frame would be useful to the Navy for navigation. Hipparcos will yield a grid that is good for a short time, but proper motion uncertainty from this short-duration mission will quickly degrade that grid. Newcomb and Hipparcos would be complementary missions for determining proper motion. Repeated and redundant observations would insure that the program was robust and lower the position (and thus the parallax and proper motion) uncertainty well below the nominal single-observation uncertainty.

Newcomb will also provide a direct link between high-precision optical astrometry and the present radio reference frame as discussed by Fey *et al.*[6], and in the papers they cite. Observations of only a few radio quasars are needed to fix the relative rotation between the current radio reference frame and the optical reference frame which will be developed by Newcomb and Hipparcos. Newcomb will thus resolve current difficulties in relating high angular resolution observations at radio and optical wavelengths.

Newcomb could see enough of the sky to do some interesting science. A preliminary study suggests that the instrument's limiting magnitude would be about 15. However, this analysis depends on instrument parameters that are not yet fixed and are expected to be set during a series of trade studies. The Space Interferometry Science Working Group (SISWG) developed a Strawman Science Program for the Astrometric Interferometry Mission[7] as a step toward evaluating the astrophysical capability of candidate missions. Of the goals presented in the "Strawman," five could also be met by Newcomb: (1) 19 known Cepheids have parallaxes between 200 and 1000 μas and V magnitudes of less than 10; a 5% distance measurement would be useful for refining the cosmic distance scale. (2) Absolute magnitudes of O stars are uncertain because none is close enough to allow a trigonometric parallax measurement from the ground. O stars are bright targets, V=4 to 6 at 1 to 2 kpc; 25 to 50 μas parallax measurements are needed. (3) Estimates of the ages of globular clusters often exceed estimates of the age of the universe. Age determination of globular clusters depends in part on calibration of the absolute magnitude of RR Lyrae stars as a function of period. The 20 brightest RR Lyrae stars range from V=7.6 to 10. Parallax measurements are needed at the 1% level, which corresponds to 40 μas for RR Lyrae itself. (4) Distances to 90 nearby field subdwarfs cataloged by Carney,[8] ranging in magnitude from 7.2 to 12, would calibrate subdwarf luminosities, which are used in fitting the globular cluster main sequences. Parallaxes are needed with 30 μas precision. (5) Parallaxes of bright (V = 10) K giants in the galactic disk, accurate to 50 μas, would probe the dark matter in our galaxy.

With 100 μas measurements and a sufficient mission duration, Newcomb could detect Jupiter-sized planets around nearby stars. The problem here is that, if the solar system is a "typical" planetary system, signatures large enough to be seen will have periods much longer than the 27 month life envisioned for Newcomb. Hipparcos measurements might help break the degeneracy between proper motion and a short arc of orbital motion, but this speculation has not yet been tested by a sensitivity study. Similarly, Newcomb data could supplement a POINTS mission, especially in the case of a planet period long compared to the mission life possibly shortened by equipment failure.

Gravity Probe B, an experiment which will measure the general relativistic frame dragging due to the spinning Earth, needs a bright guide star (Rigel) with proper motion known in an inertial frame to ≈1 mas/year or better. Newcomb could determine the proper motion of Rigel relative to a few bright quasars tied directly to the reference grid.

5. ACKNOWLEDGEMENTS

This work was supported in part by the NASA Planetary Instrumentation Definition and Development Program (PIDDIP) Grant NAGW-2497, and by the Smithsonian Institution. The authors gratefully acknowledge the careful preparation of the camera-ready text by S.A. Silas.

6. REFERENCES

1. D.J. Schroeder, *Astronomical Optics*, p. 102, Academic Press, 1987.

2. R.D. Reasenberg, R.W. Babcock, M.C. Noecker, and J.D. Phillips, "POINTS: The Precision Optical INTerferometer in Space," *The Proceedings of the ESA Colloquium on Targets for Space-Based Interferometry*, European Space Agency, Beaulieu-sur-Mer, France, 13-16 October 1992, ESA Publications Division, Noordwijk, The Netherlands, ESA-SP-345, December 1992.

3. R.D. Reasenberg, R.W. Babcock, M.C. Noecker, and J.D. Phillips, "POINTS: The Precision Optical INTerferometer in Space, in *Remote Sensing Reviews* (Special Issue Highlighting the Innovative Research Program of NASA/OSSA), Guest Editor: Joseph Alexander, 1993.

4. R.D. Reasenberg, "Microarcsecond Astrometric Interferometry," in *Proceedings of IAU Symposium, 109, Astrometric Techniques* (Gainesville, 9-12 January 1984), H.K. Eichhorn and R.J. Leacock, eds. pp. 321-330, Reidel, Dordrecht, 1986.

5. C.W. Allan, *Astrophysical Quantities*, The Athlone Press, p. 244, London, 1976.

6. A. Fey, J.L. Russell, C. Ma, K.J. Johnston, B.A. Archinal, M.S. Carter, E. Holdenreid, and Z. Yao, *Astron J.* **104**, p. 891, 1992.

7. "Astrometric Interferometry Mission Strawman Science Program," unpublished memorandum, 1992.

8. B.W. Carney, "The Subdwarf Helium Abundance and the Rotation of the Galactic Halo," *Astrophysical Journal*, **233**, p. 877, 1979.